POLITECNICO DI MILANO

Facoltà di Ingegneria Industriale

Dipartimento di Scienze e Tecnologie Aerospaziali

Corso di Laurea Magistrale in Ingegneria Aeronautica

POLITECNICO
MILANO 1863

CHARACTERIZATION OF A SELF-HEALING COMPOSITE: MECHANICAL AND FUNCTIONAL PROPERTIES

Relatore: Dott. Ing. Antonio Mattia GRANDE

Tesi di Laurea di:

Clara SIMÓN GARCÍA

Matricola 894522

Anno Accademico 2018 – 2019

Contents

List of Figures

List of Tables

Sommario

Il presente elaborato si concentra sulla valutazione delle proprietà meccaniche e funzionali di un composito autorigenerante formato da una resina epossidica covalente dinamica e un rinforzo industriale in fibra di vetro a 0°/90°.

Nella tesi verranno brevemente presentati i progressi raggiunti in questo ambito, focalizzando l'attenzione sui reticoli reversibili polimerici caratterizzati da disolfuri aromatici. In primo luogo verranno esaminate le proprietà termomeccaniche del materiale composito dinamico attraverso lo studio comparativo con un materiale composito di riferimento. La seconda parte sarà dedicata alla valutazione di altre proprietà funzionali come il meccanocromismo, la rielaborazione, la riparabilità o la riciclabilità.

L'idea della tesi deriva da precedenti progetti realizzati al Politecnico di Milano che miravano a caratterizzare termomeccanicamente la resina epossidica dinamica. Grazie a questo lavoro verranno ampliate le potenziali applicazioni dei materiale multifunzionali, poiché prende in considerazione i materiali compositi, che rappresentano la rivoluzione tecnologica in corso nel settore aerospaziale.

Abstract

The present thesis focuses on assessing the mechanical and functional properties of a self-healing composite constituted by a dynamic covalent epoxy resin and a 0°/90° commercial glass fibre reinforcement.

Advances in the field are briefly explained, since different healing strategies are under research, but the focus is made on the investigation of reversible crosslinked composites based on aromatic disulphides. First, thermomechanical properties are assessed making a comparative study with a composite manufactured using commercial, industrial-tested materials and secondly additional functional properties are examined, such as mechanochromism, reprocessability, repairability or recyclability.

The idea of the dissertation stems from previous projects carried out at Politecnico di Milano which aim was characterizing the pure dynamic resin. Upscaling the project focusing on composites, which still are the ongoing technological revolution in aerospace manufacturing industry, potential applications of multifunctional materials are expanded.

Nomenclature

A	Pre-exponential Arrhenius factor
AFM	Atomic Force Microscope
AHEW	Amine Hydrogen Equivalent Weight
BDSER	Bis-disulphide bond Dynamic Epoxy Resin
CAN	Covalent Adaptable Network
CFRP	Carbon Fibre Reinforced Polymers
DA	Diels Alder
DA-rDA	Diels Alder/retro Diels Alder
DETDA	Diethyltoluenediamine
DGEBA	Diglycydil Ether of Bisphenol A
DCC	Dynamic Covalent Chemistry
DMA	Dynamic Mechanical Analysis
DMF	Dimethylformamide
DSC	Differential Scanning Calorimetry
E	Young modulus
E'	Tensile storage modulus
E''	Tensile loss modulus
E*	Complex modulus
E_a	Activation energy
EEW	Epoxide Equivalent Weight
FRP	Fibre Reinforced Polymers
FRPC	Fibre Reinforced Polymer Composites
G'	Shear storage modulus
G''	Shear loss modulus
GFRP	Glass Fibre Reinforced Polymers
ILSS	Interlaminar Shear Strength Test
K(T)	Temperature dependent separable function
NDI	Non-Destructive Inspections
PUU	Poly(urea-urethane)
R	Universal gas constant

RTM	Resin Transfer Moulding
SEM	Scanning Electron Microscopy
T_d	Degradation temperature
T_g	Glass transition temperature
T_v	Freezing transition temperature
TGA	Thermogravimetric analysis
TRL	Technology Readiness Level
UV	Ultraviolet
V	Volume
V_v	Void volume fraction
WLF	Williams-Landel-Ferry
f	Fibre volume fraction
o-EPO	Ortho Epoxy
p-EPO	Para Epoxy
phr	Parts per 100 grams of epoxy resin
tan δ	Loss factor
2-AFD	2-Aminophenyl disulphide
4-AFD	4-Aminophenyl disulphide
α	Degree of cure
ε	Strain
η	Efficiency
η	Viscosity
ρ	Density
σ	Stress
ω	Oscillation frequency
ΔH_{cure}	Heat of cure

Introduction

Aerospace industry is well known for its role as technological driving force. Thus, high-performance materials have been developed. Composite materials evolution began in the 1960s motivated by the heavy weight of metallic components, the expansion of polymer industries and the discovery of high strength materials, such as glass fibres. Since then its implementation in the aerospace industry has grown exponentially.

Composite materials consist of a load carrier material embedded in a matrix, so that constituent materials properties are combined to exploit their synergies. They show greater strength characteristics, lower weight and higher fatigue and corrosion resistance than metallic alloys, so even if their manufacturing can be problematic, their advantages outweigh the disadvantages and new generation large aircraft, such as Airbus A350XWB and Boeing 787, are mainly designed using a primary composite structure.

Notwithstanding the above, composites still present major drawbacks that should be overcome to expand their application not only in the aerospace field, but also the automotive, construction and wind energy sectors. At present, composites manufacturing is very expensive and due to their nature, they cannot be reshaped, making their repair and recycling almost impossible. A solution is to entitle composites to repair themselves, just like biological systems, so that they can restore their mechanical properties. This kind of materials are known as self-healing materials.

The main objective of this thesis is to characterize mechanically a modified dynamic fibre reinforced polymer (FRP) comparing it with a reference glass fibre reinforced polymer (GFRP) and assessing several functionalities of the material, such as mechanochromism, thermoforming or adhesion to evaluate its repairability and

reprocessability capabilities, which will make it outperform the current composite materials.

This thesis will be presented in accordance to the following scheme:

1. **State of the Art**

   Fundamentals and description of the main self-healing approaches and healing strategies, and self-healing materials additional functional properties.

2. **Processing and Manufacturing**

   Description of the materials and manufacturing processes used within the development of the thesis. Observation techniques (SEM, mainly) are also included in this chapter, as a visual assessment is important to complete a material's analysis. SEM is used throughout the thesis to evaluate the composite void volume fraction, fibres morphology and structural defects.

3. **Mechanical Characterization**

   Explanation of the fundamentals of the used experimental techniques (namely DMA, DSC and Mohr – Westphal balance) for the material's examination, as well as an overview of the experimental layout.

4. **Experimental Results**

   Presentation and interpretation of the experimental results, comparing a reference composite with the thesis subject self-healing material.

5. **Additional Functionalities**

   Evaluation of significant functional properties which the dynamic composite may show. Considering the research conducted at the IK4-CIDETEC Research Centre [50], experiments are realized to evaluate the material's reprocessability and repairability.

6. **Conclusions**

   Summary of the experimental results including the most remarkable differences, advantages and disadvantages of the assessed dynamic composite in comparison with the reference composite.

1 State of the Art

1.1 Smart Materials

Smart materials are materials which properties can be modified in a controlled way when an external stimulus is applied. These changes apply to their mechanical, thermal, optical or electromagnetic properties.

Inspired by living organisms, smart materials mirror the functionalities found in nature. If compared with the human body, it is observed that the host material must be endowed with sensors which process the received stimuli mimicking the nerves and actuators which adequately respond to the incoming signals imitating the muscles [1]. Furthermore, everything must be controlled by a data analysis system or brain which monitors the received signals, elaborates the acquired information and generates the proper reaction. Smartness describes the self-sensing and self-adaptability capacity.

Smart materials can be classified according to their working principle as active or passive materials. Active materials have the capacity to modify their properties under the application of an electric, thermal or magnetic field by transforming energy. Examples include piezoelectric materials (they generate a voltage when subjected to a mechanical stress and vice versa), shape memory alloys or polymers (these materials can be deformed and then returned to their original shape by heating) or magnetostrictive materials (they generate a magnetic field upon application of a stress).

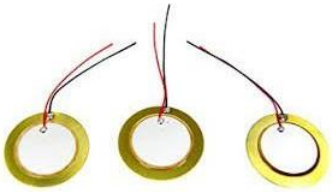

Figure 1.1.1. Active material: Piezoelectric Transducers

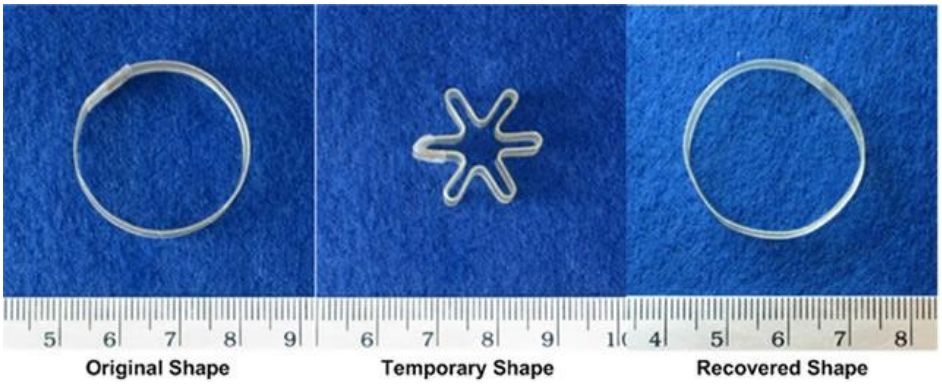

Figure 1.1.2. Active material: Shape Memory Polymer

Passive materials cannot transduce energy but are able to change one of its properties under a stimulus. Within this group fibre optics (light properties change when a strain is implemented), pH-sensitive materials (they change their colour when acidity varies) or chromogenic systems (they change their colour in response to a stimulus) are included.

Figure 1.1.3. Passive material: Fibre Optics

The versatility of smart materials makes them suitable to solve actual engineering problems, in addition to providing the opportunity to design new generation products. Some of the possible applications of smart materials are vibration control, lifetime monitoring, self-healing, damping aeroelastic stability or active and passive controls. [2]

1.2 Self-healing Materials

1.2.1 Basic Principles

Within smart materials, this thesis focuses on self-healing materials. Following the biomimetic approach, self-healing materials are materials which can retrieve a functionality which has been diminished due to a damage.

Traditionally, the main goal of materials development was to improve them by enhancing their properties and optimizing their manufacturing process. Although materials with extraordinary properties have been developed, even smallest defects are not avoidable. That leads to the need of periodical inspections and repairs which are highly time-consuming and expensive. Fibre-reinforced polymer composites (FRPCs) are especially critical because they can suffer extreme internal damage from low velocity impacts without any external indication. Thus, non-destruction inspection techniques are needed to check for any possible defect. When damage is found, no repair technique can be used as standard since composites undergo several failure modes, such as fibre breakage, fibre pull out, matrix micro-cracking, interface debonding or delamination.

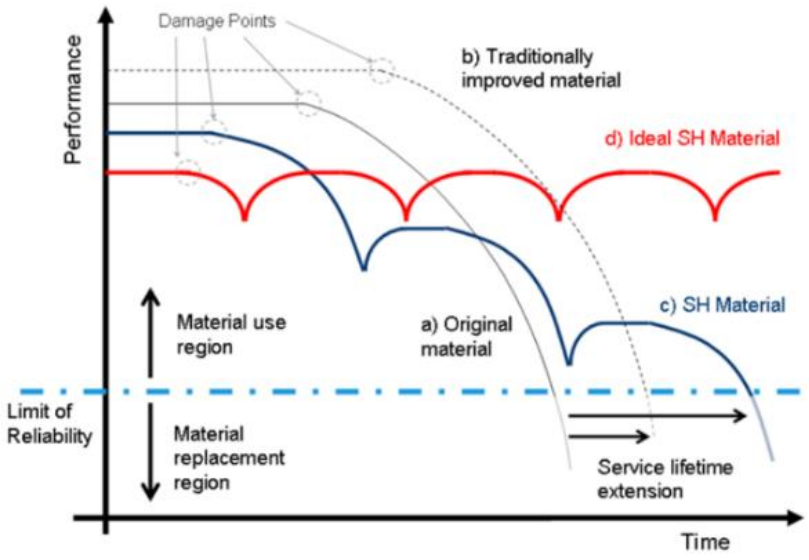

Figure 1.2.1. Damage management concept: traditional and self-healing materials [3]

Developing self-healing materials therefore means a change in the material research philosophy: from damage prevention to healing. That means from avoiding crack creation to making the repair intrinsic to the material. Ideally self-healing materials could recover periodically their performance, extending their lifetime to an unlimited extent, hence enhancing their reliability. [4]

For the time being, self-healing technology has not reached the required 'Technology Readiness Level' (TRL) to be applied on a large scale, but the prospect is that these materials will be economically beneficial in the long run due to their higher reliability and durability [5]. Its application is anticipated in almost every industry. So far, it is being developed mainly in the aerospace, automotive, biomedical, civil and energy industries. Focusing on aerospace industry, self-healing materials offer huge advantages since reliability and safety are critical aspects. Furthermore, its implementation in spacecrafts is interesting since space maintenance is extremely difficult and expensive. [4]

Self-healing concepts can be applied to different material classes, such as metals, ceramics and polymers. These materials have different intrinsic properties, but the general healing process can be defined regardless of the material.

Whenever a damage is caused on the material, a crack can be generated. To repair the defect, a healing agent triggered either by the damage itself or an external stimulus is activated. The agent acts in the damaged area either by physical or chemical interactions assuring the crack planes reconnection. Once the healing action is performed, the agent action vanishes resulting in the restoration of the material mechanical properties.

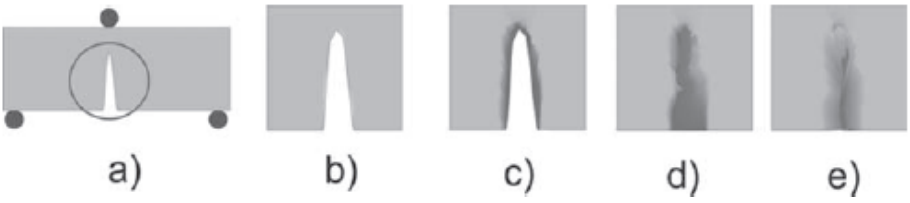

Figure 1.2.2. Basic healing process [6]

Self-healing polymers are the most developed self-healing materials, since their structure makes them relatively easy to be modified. Metals and ceramics are characterized by the fact that atoms in the solid phase form rigid three-dimensional structures, but still are gaining attention due to their promising features.

1.2.2 Classification

Current self-healing polymers can be sorted in two main groups depending on the need of an external trigger to initiate the healing process: non-autonomic and autonomic. Non-autonomic self-healing materials require an external stimulus, like heat or light. By contrast, autonomic materials use the own damage as starter of the healing action. [7]

A second way of categorising self-healing composites is represented by the healing strategy: extrinsic and intrinsic healing. [8]

Extrinsic healing techniques consist in the use of a healing agent placed in the matrix as a separate phase. The reservoir breaks when damage occurs releasing the healing agent. The agent occasionally can self-react, but generally a catalyst is needed, which can be dispersed in the matrix or directly combined with the healing agent. The main approaches are the use of capsuled-based structures, liquid-filled hollow fibres or a mesoporous network. Consistent with the biological simile, capsules act like cells while hollow fibres and mesoporous networks mimic the vascular and circulation systems in animals. [9]

Capsule-based self-healing materials incorporate microcapsules in which the healing agent is embedded. When a crack appears and breaks a capsule, the healing agent moves towards the defect and repairs it. The first successful attempt was developed by White *et al.* [11] which included polymeric microcapsules filled with a cross-linkable liquid oligomer placed into a low viscosity epoxy matrix containing Grubbs catalyst, which yield a 75% recovery in toughness in fracture tests. Since

then this strategy has been extensively researched due to its ease of implementation, potentially even for mass production. Consequently, different combinations of healing agents and catalysts, capsules sizes and encapsulation techniques have been developed.

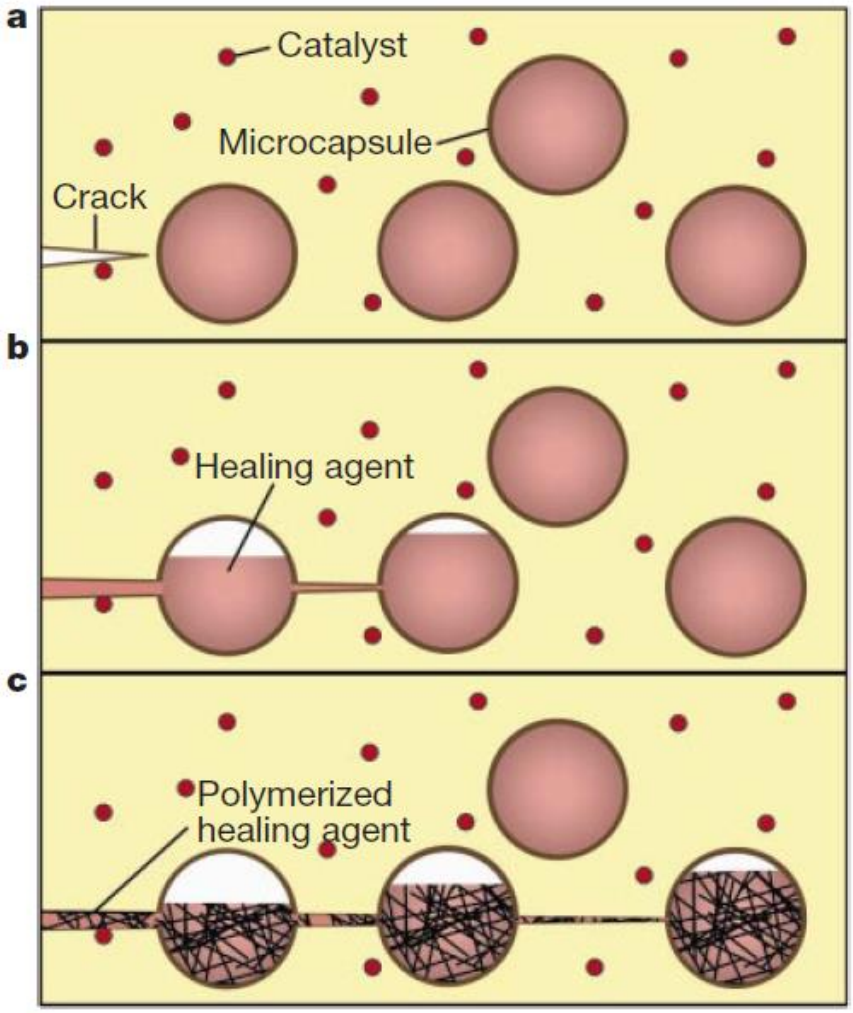

Figure 1.2.3. Capsule-based self-healing composite [11]

Changing the healing agent container, liquid-filled hollow fibres self-healing composites are obtained. Based on the previous research findings, Bond *et al.* [12] first showed an effective behaviour of this technique, obtaining a recovery of 97% in flexural strength and an easy way to trace the defects, since the used dye offered a proper damage visualization. The working principle is in line with the one of

microcapsules, but fibres offer the advantage of a better integration within an FRP and a larger potential recovery power, since the volume of healing agent is higher than the one contained within capsules. To obtain an effective healing action, it is necessary to optimize the number and spatial distribution of the hollow fibres.

Extending the 1D vascular concept of liquid-filled hollow fibres, 2D and 3D networks have also been developed. [13] Its invasiveness must be minimized so that its effect does not undermine the polymer mechanical properties. Therefore, its structure and the healing agent characteristics, such as fluidity and stability, should be carefully selected.

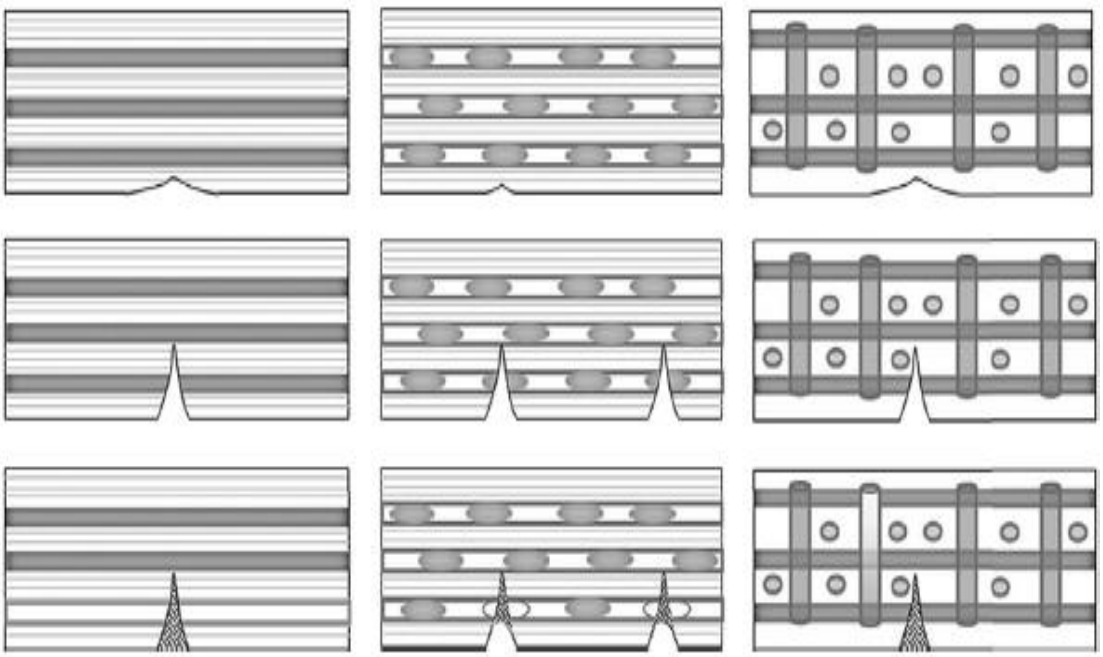

Figure 1.2.4. Vascular self-healing approaches [3]

Although at present none of these strategies have been applied on large scale, it is likely that the integration of extrinsic healing systems to existing materials will be more straightforward than intrinsic approaches. Yet they present some inconveniences such as the potential chemical incompatibility between the healing agent and the composite, which is itself inhomogeneous, the scarce design window to introduce the healing agent in the structure and the fact that the healing action is

linked to the healing agent presence leads to singular healing events which magnitude is also limited by the healing agent quantity [5].

Intrinsic healing is based on the own healing capability of the matrix material. When subjected to an external stimulus or an internal damage, the material can repair itself through the reversibility of chemical or physical bonding in the matrix phase. No external agents are needed, so beforehand they have the advantage that multiple healing events can take place. The most significant strategies are based on reversible covalent bonds, thermoreversible physical interactions and supramolecular chemistry. [10]

Reversible covalent bonds are the basis of the self-healing behaviour of the fibre-reinforced composite used within the development of this thesis. Thus, a detailed explanation of the different investigated mechanisms is given down under the heading “Dynamic Covalent Chemistry”.

Self-healing behaviour based on reversible physical interactions involves the use of ionomeric polymers. Ionomers are polymer groups containing ionic species, such as metal salts, which form reversible clusters inducing mobility within the polymeric structure [14]. It has been extensively applied to study high velocity ballistic impacts [15], which could lead to its application in military aircraft, but also the general effect of cluster plasticisation on the self-healing behaviour [16].

Supramolecular chemistry works with interactions which are neither covalent nor physical, including π-π stacking, metal coordination and hydrogen bonding, being the latter the most researched approach. It seems to be an encouraging way to induce self-healing behaviour due to their low energy. Low molar mass monomers are held together by these interactions to obtain additional features, such as switchable environment-dependent properties or improved processing. The main challenge is finding the balance between having a reversible polymer and the association constant, since having a high reversibility can also be a synonym of smaller assemblies and poor mechanical properties. [17]

1.3 Self-Healing Fibre-Reinforced Composites

1.3.1 Current Fibre-Reinforced Composites

Thermosetting materials are cross-linked polymers formed by an irreversible exothermic chemical reaction. The formed covalent polymer network is insoluble and mostly inert, which makes it almost impossible to recycle or reprocess once it has been formed. Their application cannot be at present substituted by thermoplastics, so it has become of critical importance to find a method to efficiently recycle this kind of polymers.

In the case of aerospace industry, the focus is made on obtaining reprocessable, repairable and recyclable fibre-reinforced thermoset composites using epoxy resins as matrix. Epoxy resins are thermosetting low-molecular-weight pre-polymers containing more than one epoxide group which properties depend on the type of epoxy resins and curation agents used during their manufacturing. The epoxide group is a three-membered ring formed by an oxygen and two carbons. Most of the commercially available epoxy resins are oligomers of diglycydil ether of bisphenol A (DGEBA) which react with a hardener [28]. DGEBA is extended due to its good mechanical properties and high glass transition temperature (T_g).

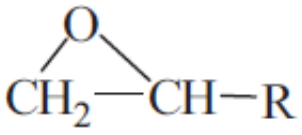

Figure 1.3.1. Epoxide group [21]

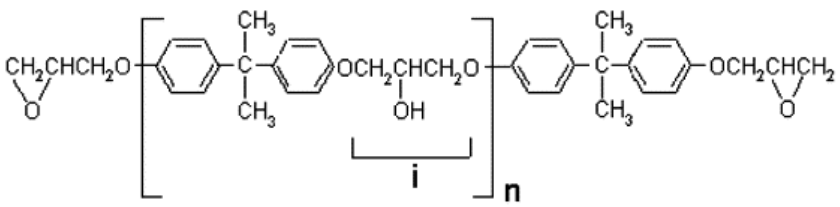

Figure 1.3.2. DGEBA resin [33]

Among the thermosetting resins, epoxy resins are of interest due to their magnificent chemical and mechanical properties, heat, electrical and water resistance, adhesion strength, low cure shrinkage, long shelf lives, availability and relatively cheap price. These outstanding characteristics have led to their extensive use as electronics encapsulation, sealants, coating, adhesives and of course matrices for fibre-reinforced composites. [20][21]

	Thermosetting resins				
Property	**Poly-ester**	**Epoxy**	**Phenolic**	**Bismale-imide**	**Poly-imide**
Processability	Good	Good	Fair	Good	Fair to difficult
Mechanical properties	Fair	Excellent	Fair	Good	Good
Heat resistance	82 ºC	93 ºC	176 ºC	176 ºC	260 – 315 ºC
Price range	Low to medium	Low to medium	Low to medium	Low to medium	High
Delamination resistance	Fair	Good	Good	Good	Good
Toughness	Poor	Fair to good	Poor	Fair	Fair

Table 1.3.1. Comparison of properties for general thermoset matrices [32]

Although epoxy resins have been presented as outstanding materials, they still present some major drawbacks in their use as structural materials such as their inherent brittleness and rigidity, which make them prone to delamination and induce a poor impact resistance. To improve their physical properties, several paths can be followed. Within the aerospace industry, as well as toughening the matrix using a solid solution with a more ductile polymer, precipitating an elastomeric second phase or developing of interpenetrating polymer networks, fibres have been chosen as toughening agents. [31]

The ever-increasing use of high-performance fibre composites within aerospace applications is driven by the improvements in specific (property/density) strength and stiffness in comparison with metallic alloys. The main advantages are summarized in the following table.

Weight Saving	Higher range Lower fuel cost Increased payload Rising manoeuvrability
Lower Acquisition Cost	Lower manufacturing cost Better “fly-to-buy” ratio Lower assembly costs
Higher Performance	Improved aerodynamics Good aeroelastic properties Higher temperature capability Better damage tolerance Lower detectability
Lower Maintenance Cost	Better fatigue and corrosion resistance Better mechanical damage resistance

Table 1.3.2. Advantages related to the use of fibre composites [31]

Reinforcement fibres are generally circular cross section tubes made of low atomic number elements, including carbon, boron, aluminium and silicon, which can be formed into stiff, low density materials. These materials are manufactured in the form of fibres due to their strong directional interatomic bonds. This entails that

they cannot relieve stress concentration by plastic flow and are notably weakened by defects, especially when they are superficial. According to Weibull statistics, the probability of a defect existing per unit length is an inverse function of the material volume; hence as a fibre presents a low volume, it is less susceptible to damage. [31]

Within this thesis the focus is made on glass and carbon fibres, as their use is widely extended in the aerospace industry due to their high strength-to-weight and stiffness-to-weight ratios. In Table 1.3.3 and Table 1.3.4 the properties of the main commercially glass and carbon fibres are shown.

	Glass Fibres	
Property	*E-Electrical*	*S-High Strength*
Specific gravity	2,6	2,5
Tensile modulus (GPa)	73	87
Tensile strength (MPa)	3445	4890
Ultimate strain (%)	3,5	4,5
Thermal expansion ($x10^{-6}\ mm^{-1}K^{-1}$)	5	5,6

Table 1.3.3. Properties of the major types of glass fibres [31]

	Carbon Fibres		
Property	*HM Type I*	*HS Type II*	*IM Type III*
Specific gravity	1,9	1,8	1,8
Tensile modulus (GPa)	276 – 380	228 – 241	296
Tensile strength (MPa)	2415 – 2555	3105 – 4555	4800
Ultimate strain (%)	0,6 – 0,7	1,3 – 1,8	2,0
Thermal expansion ($x10^{-6}\ mm^{-1}K^{-1}$)	- 0,7	- 0,5	N/A
Thermal conductivity ($Wm^{-1}K^{-1}$)	64 – 70	8,1 – 9,3	N/A
Electrical resistivity (μΩm)	9 – 10	15 – 18	N/A

Table 1.3.4. Properties of the major types of carbon fibres [31]

Glass fibre-reinforced composites are used due to the simplicity and low cost of glass fibres manufacturing from the molten state, their strength and their chemical inertness, which helps corrosion inhibition. In the aerospace industry glass fibre composites are used in the secondary aircraft structure, where no heavy loads are applied such as window surrounds, storage compartments, wing fairings and wing fixed trailing edge panels. [32]

Carbon fibre-reinforced polymers have the highest specific modulus and specific strength of all reinforcing fibre materials, so their application is highly extended in the aerospace industry. Carbon fibres can retain these properties even at high temperatures and at room temperature they do not chemically react with most of solvents, acids or bases. [54]

Present solutions for the disposal of fibre-reinforced polymers are heavily polluting, highly energy consuming and generate a significant material waste. Landfill is the current cheapest option, but also the least preferred option under the European Union's Waste Framework Directive, which means that it is prone to be prohibited at least on European territory as environmental legislation is becoming more and more restrictive. Other recycling techniques include mechanical processes such as grinding, pyrolysis and solvolysis. Pyrolysis is commonly used in the chemical industry, so its extension as an industrial scale process was the most straightforward. During the process, fibres are contaminated and degraded at high temperature, so chemical treatments have been thought as a reasonable alternative to pyrolysis. Solvolysis techniques can be extensively tuned using different solvents, temperature and pressure levels, and catalysts depending on the material, but still they are not commercially exploited. [22]

1.3.2 Dynamic Covalent Chemistry

Dynamic Covalent Chemistry (DCC) consists in extending the dynamic features found in supramolecular chemistry to molecular chemistry using reversible covalent bonds. DCC covers dynamers, covalent adaptable networks (CANs) and vitrimers.

The first step in the development of dynamic components are dynamers, which are *"constitutional dynamic polymers of either supramolecular or molecular nature whose monomeric components are linked through reversible connections, which can be either non-covalent interaction or reversible covalent bonds"*, according to Skene and Lehn [29]. They can respond to physical and chemical stimuli by establishing reversible networks.

The most studied dynamic covalent reaction within the self-healing materials field is the Diels-Alder/retro-Diels-Alder (DA-rDA) reaction for cross-linking linear polymers. The reversible bond was first reported in the late 1960s, but first implemented by Chen *et al.* [36] using furan-maleimide polymers. It has also being used to create a thermally activated self-healing carbon fibre composite including a bis-maleimide tetrafuran which presented almost a 100% strength recovery [7] [37].

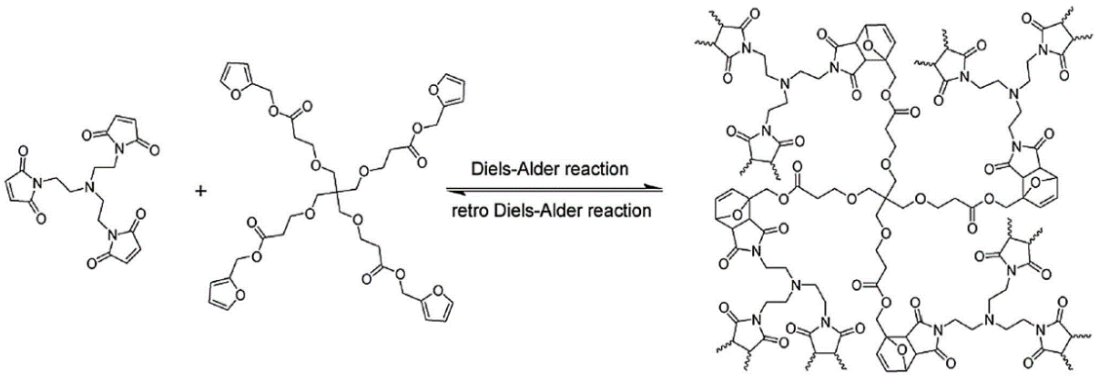

Figure 1.3.3. Furan and maleimide bases polymers using reversible DA reactions [38]

CANs refer to the networks in which a cross-linked structure is present due to the number and topology of reversible covalent bonds and can be modified under an applied stimulus. The network does not suffer any degradation; hence, it maintains the initial bond density while the material responds to the stimulus. CANs can be manufactured from monomers connected through reversible linkages, as part of the fabrication process or by using proper functional groups [30].

CANs can be classified according to their exchange mechanism: dissociative and associative networks. Both mechanisms are schemed in Figure 1.3.4.

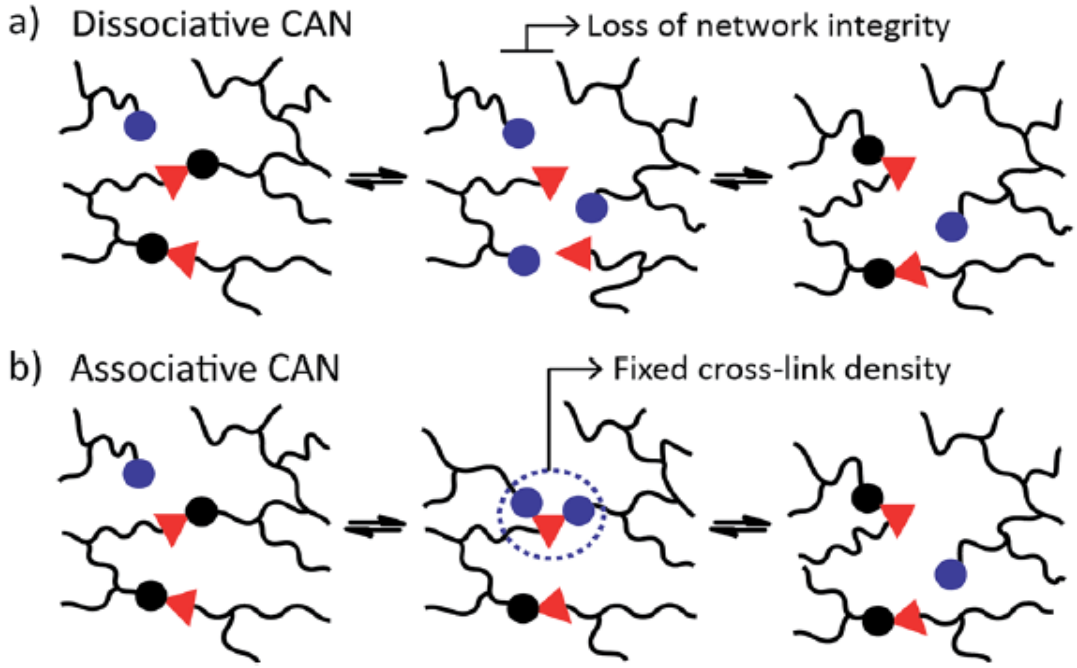

Figure 1.3.4. CANs Classification [34]

In dissociative networks, bonds are first broken and then reformed, which make them momentarily lose their integrity. The most common dissociative networks are again based on DA reactions between furans and maleimides. Cross-linking becomes a reversible reaction upon heating leading to a fast reorganization of the network and a significant viscosity drop. Upon cooling, the network recovers its stiffness and insolubility properties, allowing thermal reprocessing and healing of the material. [34]

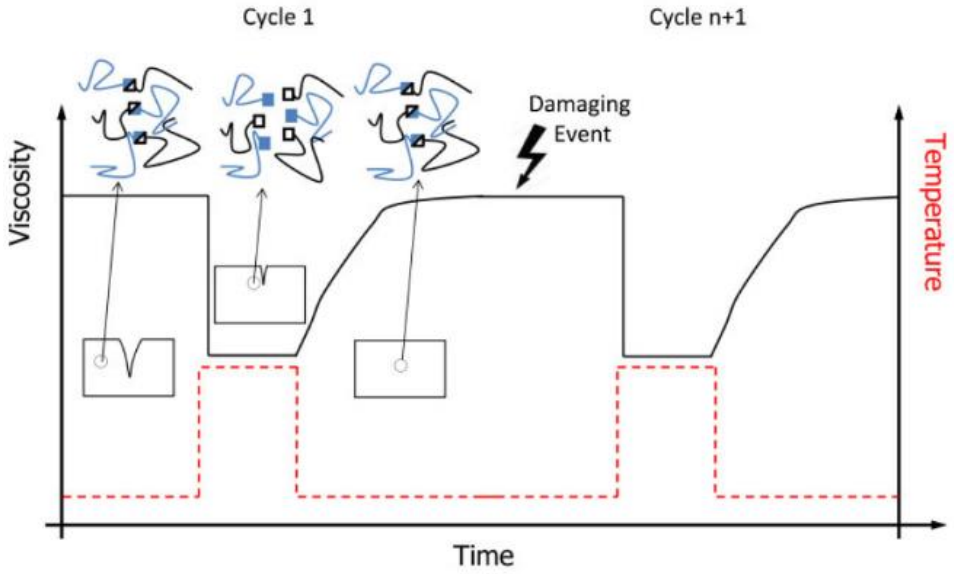

Figure 1.3.5. Viscosity vs temperature within dissociative networks [3]

Associate networks main characteristic is their fixed cross-link density; hence, they are both dynamic and permanent, since a bond is only broken after a new covalent bond has been formed. Several networks were reported during the first decade of the 21st century, but it was not until Leibler *et al.* [39] found in 2011 a network formed by a transesterification catalyst and an epoxy/acid or epoxy/anhydride that these polymers showed relevant functionalities. These networks have a gradual viscosity reduction upon heating, such as vitreous silica. Honouring this feature, these materials were named vitrimers.

Vitrimers behaviour is mainly dependent on temperature and their covalent bond structure. At high temperatures, viscosity is driven by chemical change reactions; thus, viscosity decreases following the Arrhenius law, unlike thermoplastics and dissociative CANs which are ruled by the Williams-Landel-Ferry model (WLF). Until degradation temperature range is reached, vitrimers maintain their integrity, that meaning that they do not dissolve in chemically inert solvents.

Vitrimers viscoelastic behaviour can be defined using two transition temperatures: glass-transition temperature (T_g) and freezing transition temperature (T_v).

T_g is one of most important thermophysical properties of polymers and its meaning is equivalent to the melting point of non-amorphous materials. It divides the glassy, hard and brittle, and the rubbery and soft states and therefore is correlated to molecular motion.

T_v depends on the cross-linking exchange reactions and marks the transition between viscoelastic solid and viscoelastic liquid, as the network begins to flow (the timescale of bond exchange reactions is lower than the timescale of material formation). It is hereby established that the temperature coincides with the point in which a viscosity of 10^{12} Pa·s is reached.

Both temperature values need to be considered when designing the polymer, so several parameters are used to control them, such as exchange reaction kinetics, intrinsic rigidity of monomers or cross-linking density. [35]

1.3.3 Dynamic Sulphur Chemistry

Among the chemical bonds prone to be used to manufacture dynamic polymers, sulphur-containing compounds have been extensively researched, especially networks including thiol/disulphide exchange and disulphide exchange. Disulphide bonds are weaker than carbon bonds, facilitating the mechanical scission [45].

Thiol/disulphide exchange mechanism is based on the nucleophilic displacement of a thiolate anion from the disulphide when attacked by another thiolate anion. It is highly influenced by changes in pH, which is an advantage when using a pH trigger as catalyst, but also a disadvantage when polymers are subjected to aerial oxidation or work in acidic conditions, as no enough reactive thiolates are present, weakening the network dynamic properties. [26]

One successful investigation was presented by Wei *et al.* [42]. Due to the mild transformation conditions of the thiol/disulphide a reversible ion gel with high

toughness, high conductivity and recyclability was produced. The gel could be six times reshaped under relative low values of temperature (60 °C) and pressure (0.04 MPa) with no relevant performance loss and without the need of an external agent.

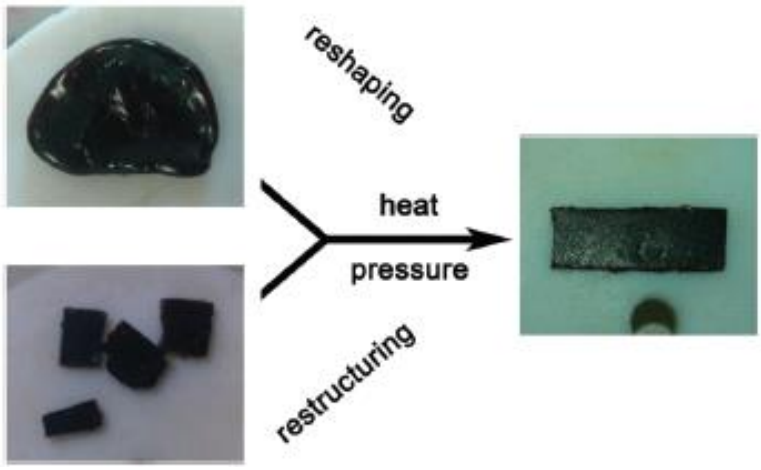

Figure 1.3.6. Recyclable ion gel using thiol/disulphide exchange mechanism [42]

Disulphides respond at room temperature, as a reasonable level of bond strength is achieved. It usually needs to be triggered by chemicals, heat or UV light, but some autonomous examples have also been reported. Disulphide chemistry owes its versatility to the reversibility of the S-S bond cleavage which generates sulphenyl radicals.

Being recyclability one of the main reasons for the use of dynamic covalently bound materials, Johnson *et al.* [43] presented a disulphide-containing epoxy which degradation kinetics can be controlled by temperature, concentration of disulphide groups and monomer stoichiometry. This study also proved that disulphide-containing epoxy thermosets are stable under severe conditions.

Takahashi *et al.* [41] reported the development of degradable epoxy resins using disulphide linkages synthetized from bis(4-glycidyloxyphenyl) disulphide and several diamines. While mechanical properties were comparable to the ones of the reference resin, the dynamic epoxy resins showed the ability to fragment rapidly, allowing the resin recyclability.

Also, vitrimer materials containing disulphide bonds have been researched by Zhou *et al.* [46], which synthesized BDSER by the reaction of a difunctional epoxy monomer with 4,4'-disulfanediyldianiline (4-AFD). The introduction of more disulphide bonds was expected to increase the repair capacity of the matrix. The material showed excellent mechanical and thermodynamic materials, as well as good reprocessability, self-healing, degradability, low activation energy and fast relaxation times.

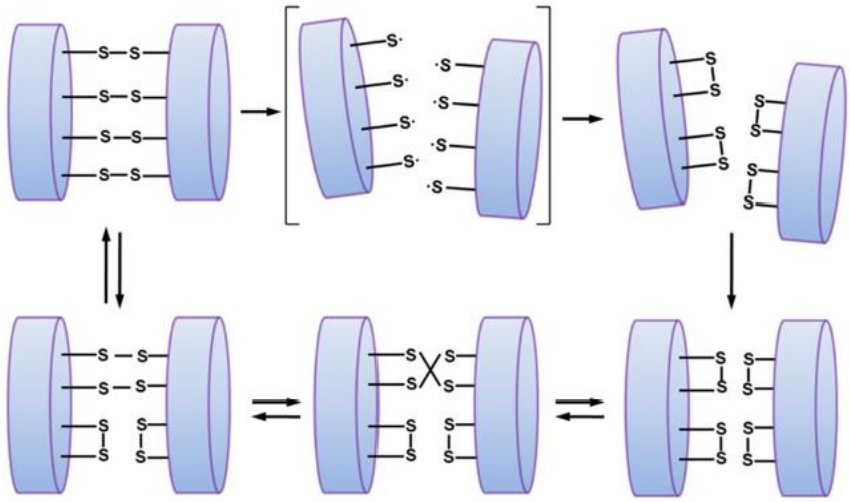

Figure 1.3.7. Representation of network healing through disulphide exchange reactions [27]

To improve the bond interchange rates and lower the bond strength, disulphide bonds can be replaced with tetrasulphides, as the stability of the S-S bridge is reduced when a higher number of sulphur atoms is present. Abdolah Zadeh *et al.* [47] developed a dual organic-inorganic crosslinked network by sol-gel process. Tetrasulphide content revealed to have an important effect on healing temperature and polymer structure when repairing a crack. Dynamic exchanges induce the flow of the crosslinked network while irreversible linkages keep the mechanical integrity of the polymer. The industrial implementation of this innovative technology depends on the long-term performance of the healed material, so as well as the dependence of the material on the dynamic covalent bonds, the effect of curing time was studied [44]. It was found that increasing the curing time improved the material

stability and mechanical properties, but was not related to the healing efficiency, as the number of available S-S bonds does not change.

Within disulphide exchange mechanisms, the most promising is the aromatic disulphide exchange. Little was known regarding the reaction mechanism and electronic structure allowing the dynamic network behaviour, so a theoretical approach was developed by Matxain *et al.* [23]. The scope of this study was achieving a better understanding of the reaction at molecular level, so that self-healing behaviour implementation could be improved. Several compounds where derived from diphenyl disulphide to analyse the effects of substitution on the chemistry of the process. The research concluded that the chemical structure is significant to improve self-healing materials properties and deduced that the main reaction mechanism of the aromatic disulphide exchange is a radical mediated mechanism.

Self-healing behaviour depends on the disulphide cleavage, hydrogen bond between polymer chains and the capability to overcome the reaction barrier at room temperature. Bond dissociation energy is lowered when *para*-substituting phenyl groups with ring-activating moieties, making the aromatic ring more stable and promoting bond division. Hydrogen bonding keeps the disulphide chains close, that meaning that they are fundamental for the polymer structure. [23][45]

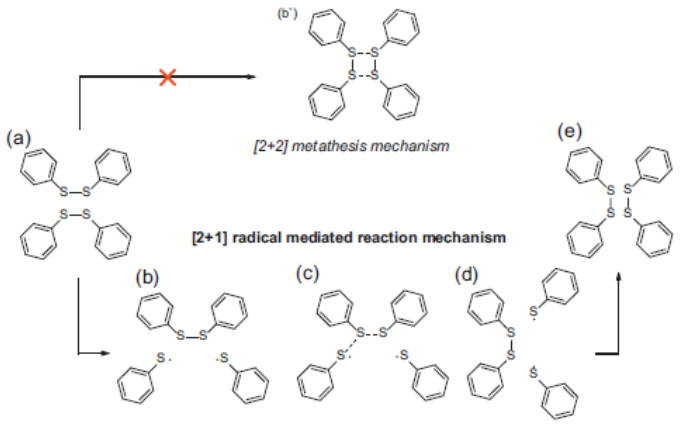

Figure 1.3.8. Schematic representation of the aromatic disulphide exchange reaction mechanisms [23]

Aromatic disulphide exchange has been used to modify polyurethanes, poly(urea-urethanes), polyimides and epoxy resins.

Rekondo *et al.* [49] reported self-healing poly(urea-urethane) elastomers with 97% healing efficiency in tensile strength tests at room temperature after being cut in half with a razor blade, just by contact between the halves. The significant healing efficiency has been attributed to the aromatic disulphide content, as well as the presence of two urea groups, capable of forming a quadruple hydrogen bond. Its easy preparation from commercially available materials makes the industrial use of these kind of elastomers promising in the short run.

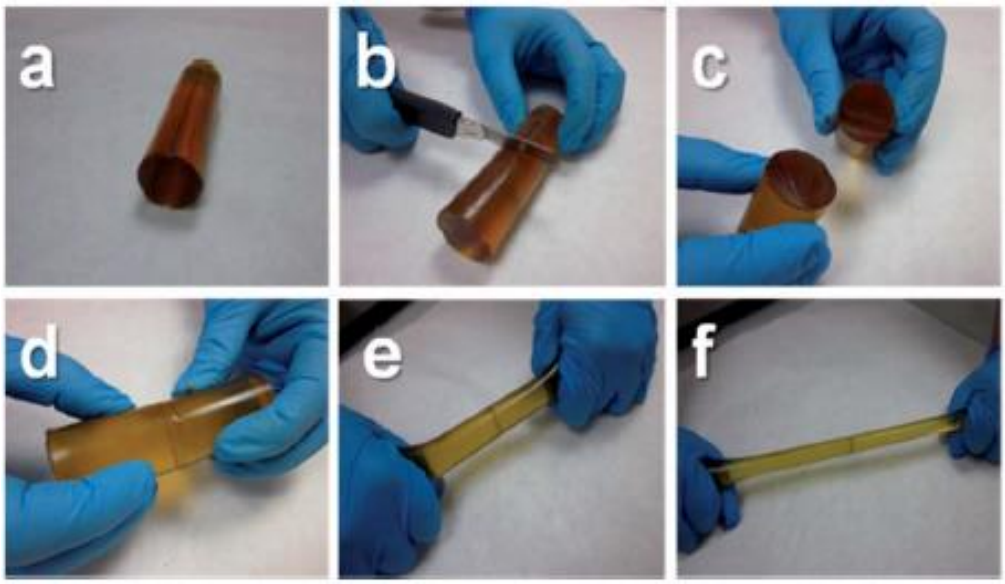

Figure 1.3.9. Sequence of the healing event in a PUU elastomer [49]

Moreover, this research group [50] demonstrated that poly(urea-urethane) elastomers based on aromatic disulphides can also be manufactured for reprocessing by applying temperature and pressure on a mould. The obtained polymer shows the same mechanical properties as the pristine sample. Reprocessing was achieved using both a cylinder sample and powder, which offers the advantage of using the cured resin directly as starting material. Although mechanical tests show that aromatic disulphides can rearrange the material at room temperature, it is necessary to carry out rheology experiments to study the stress

relaxation. Rheology tests showed that the polymer needs to be treated above 100 °C to completely relax.

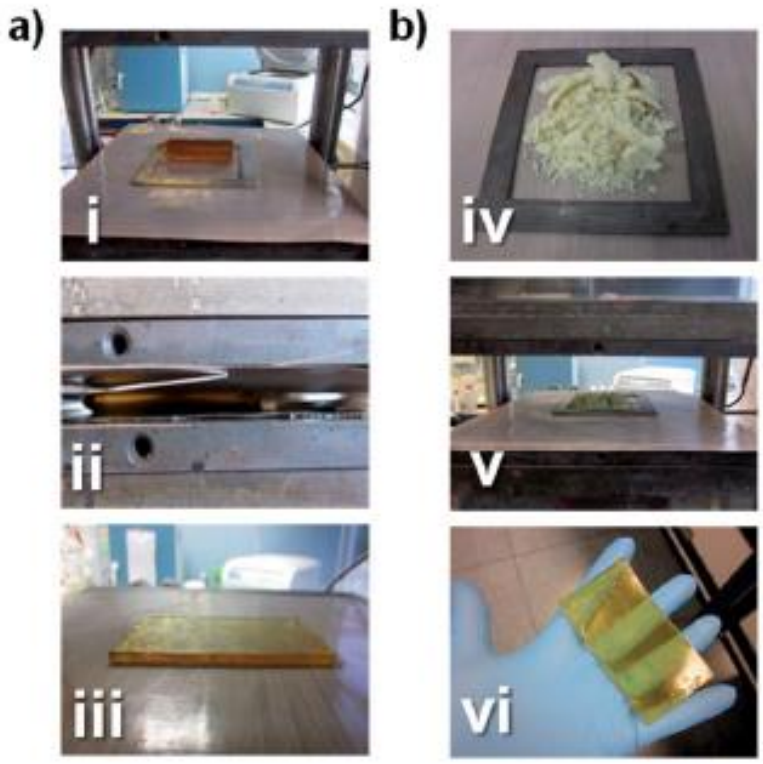

Figure 1.3.10. Reprocessing of a PUU sample in the form of a cylinder (a) and from powder (b) [50]

Grande *et al.* [24] deepened in the study of poly(urea-urethanes) examining the function of the hydrogen bonds and disulphide content; thus, the polymer structure. Different samples were prepared maintaining the number of disulphide linkages but changing the crosslinking density. The change in the network was proved to be directly correlated to the mechanical properties and healing efficiency.

Also based on the reversible exchange of aromatic disulphides, Ruiz de Luzuriaga *et al.* [40] have developed an epoxy vitrimer system which shows the following interesting features: synthesis from available starting materials, easy reprocessability, repairability and recyclability. To analyse the advantageous properties of the new system, a comparison between DGEBA with 4-aminophenyl disulphide (4-AFD) as dynamic hardener and DGEBA with diethyltoluenediamine

(DETDA) as reference hardener was made. Mixing of the resin prepolymer and the corresponding hardener was made at 60 – 80 °C followed by a curing process at higher temperatures.

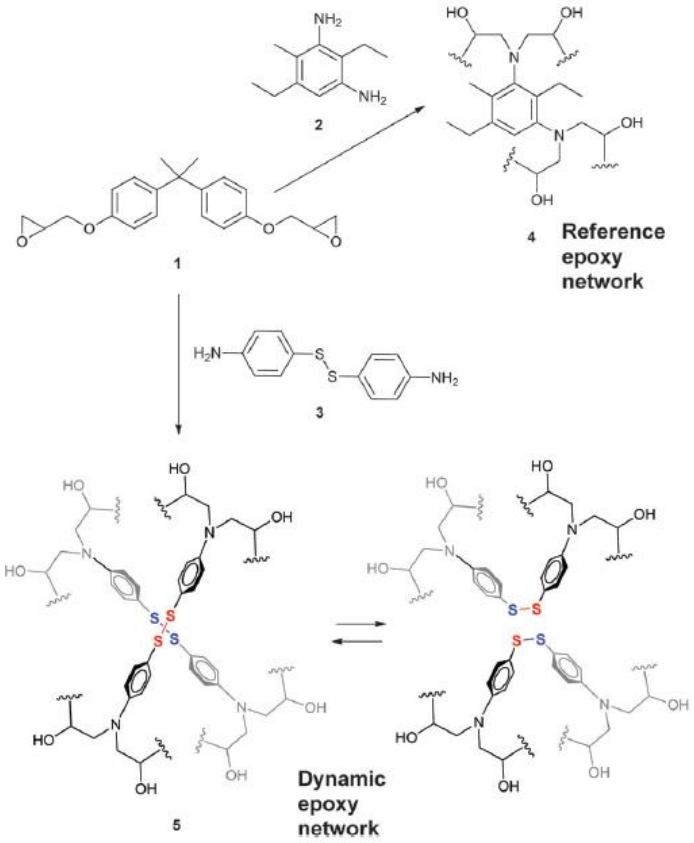

Figure 1.3.11. Structure of the reference and dynamic epoxy networks

Thermomechanical analysis was carried out to determine the T_g, inferior degradation temperature (T_d), storage modulus (E'), stress and strain at break. T_g values are comparable using both differential scanning calorimetry (DSC) and dynamic mechanical analysis (DMA). Thermogravimetric analysis (TGA) showed a difference in thermal stability, as the dynamic network has a lower T_d, which is likely to be linked to the presence of the disulphide bond. E' values are analogous in both networks regardless the test temperature. Tensile tests revealed a similar behaviour of the thermosets, which means that mechanical properties are not affected by the dynamic hardener below T_g.

	$T_{g\ (DSC)}$ [°C]	$T_{g\ (DMA)}$ [°C]	T_d [°C]	E' (25 °C) [GPa]	E' (150 °C) [GPa]	Stress [MPa]	Strain [%]
Reference network	127	130	350	2,5	20	81	7,3
Dynamic network	130	130	300	2,6	20	88	7,1

Table 1.3.5. Thermal and mechanical properties of both reference and dynamic epoxy networks [40]

Following the usual thermomechanical tests, dynamic properties were assessed. First, stress relaxation was considered. The time and temperature dependent relaxation modulus of the dynamic epoxy resin were tested by DMA. The obtained results showed that complete relaxation and flow occur when reaching a temperature higher than T_g. Relaxation times were found using the Maxwell's model for viscoelastic fluids and ranged from 3 hours at 130 °C to 20 seconds at 200 °C. To prove that the dynamic epoxy network presents a vitrimer behaviour, it is necessary to determine T_v. Fitting the relaxation time as a function dependent on temperature following the Arrhenius's law, T_v was extrapolated.

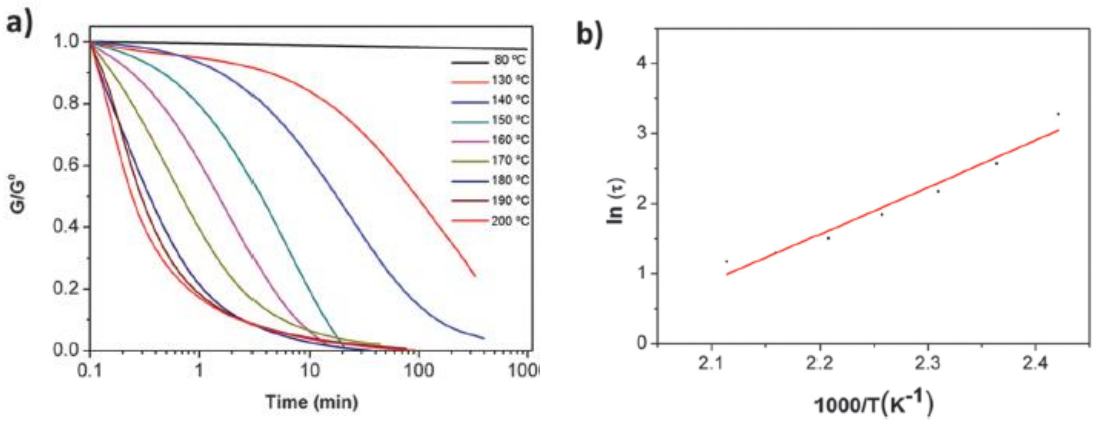

Figure 1.3.12. Normalized stress relaxation curves of dynamic epoxy network (a) and fitting of relaxation times (b)

After obtaining the reference vitrimer temperatures, reprocessability, repairability and recyclability of the material was tested. Three different experiments were carried out.

The first one consisted in processing two samples, one of each epoxy resin, in a hot press at 200 °C and 100 bar for 5 minutes. The reference epoxy led to a powder state material, while the dynamic epoxy created a new sample in the form of a film. Its mechanical properties were identical to the ones showed by the original sample.

The second test involved the ability of the dynamic network to self-repair. A small superficial scratch was made on two samples and heat and pressure were applied. The reference epoxy showed no change, but the dynamic epoxy could be repaired when the temperature reached a value above T_g.

The final test was planned to evaluate the material recyclability. Two resin samples were grinded and then compacted into a mould in which heat and pressure were applied. The reference epoxy resin could not be recovered, but the dynamic sample showed perfect visual appearance and its mechanical properties were like the ones of the pristine sample.

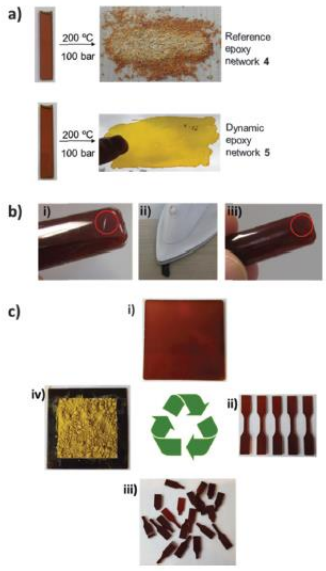

Figure 1.3.13. Reprocessing experiments to characterize the dynamic epoxy network [50]

Following the work of Ruiz de Luzuriaga *et al.* [40], Paolillo [48] completely characterized the behaviour of an epoxy resin at Politecnico di Milano, which will be used within the development of this thesis. DGEBA and 4-AFD will be used as resin prepolymer and hardener of the dynamic epoxy and DGEBA with 4,4'-ethylenedianiline will constitute the reference epoxy to manufacture both the dynamic and reference composites which will be analysed.

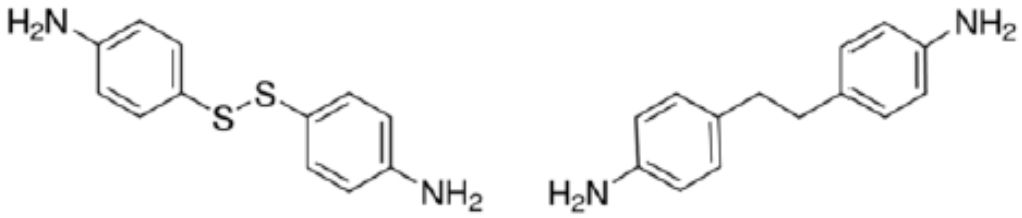

Figure 1.3.14. 4-AFD (left) and 4,4'-ethylenedianiline (right) [48]

Few examples of FRPs containing reversible polymer networks have been yet researched. The dynamic behaviour is usually induced into the polymer matrix using a hardener which generally does not generate any additional features within the polymer. Again Ruiz de Luzuriaga *et al.* [25] reported that the previously described 4-AFD, used as dynamic hardener for the generation of dynamic epoxy networks or vitrimers, can induce a mechanochromic functionality within the polymeric network. This group developed a dynamic epoxy resin based on reversible aromatic disulphide crosslinks (*p*-EPO), which showed a green coloration when machined or hit which disappeared spontaneously after several hours. To understand which chemical species are inducing this functionality and its time dependency an additional epoxy network was studied (*o*-EPO) including 2-AFD as hardener.

p-EPO showed green coloration when hit and grounded to power, that meaning, when broken. The colour disappeared gradually after 24 hours at room temperature. To analyse the temperature dependency a sample was placed into an oven at 150 °C and another in a freezer at -20 °C. The oven sample lost its green

coloration within 30 seconds, while the frozen one maintained the colour for days. A suitable explanation is the direct dependence between temperature and chain mobility.

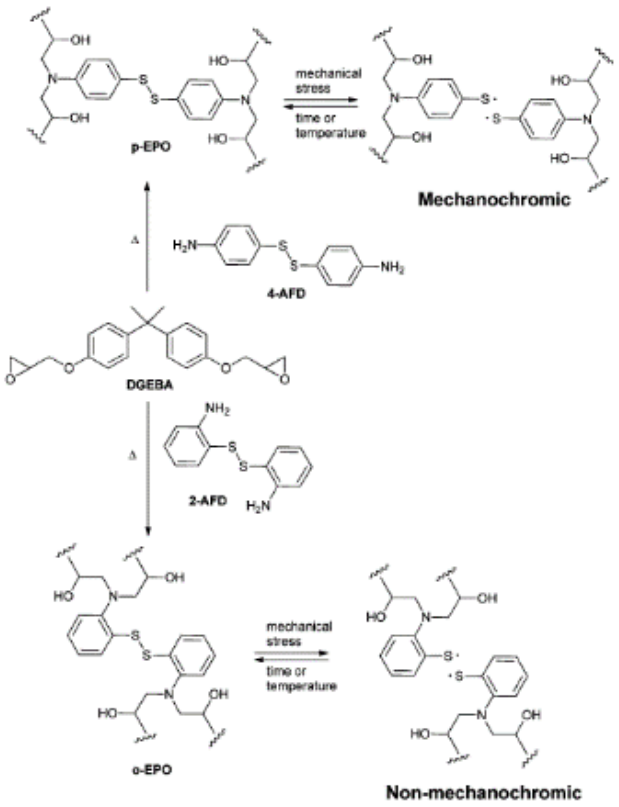

Figure 1.3.15. Synthetic procedure and chemical structure of the p-EPO and o-EPO [25]

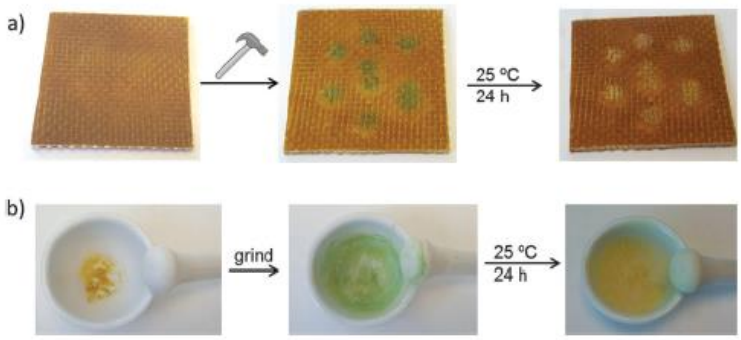

Figure 1.3.16. Hit and grounded *p*-EPO simples [25]

o-EPO samples were subjected to the same mechanical tests, but no green coloration appeared. 4-AFD and 2-AFD are isomers which only difference is the relative position of the disulphide and the amino substituents, so its different behaviour seemed surprising, but highlighted the important of the chemical structure.

Mechanochromism is a significant functionality since it can be used to detect stress, strain and deformation, as well as damage, which is especially useful in the evaluation of FRPs. [26]

As well as FRPs monitoring, composites manufacturing processes can highly benefit when introducing the previously described dynamic epoxies. Currently, the epoxy matrix is partially cured before the lay-up of the composite, so that fibres are maintained within the matrix and enough functional groups are present to complete the curing of the thermoset. Since the matrix has not reached its final state, it has a limited shelf-life (in which it must be refrigerated) and out-life before it loses its ability to self-adhere or adhere to the tool. If dynamic networks were introduced, these disadvantages could be overcome, as this group reported that a compacted multilayer composite was obtained when laying up and hot pressing eight single enduring prepreg sheets using the dynamic epoxy, while no attachment was achieved when using regular prepregs.

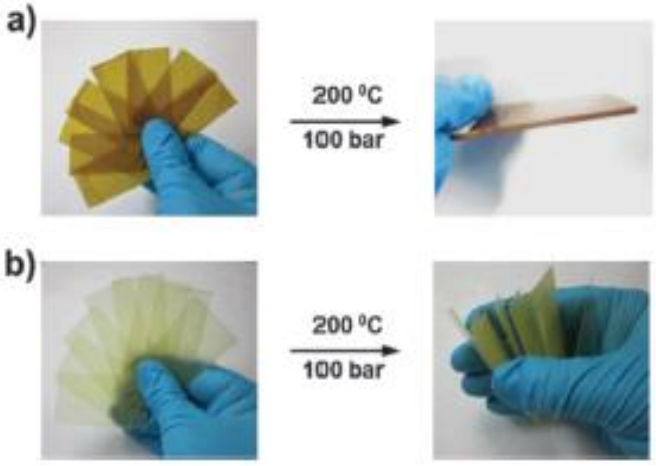

Figure 1.3.17. Composite manufacturing using dynamic epoxy prepregs (a) and reference epoxy prepregs (b)

Extending the reshaping capability of the dynamic epoxy, thermoforming can be introduced, which is the deformation of the composite even after curing. Actual techniques to manufacture 3D composites are extremely complex or even impossible when using conventional epoxy composites, while thermoforming offers the possibility to produce 3D composites from 2D laminates. Thermoforming was analysed using a sheet of multi-layered dynamic CFRP using resin transfer moulding (RTM) which was then placed in a preheated zig-zag mould and processed in a hot press. After cooling, the desired shape was obtained. When using a regular epoxy, the used specimen could not withstand the process.

Figure 1.3.18. Thermoprocessing of a cured composite laminate [50]

Repairing composites requires at present time special techniques and skilled workers, therefore more automated maintenance methods need to be created.

Within the most common failures in multilayer composites, delamination is found. This problem could be solved by the self-adhesion capability of dynamic epoxy resins. Several samples where cut from a CFRP sheet (ISO 14130) manufactured from prepregs and then delamination was induced. Then heat and pressure were applied, and delamination disappeared. Subjecting the samples to interlaminar shear strength tests (ILSS), it was shown that mechanical properties were approximately recovered.

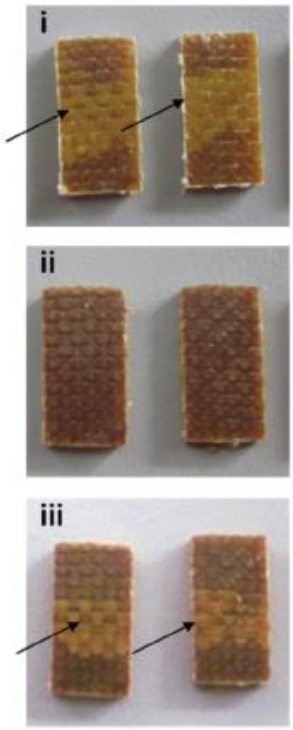

Figure 1.3.19. Samples of FRPs subjected to delamination (i) First ILSS (ii) Under heat and pressure (iii) Second ILSS test

Finally, both mechanical and chemical recycling have been assessed. Mechanical recycling was achieved by grinding the CFRP and compressing the obtained powder in a mould. As reinforcement fibres lose its form, mechanical performance cannot be as high as the one obtained with the original material, so it could not be used as structural material.

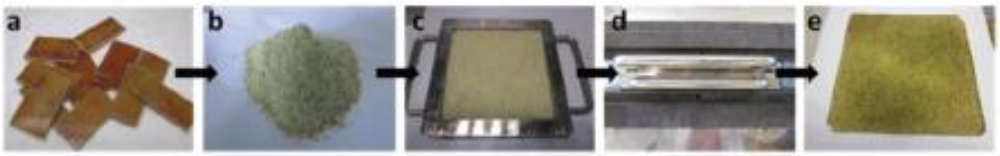

Figure 1.3.20. Mechanical recycling of a CFRP [50]

Dynamic epoxy showed a good resistance to several chemical substances, but the reversible nature of the crosslinks allows the network to be dissolved in the presence of a thiol, following the thiol/disulphide exchange mechanism. Introducing

a sample in a solution of 2-mercaptoethanol in DMF, after 24 hours under vacuum in an oven at 100 °C, the reinforcement fibres could be recovered undamaged after matrix dissolution.

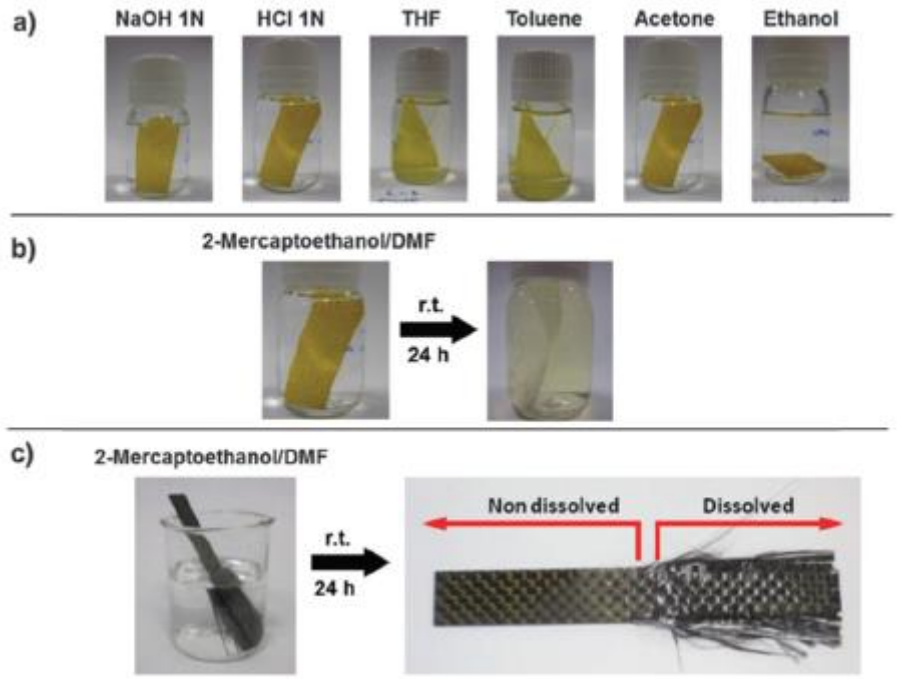

Figure 1.3.21. Behaviour of FRPs under the effect of several chemical substances [50]

1.4 Self-healing Performance Evaluation

Self-healing processes include both structure and functionality restoration. The first step in assessing self-healing performance consists on the observation of the structure recovery. Some of the techniques applied for the optical characterization involve the use of optimal microscope, laser microscope, scanning electron microscope (SEM) and atomic force microscope (AFM). [18]

With a view to evaluate quantitatively the quality of healing, the healing efficiency, denominated η, is used. It is defined as the ratio of a material property of the healed sample to that of the virgin sample.

$$\eta = \frac{P_{healed}}{P_{virgin}} \cdot 100\%$$

Despite being a quantitative parameter, its direct interpretation may not be accurate. Some polymers can show a very fragile behaviour, while the ones used in real applications have stronger matrices. If they are used indistinctly as reference materials, the results can significantly vary. Furthermore, the effect of the healing additives on the virgin polymer can help or suppress the healing efficiency and it changes depending on the applied loadings. Alternate definitions can then be used to normalise the healing material properties comparing the properties of the healed material with the ones of the original material without added healing components.

$$\eta = \frac{P_{healed}}{P_{nohealing}} \cdot 100\%$$

Another factor that can considerably affect the healing efficiency is the extent of the damage. When using samples that have catastrophically failed, healing effect measurements are more reliable, but it does not respond to the target application of self-healing materials, which is restoring the original material properties when partial damage is present.

As stated before, FRPs suffer several failure modes, so in order to assess the healing effect, several different damage methods should be studied. Currently no standard processes have been described, but most often mechanical properties are primarily tested using tensile, compression or bending test protocols. Other experimentations which have already been carried out include impact, scratching, hammering or indentation tests. Depending on the test, several healing efficiency definitions can be applied using the appropriate property. [19]

2 Processing and Manufacturing

2.1 Introduction

Manufacturing is a key factor in the composites design process, since it heavily influences the properties and cost of the material. Preparation for a composite manufacturing should proceed in coordination with the early design concepts and includes the selection of materials, composites quality assurance, development of a manufacturing plan, setting of the material requirements and tools, and production process development.

Figure 2.1.1 describes the generic phases of a laminate thermosetting composite manufacturing process.

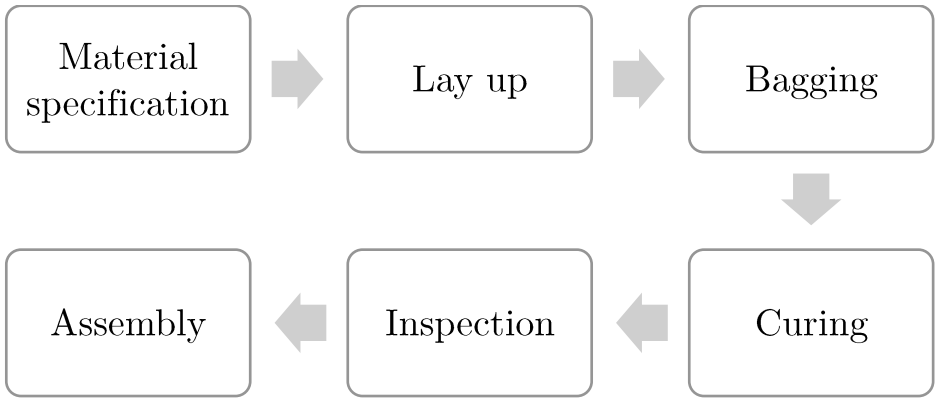

Figure 2.1.1. Flow chart of composite laminate part fabrication [32]

Within this thesis only small samples with a relatively simple geometry will be manufactured, so this chapter focuses on the used materials to produce both the self-healing material and reference samplings, the explanation of the different implemented manufacturing strategies and the observation of the produced specimens using Scanning Electron Microscopy (SEM) to determine which manufacturing process is more suitable to fit the material required criteria.

2.2 Materials

HEXFORCE ® - HEXCEL ® E glass fabric, nominal weight 290 g/m^2, thickness 0,23 mm, 7 yarn/cm warp and 7 picks/cm weft, SX8 EVO A epoxy resin and SX8 EVO B hardener purchased from Mike Compositi were used to manufacture the reference samples. [68][69]

D.E.R. ™ 332 diglycidyl ether of bisphenol A (DGEBA) and 4-aminophenyl disulphide (4-AFD, 98%) were used for manufacturing the dynamic samples and were purchased from Sigma-Aldrich. Glass fibre reinforcement is maintained in the dynamic samples production.

2.2.1 Synthesis of Specimens

2.2.1.1 First procedure: Vacuum Bag + Heating

The first sample manufactured within this thesis consisted on a 10 x 10 cm four-layer glass fibre reinforced composite using the reference epoxy resin and hardener. The objective was achieving a composite with 50% fibre reinforcement, so the first step before beginning with the lay-up was weighting the fibre fabric so to introduce a proper amount of resin. The fibre reinforcement weight was 12,14 g, so to assure a proper fibre content, 15 g of matrix were used, since part of the resin is lost during curing. According to the resin properties, to have a complete cross-linking reaction, the ratio of epoxy resin and hardener is 100:30, so within 15 g, theoretically, 11,5 g of resin and 3,5 g of hardener were needed. In the actual sample 11,48 g of resin and 3,52 g of hardener were introduced.

Once the epoxy resin and the hardener were mixed, fibre fabric and matrix were manually laid up using a regular plastic spatula so that resin is homogeneously distributed. As it is a manual process, it is difficult to avoid the generation of void within the material, so a grid is placed above to facilitate the extraction of the

retained air. After the grid, the composite is covered by a release peel ply which enables the separation of the composite from the bleeder, which is the next layer. The bleeder holds the excess resin from the composite. The vacuum bagging film in which all the mentioned materials are placed is then sealed using a rubber and connected to the vacuum pump via a vacuum connector.

Resin data sheet suggested 20 h at room temperature and 5 h at 70 °C for complete curing, but in this trial the sample was directly introduced 5 h in the oven maintaining vacuum [53]. After 1 h in the Memmert oven, the vacuum bag was checked to see if the sealing was properly working or if the bag was partially opened. The rubber was not perfectly hermetically closed, so silicone adhesive was introduced in the vacuum bag critical points.

Figure 2.2.1. Memmert oven

The obtained sample weighted 16,36 g, so to determine the volume fraction of fibre reinforcement present within the specimen, rule of mixtures is applied,

$$f = \frac{V_f}{V_f + V_m}$$

where f is the fibre volume fraction and V_f and V_m, the volume of both the present phases, fibre reinforcement and matrix. The achieved fibre volume fraction was 53,54%, which is above the target value. Reformulating the rule of mixtures, theoretical density can be calculated. Rule of mixtures is generally applied in materials science, especially in the composites field, since it theoretically delimits the values of properties such as the elastic modulus or the density. It consists on a volume-weighted mean which considers both the properties of the matrix and the fibres. In the present case, the rule can be described as

$$\rho_c = f\rho_f + (1 - f)\rho_m$$

The resultant value will be later compared to the measured density value, so to assess the presence of voids within the material.

2.2.1.2 Second Procedure: Hot Press

Before starting the manufacturing of the dynamic samples, a second manufacturing technique was tried to attempt to reduce the defects present in the specimen.

The first step in this manufacturing process is analogous to the one followed in the first trial: manual lay-up. In order to measure and optimize the quantity of needed resin, 15 g of epoxy and 4,5 g of hardener were mixed to ensure that enough resin was available for the lay-up. 11,15 g of resin were needed for the lay-up, that meaning that using this method the fibre-matrix weight ratio, considering that 10,83 g of fibre were used, is of 97,13%. Minimization of resin utilization is important not to waste material, but in the case of the dynamic epoxy is crucial, as its cost is considerably higher than the one of a regular polymer. Cost optimization falls

beyond the scope of this thesis, but since it is one of the factors limiting the current feasibility of self-healing materials, it should be accounted.

The composite was laid up onto a vacuum bag film and covered by Teflon. It was then introduced within another vacuum bag film to create a double layer coverage. After that, it was placed in a hot press for 20 h at room temperature and 5h at 70 °C. The pressure within the press is controlled by a built-in barometer which scale is 2 bar, so a precise control is not provided. The real pressure ranges from 5 to 6 bar.

After its curing, the specimen weighted 13,66 g, which lead to a theoretical volume fibre fraction of 60,52%, which constitutes an improvement with regard to the first trial.

Figure 2.2.2. Hot press

2.2.2 Dynamic Samples Manufacturing

When manufacturing the reference samples, the suggested resin hardener ratio was used, while in order to produce dynamic samples, no supplier recommendation is available. In order to achieve the optimum performance from a resin/hardener system, it is necessary to use an appropriate stoichiometric mix ratio. When using functional epoxide/reactive curing agents, it is desirable to make react resin and hardener at approximately stoichiometric quantities. [67] To calculate the stoichiometric quantity of amine in weight parts per 100 grams of epoxy resin (phr), the amine hydrogen equivalent weight (AHEW) of the hardener and the epoxide equivalent weight (EEW) of epoxy resin are needed.

$$AHEW = \frac{Molecular\ Weight\ of\ Amine}{No.of\ active\ hydrogens}$$

$$EEW = \frac{Molecular\ Weight\ of\ Epoxy\ Resin}{No.of\ epoxy\ groups}$$

$$phr = \frac{AHEW}{EEW} \cdot 100$$

Considering 4-AFD with a molecular weight of 248,37 g/mol and number of active hydrogen atoms equal to 4, and D.E.R. ™ 332 diglycidyl ether of bisphenol A with 340,41 g/mol and number of epoxy groups equal to 2, the phr is 36,48%, that meaning a 100:36,48 mixing ratio.

While the reference epoxy resin and hardener where mixed at room temperature, to prepare the dynamic matrix it is necessary to mix both components at 80°C with a VELP Scientifica ARE magnetic stirrer and degassed under vacuum with a Thermo Scientific Heraeus Oven. Magnetic stirrer provides no precise control on temperature, so temperature was externally monitored by using thermocouples.

Figure 2.2.3. VELP Scientifica ARE magnetic stirrer

Figure 2.2.4. Thermo Scientific Heraeus Oven

2.3 Scanning Electron Microscopy (SEM)

Before the mechanical assessment of the samples, they were observed by scanning electron microscopy (SEM) using the Hitachi TableTop Microscope TM3000. The observation of each sample allows the analysis of the specimen thickness, internal defects and fibre reinforcement diameter.

Before observing the samples, the analysed surface is prepared. Two different sanding techniques were used. The first way consisted in manually sanding the samples using three different grain abrasive papers, while the second method include the use of a Bitech Europe grinding and polishing machine, again using three different grain sandpapers (P320, P600 and P1200).

Figure 2.3.1. Bitech Europe grinding and polishing machine

Figure 2.3.2 corresponds to a scanning electron microscope schematic diagram. The electron gun creates an electron flow which is accelerated towards the anode. Electrons go through one or several electron lenses, so that the image of the electron source is created in the specimen plane. The electron beam is controlled by the scanning generator which deflects the beam to move all over the sample surface. The primary electrons generate likewise secondary electrons on the specimen sample which are detected by the electron collector and subsequently amplified to enable its display.

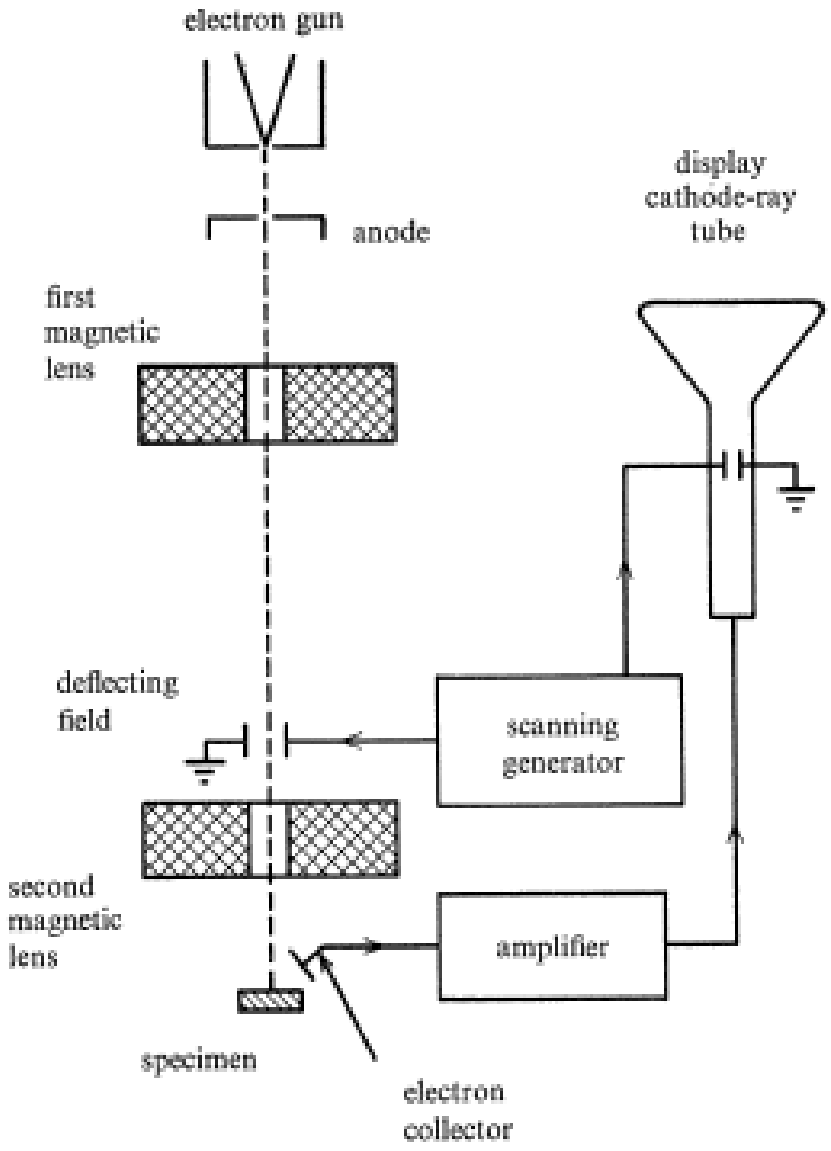

Figure 2.3.2. Scanning electron microscope scheme [57]

The advantages of this technique in comparison with optical microscopy are its higher resolution with a greater depth of field, and that the sample is later on available for experimentation. [57]

The image processing will be done using ImageJ/Fiji, which is an open source Java-based image processing program. Fibres are presented as an illuminated white, matrix as shades of grey and voids or defects in black. Evaluation of void contents by image analysis are done on sets of 12 to 16 micrographs taken at different locations.

The first assessment is related to the panels' geometrical parameters: thickness and fibres mean diameter.

	Thickness (mm)	**Fibres diameter(μm)**
Reference 1	0,917	7,881
Reference 2	0,868	6,77
Dynamic	0,815	6,077

Table 2.3.1. Samples geometrical parameters

While the first reference sample shows a higher thickness and fibres with an almost circular section (nominal fibre diameter is 9 μm**)**, hot press samples reinforcement shows a more pronounced ovalization which leads to a lower thickness.

Any geometrical deviation from a cylinder may be a preferential point to initiate buckling, making the matrix accountable for the composite compressive strength sustenance. Microbuckling is the typical failure mode of composites loaded by compressive stress states along the reinforcement direction. Matrix is loaded in shear conditions as the fibre tends to kink leading to catastrophic failure. [71]

The second and most important analysis is the assessment of the internal defects or voids. A good contrast between void and matter must be assured, so that the qualitative analysis has an accurate quantitative counterpart. Still discrimination of the different features is not always straightforward and small voids with

characteristic dimensions of few microns can be difficult to detect. A sweep of the complete sample is done so that the hole length is considered. Changes in the microscope zoom or the appearance of white spots due to the own SEM working principle may lead to a partial superposition of the images, so some voids may be taken into account twice. A thorough scanning is carried out in order to minimize these errors. Increasing the scanning area, a better correspondence between the areal and volume void fractions is found, but under the assumption of small void dimensions (< 0,1 mm) and low void content (<10%), it has been shown than an analysis area of 10 to 100 mm^2 is enough to estimate void volume fraction within 20% error. [76]

By way of illustration, the most relevant recorded SEM images are included hereunder. The obtained numerical void fraction results will be detailed in section 4.1 along with the density tests outcome, so that both characterization techniques are compared.

First reference sample presents the less homogeneous profile and lack of resin diffusion in the panel's boundaries. Generally the most noticeable defects are present in interfaces, so even if the superficial defects are relevant, the analysis focuses more on the composite core.

Second reference specimen mainly shows small voids, but some bigger defects can be also observed (Figure 2.3.8). Looking at the image scale, the observer can state that even the bigger defects are under a reasonable area threshold.

Finally, the dynamic composite sample was observed. Figure 2.3.9 shows a marked delamination which opens to the surface. No further samples were analysed in the microscope, so the extension of the delamination cannot be determined, but still it is the only remarkable defect. Exploring the whole specimen length, it is seen that the quantity of defects is reduced if compared with the reference samples.

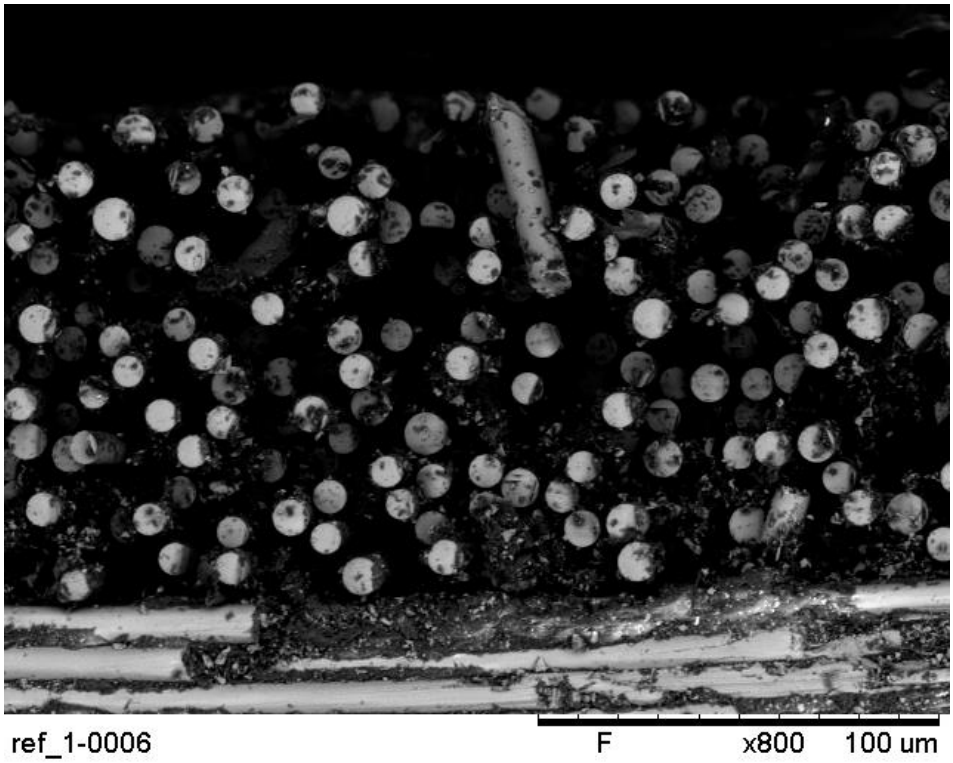

Figure 2.3.3. Reference composite 1: fibre reinforcement detail

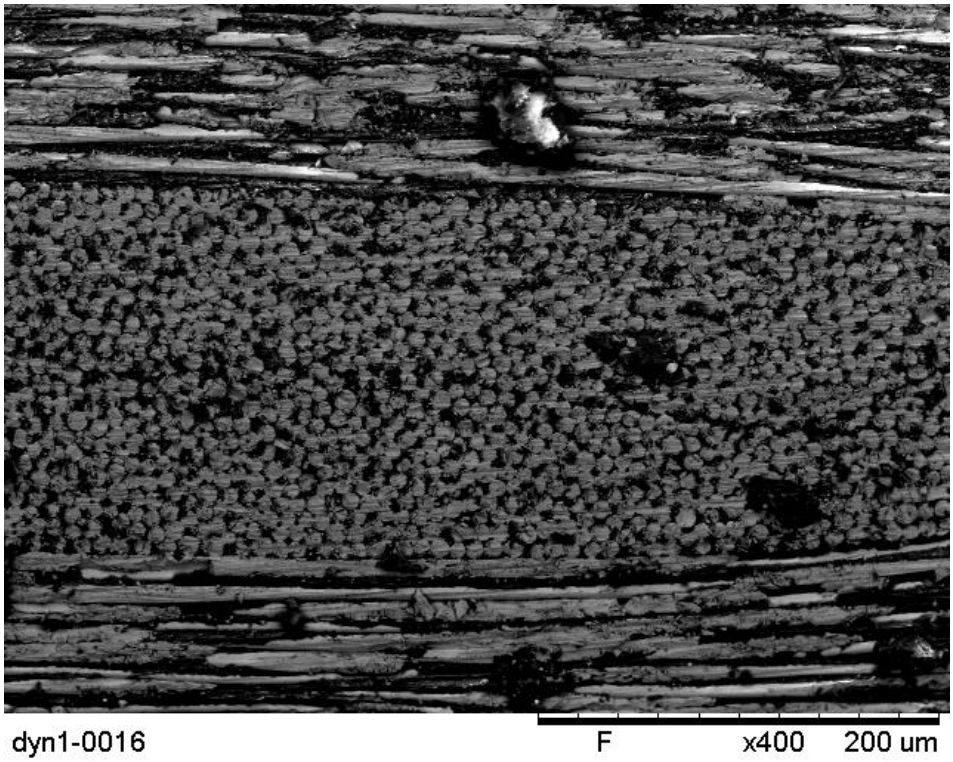

Figure 2.3.4. Dynamic composite: fibre reinforcement detail

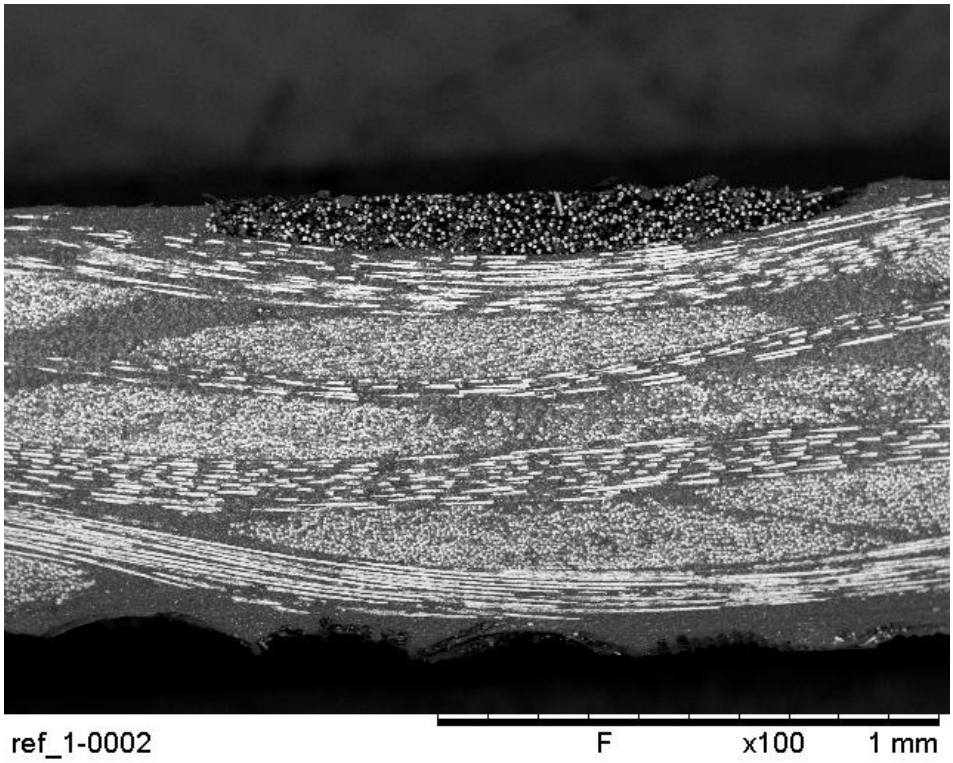

Figure 2.3.5. Reference composite 1: SEM image 1

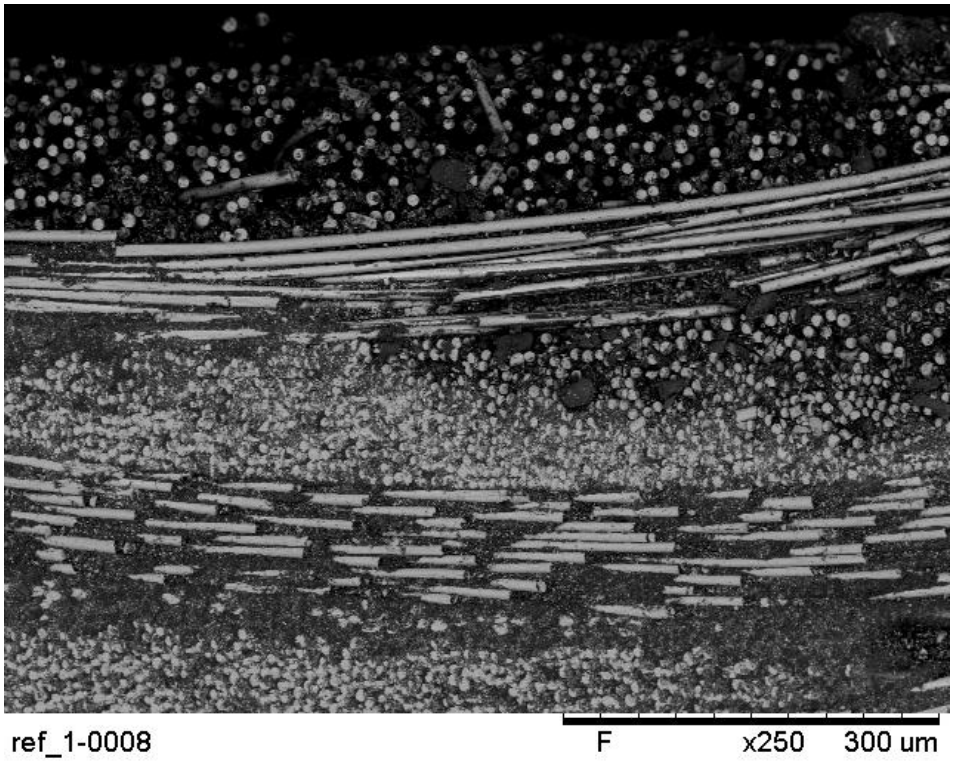

Figure 2.3.6. Reference composite 1: SEM image 2

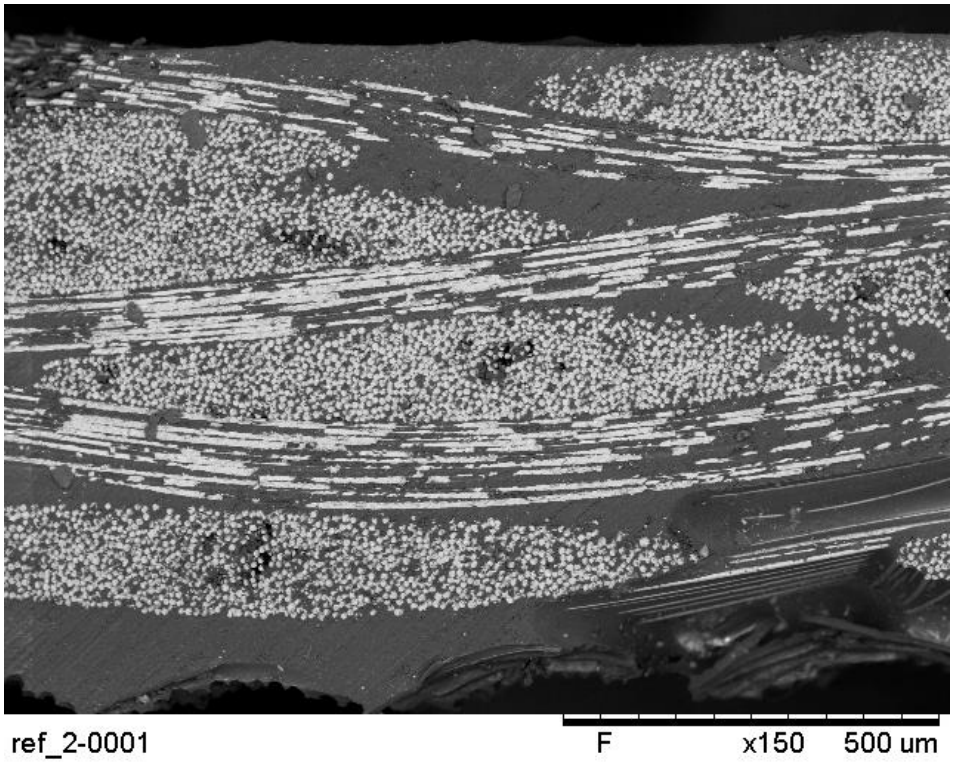

Figure 2.3.7. Reference composite 2: SEM image 1

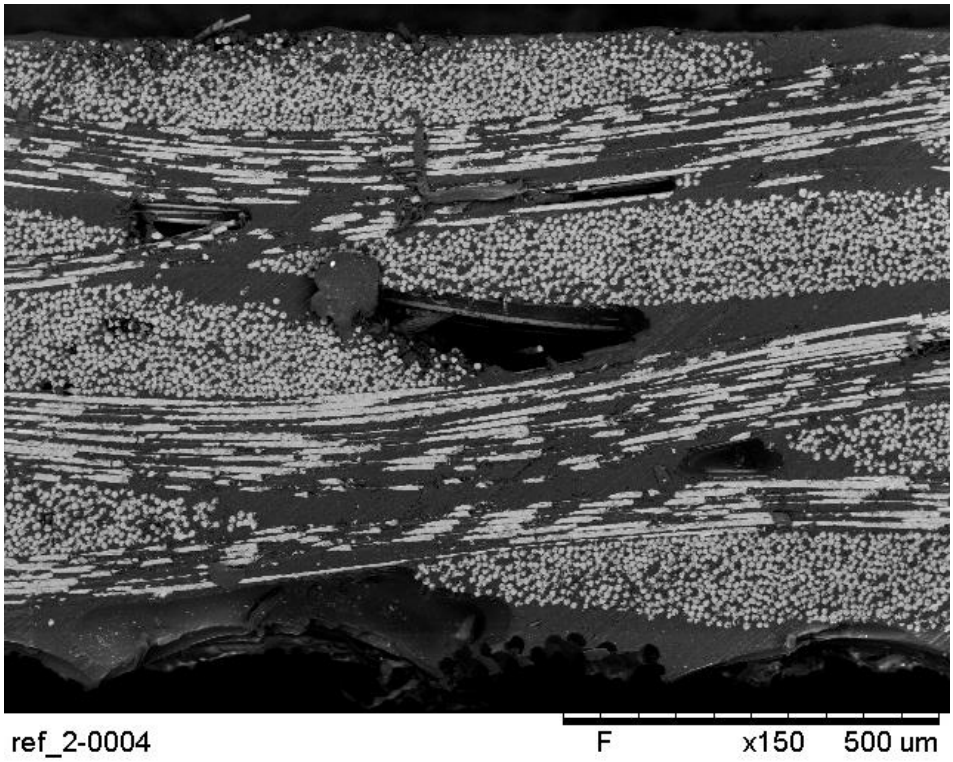

Figure 2.3.8. Reference composite 2: SEM image 2

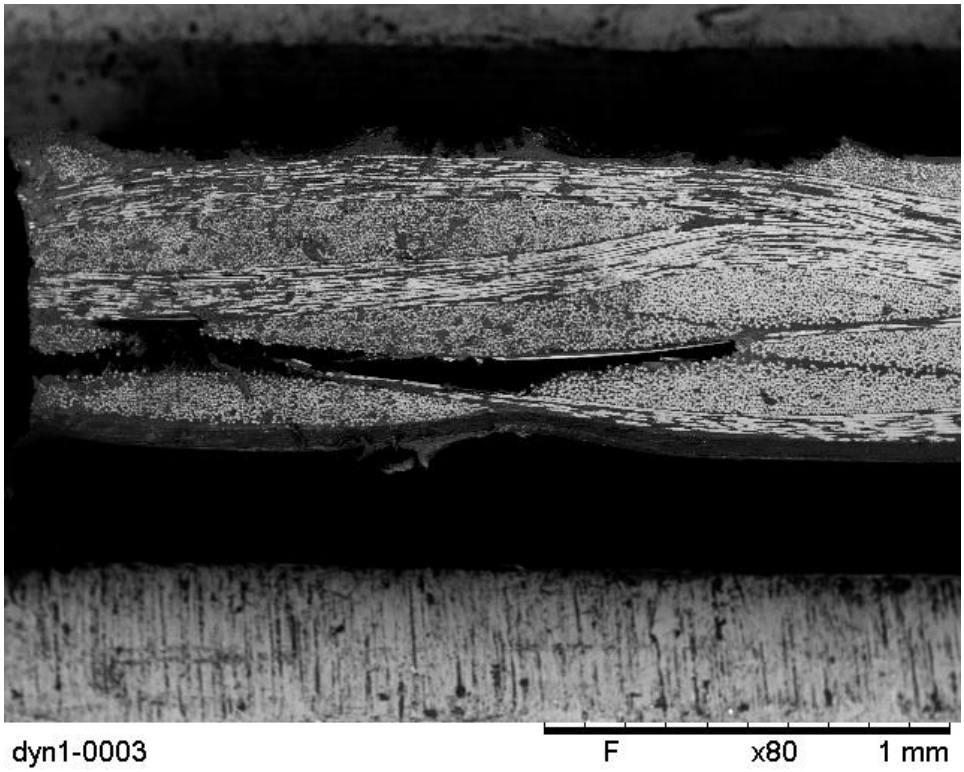

Figure 2.3.9. Dynamic composite: SEM image 1

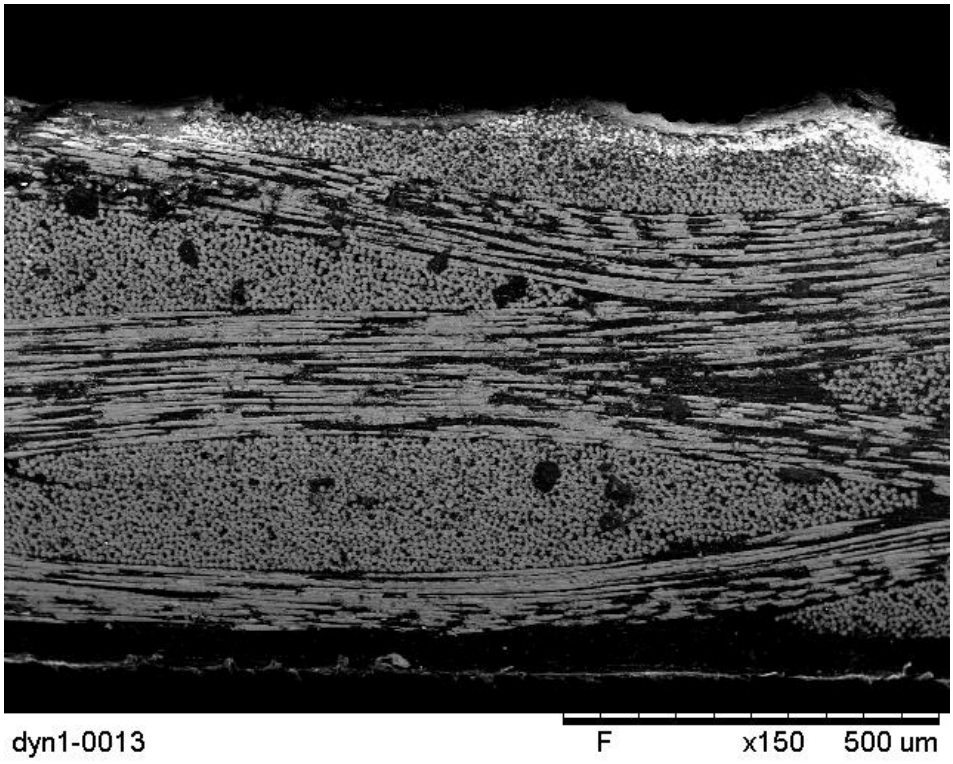

Figure 2.3.10. Dynamic composite: SEM image 2

3 Mechanical Characterization

3.1 Density Tests

Composites mechanical properties are highly influenced by the fibre reinforcement volume fraction. To assess this value, measuring the composite's density is required. Throughout this thesis, density measurements are made with the help of a Mohr-Westphal's balance.

The working principle of the Mohr-Westphal's balance's is based on the Archimedes' principle, which stipulates that a body submerged in a liquid receives a vertical upward thrust equal to the weight of the displaced liquid.

The balance consists of a height adjustable primary structure on which a shaft is mounted. This shaft is divided in two parts: a short arm, which is used to calibrate the balance, and a long arm, in which different weights are hung to measure the weight of the sample when introduced in water. Distilled water is used as reference liquid.

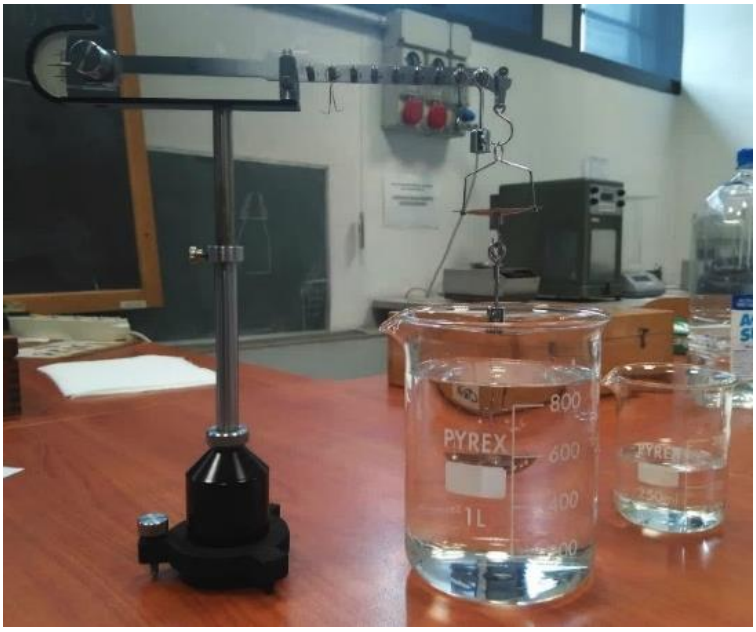

Figure 3.1.1. Mohr Westphal balance

The composite's density is calculated according to the formula

$$\rho_c = \frac{P_{air}}{P_{air} - P_{water}} \rho_{water}$$

where P_{air} and P_{water} are the sample's weight in air and in water and ρ_{water} is the distilled water's density.

As explained in section 2.2.1.1, both the theoretical and measured density values are compared.

3.2 Dynamic Mechanical Analysis (DMA)

Dynamic Mechanical Analysis (DMA) is a technique used to determine material's properties as a function of temperature, time, frequency, stress, atmosphere or a combination of the prior parameters. It consists in applying a deformation to a sample of known geometry and analysing the changes in its stiffness and damping, namely how much energy is stored or dissipated during the process. Deformation is made by subjecting the sample to a controlled stress or a controlled strain.

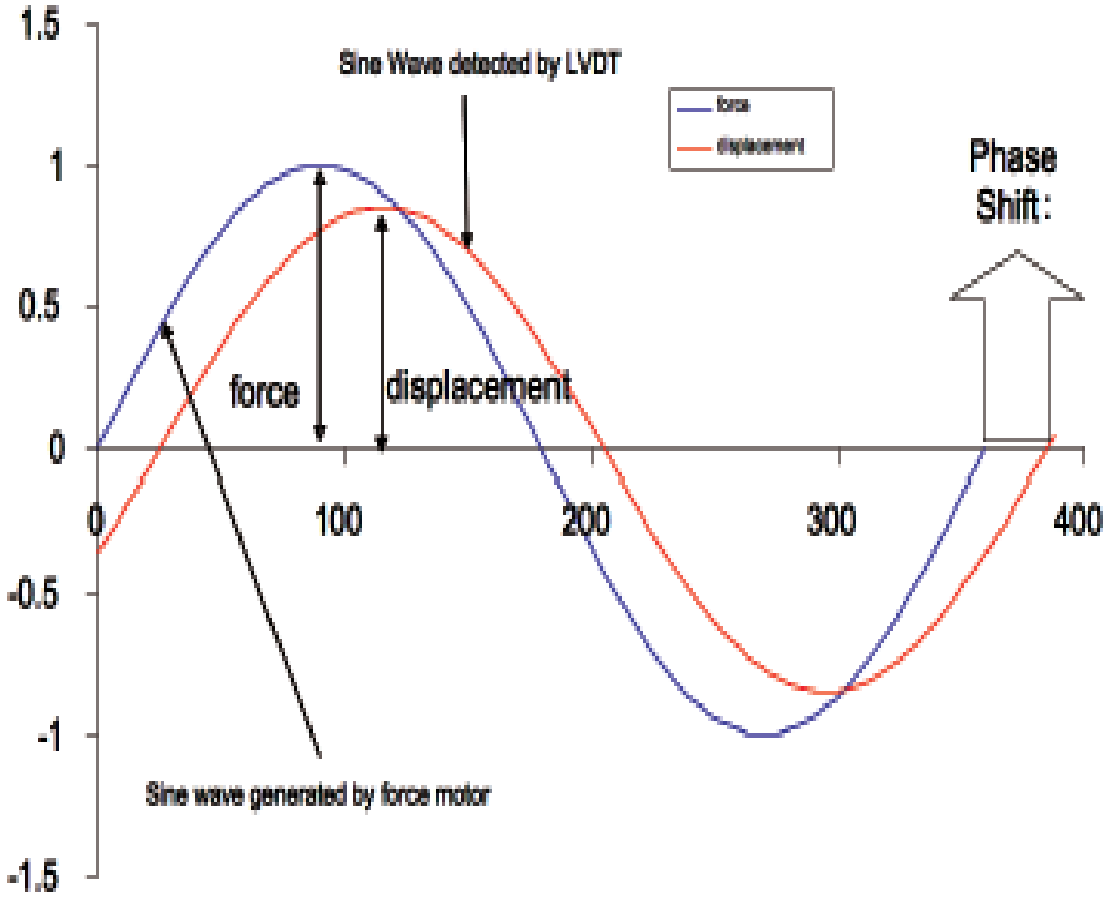

Figure 3.2.1. Relationship between the applied stress and the resulting strain [55]

Subjected to a constant load, the sample starts to oscillate sinusoidally and it deforms sinusoidally if the sample's material is within its linear viscoelastic behaviour region. The applied stress is described as a sinusoidal function

$$\sigma(t) = \sigma_o \sin \omega t$$

where σ is the stress corresponding to each time t, σ_o is the maximum stress value, ω is the oscillation frequency, and t is the time. Elastic and viscous behaviour set the shape limits of the resulting strain wave. If the material responds as a perfect elastic material following the Hooke's law, strain can be written as

$$\varepsilon(t) = E\sigma_o \sin \omega t = \varepsilon_o \sin \omega t$$

where ε is the strain corresponding to each time t, E is the modulus, ε_o is the strain at the maximum stress and the rest of parameters are analogous to the ones present in the previous equation. This limit corresponds to Figure 3.2.2 (a) as no phase lag is present in this region and both stress and strain are in phase.

The viscous limit is proportional to the stress rate, which is calculated using the derivative of the stress equation in terms of time. The proportionality constant η is the viscosity. It corresponds to the behaviour described in Figure 3.2.2 (b) where stress and strain have a phase lag of 90°.

$$\frac{d\sigma}{dt} = \omega\sigma_o \cos \omega t$$

$$\varepsilon(t) = \eta \frac{d\sigma}{dt} = \eta\omega\sigma_o \cos \omega t = \eta\omega\sigma_o \sin\left(\omega t + \frac{\pi}{2}\right)$$

Viscoelastic behaviour is described by an analogous equation in which the difference between the applied stress and the obtained strain is a phase lag or angle δ.

$$\varepsilon(t) = \varepsilon_o \sin(\omega t + \delta)$$

Using trigonometry, it can be rewritten as a combination of the in-phase and out-of-phase behaviour. The sum corresponds to Figure 3.2.2 (c).

$$\varepsilon(t) = \varepsilon_o[\sin(\omega t) \cos \delta + \cos(\omega t) \sin \delta]$$

All the equations have been described in terms of tensile stress and strain, but DMA works also for shear stress and strain (τ and γ).

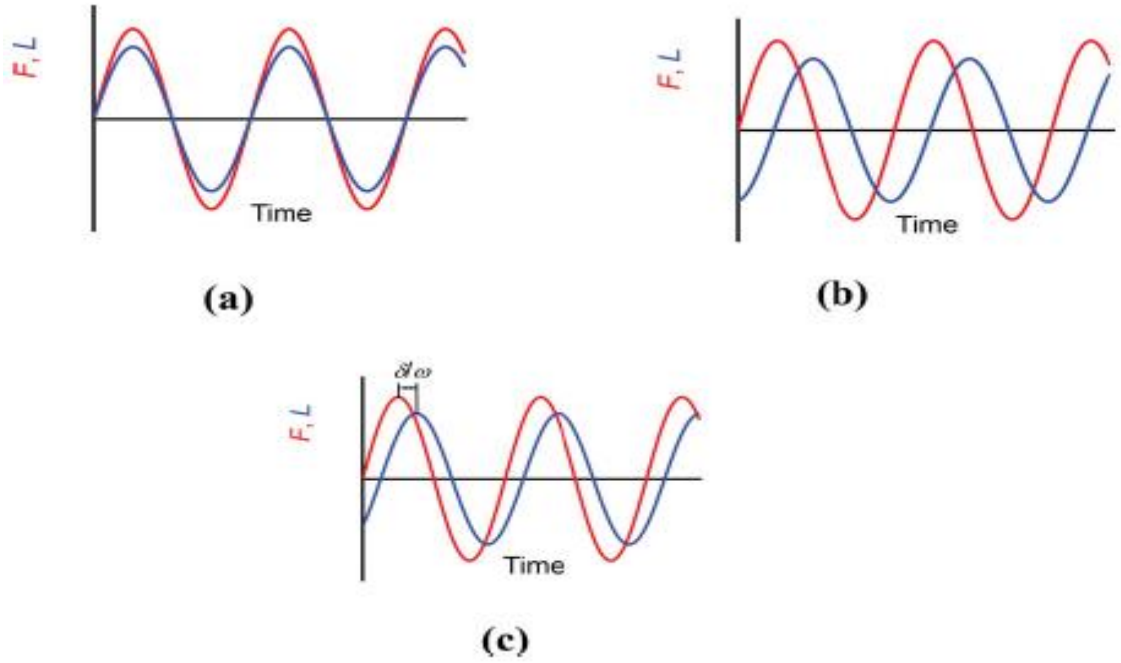

Figure 3.2.2. Material responses in DMA [54]

DMA measures the material's loss factor or loss tangent ($\tan\delta$), the storage modulus (E' for tensile tests and G' for shear tests) and the loss modulus (E'' and G'') which are independent from the applied stress and strain within the linear viscoelastic materials' theory. The parameters are described by the following equations:

$$E' = \frac{\sigma_0}{\varepsilon_0}\cos\delta$$

$$E'' = \frac{\sigma_0}{\varepsilon_0}\sin\delta$$

$$\tan\delta = \frac{E''}{E'}$$

The measured modulus using DMA does not coincide exactly with the Young's modulus used to define Hookean materials using the classic stress-strain curve. In

DMA, a complex modulus (E^*) is defined as the vector sum of both the storage and loss moduli.

$$E^* = E' + iE''$$

The use of these different moduli allows a better characterization of the material since each one reflects a capability of the material: returning energy (E'), losing energy (E'') and damping ($\tan \delta$).

Figure 3.2.3. TA Instruments DMA 2980

The instrumentation used within the experimentation is the TA Instruments DMA 2980 Dynamic Mechanical Analyzer, which works in conjunction with a TA Instruments controller and associated software to form a thermal analysis system (TA Universal Analyzer and TRIOS software).

DMA 2980 Mechanical Analyzer consists of the DMA cabinet, in which the electronics and valves are placed, and the DMA assembly. The DMA assembly is in turn formed by the mechanical section enclosure, which surrounds the air bearings, optical encoder, drive motor and the associated electronics; the clamp, in which the sample is mounted; the furnace, allowing the heating and cooling of the sample and

the CHROMEL®/ALUMEL® thermocouple, which measures the sample's temperature. [61]

Samples for DMA are obtained by cutting the pristine composite. The sample's size depends on the chosen clamp, as it is interchangeable to enable different deformation modes and the use of diverse sample's shapes and materials. Dual cantilever clamp was chosen to carry out the tests, as it is a recommended technique to assess the viscoelastic behaviour of thermosetting materials. It is formed by a movable clamp in the middle, which applies the stress and strain to the sample, and a fixed clamp on both ends fixing the sample. This system uses samples having a thickness up to 5 mm, a width up to 15 mm and a fixed testing length of 35 mm. Rectangular-based specimens of 60x10 mm were cut to meet these requirements. The sample is placed at room temperature within the clamp using a driver wrench.

Figure 3.2.4. Dual cantilever clamp assembly

Among the several offered operating modes, single frequency mode test was used. It is one of the options included in the DMA multifrequency mode, which consists in applying an oscillatory stress and strain with a constant amplitude as a function of time, temperature and frequency of oscillation. DMA single frequency tests are created using temperature ramps and holds.

The followed procedure entails equilibrating the sample temperature at 30 °C, applying a 15 μm amplitude and 1 Hz frequency sinusoidal strain to the sample while a temperature ramp of 5 °C/min is implemented until reaching 200 °C. This test method is included in the ASTM D7028 – 07. 1 Hz frequency is chosen as standard as higher testing frequencies result in a higher DMA T_g and resonance mode gives either a lower or higher temperature value which cannot be specified as a standard. Single frequency tests were carried out both for reference and dynamic composites. [62]

Further experiments were carried out using a transient mode, which implies applying a load to the sample and monitoring its response over a specified time period to analyse the stress-strain-time relationship or constitutive law. In this thesis, the stress relaxation mode is applied. Using this mode, an instantaneous strain is applied to the sample and the force required to maintain the stress is measured as a function of time. The percent of strain describes the amount of deformation applied to the sample. The main result is the stress relaxation modulus during the strain step, which is defined as

$$E(t) = \frac{\sigma(t)}{\varepsilon}$$

During the stress relaxation test, the modulus of the material generally decreases from an initial value E_0 to an asymptotic value E_∞ and its characterized by a relaxation time constant τ. Mirroring Maxwell's model for viscoelastic fluids, relaxation time is defined as the time needed to relax 1/e of the initial stress. [48][64]

Stress relaxation properties are crucial for material and engineering design because they depend on the polymer structure. Viscoelastic properties are important to assess the composite's capability in load bearing applications.

Regarding the stress relaxation procedure, it consists in heating the sample for 5 minutes up to the required temperature an then subjecting it to 1% strain. A preliminary force of 10^{-3} N is applied to assure the sample material straightness. The relaxation modulus is then monitored during the complete test running. Both composites are tested at 40, 60, 80, 100, 120, 140, 160, 180 and 200°C. Highest temperatures were included when relevant information was observed during the experimental procedure. The first test duration was 30 minutes, but the further tests were extended until 50 min to observe if any relevant information could be obtained.

3.3 Differential Scanning Calorimetry (DSC)

Differential Scanning Calorimetry is a technique which measures the difference in the heat flow between a specimen and a reference specimen as a direct function of time or temperature under heating, cooling or isothermal conditions. Within composites' characterization, it is a widely used method, since it allows to study both thermodynamic processes (glass transition or specific heat capacity) and kinetic events (onset and completion of cure, heat of cure, maximum rate of cure, percent cure or enthalpic relaxation).

Thermosetting materials' final properties strongly depend on their chemical composition, as well as the undergone conditions during their manufacturing, so DSC can be used to monitor the ending product characteristics, so that their quality and integrity are assured. [51][52]

When curing, epoxy resins undergo an irreversible chemical reaction. The related heat evolution can be measured by the DSC instrument and therefore, the exothermicity or endothermicity of the reaction can be assessed. Figure 3.3.1 shows different states of the material in different steps of the cross-linking process.

Figure 3.3.1. Representation of the advance of the cross-linking reaction [52]

The test was carried out using TA Instruments DSC 2010 CE. The differential scanning calorimeter is formed by the DSC cell, where the tested and reference

samples are placed for measuring, and the 2010 CE Instruments, which includes both the electronics and software to allow test running and data storage. Data analysis is made using TA Instruments Universal Analysis and Microsoft Office Excel. A scheme of a DSC is showed in Figure 3.3.2, while the actual used machine corresponds to Figure 3.3.3. Sample and reference capsules are heated using the same source, so the heat flow coming from the furnace must symmetrically pass through the thermally conductive disk. Sample capsules are placed on the disk symmetrical to the centre where the temperature sensors are integrated.

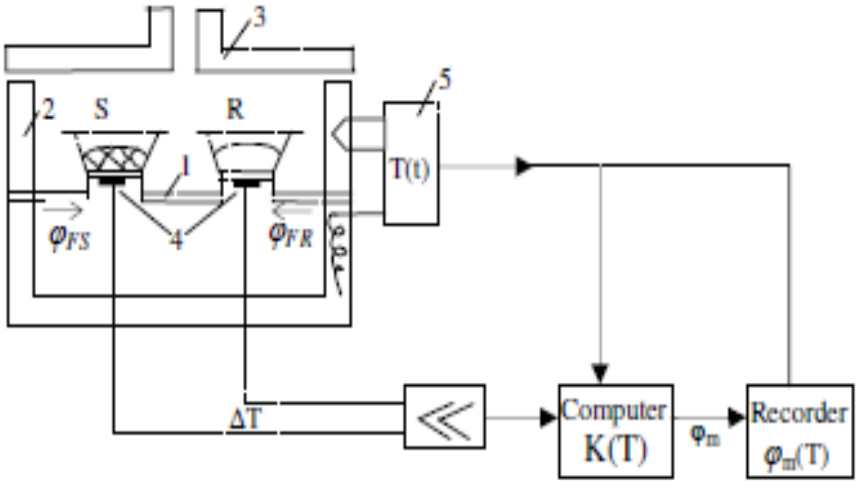

Figure 3.3.2. DSC Scheme: 1) disk, 2) furnace, 3) lid, 4) differential thermocouple(s), 5) programmer and controller, S) crucible with sample substance and R) crucible with reference sample substance [51]

Figure 3.3.3. TA Instruments DSC 2010 CE

Samples for DSC consist in capsules which are composed of aluminium pans and the material used for testing. The aluminium pans are first weighted to tare the weight of the balance to zero. A minimum amount of 10 mg is needed to carry out the test. To seal the capsule the TA Instrument Sample Encapsulating Press is used. The pan with the material is placed on the press, the lid is then laid on the pan and both are joined by pressing.

Figure 3.3.4. TA Instrument Sample Encapsulating Press

The test consists in a dynamic measurement including two heating and cooling cycles of the sample at a fixed temperature rate. Two different cycles are implemented to determine both the total heat of reaction and the T_g.-transition. To create an inert atmosphere, a nitrogen flow of 30 to 40 mL/min is needed. Once the test and reference samples are placed within the cell, the cell temperature is equilibrated at -10 °C with the help of the TA Refrigerated Cooling System. The test procedure begins with a heating temperature ramp of 20°C/min until 200 °C

followed by a cooling temperature ramp of also 20°C/min until 20°C. The process is run twice for each sample. Between each heating or cooling phase, the test is equilibrated by including a 1 min isotherm.

Difference in the heat flow between the sample and the reference is plotted against temperature. Curing is observed as a significant exothermic peak, which area can be integrated to give the heat of cure.

$$\Delta H_{cure} = \frac{1}{m_{matrix}} \int_{t_0}^{t_f} dH_{peak}(t)$$

Where ΔH_{cure} is the heat of cure, t_o and t_f are the initial and final reaction times corresponding to the initial and final temperatures of the exothermic peak, m_{matrix} is the resin mass and dH_{peak} is the heat exchanged in the peak time interval.

Complete curing is not always achieved, so to quantify the degree of cure, the parameter α is introduced

$$\alpha = \frac{\Delta H_{cure}}{\Delta H_{total}}$$

where ΔH_{total} is the total heat of reaction. The degree of cure is both characterized by the increment in T_g and the decrease of the heat of cure. When the thermoset is completely cured, the residual heat of cure is practically zero and the T_g reaches a constant value, as it depends on the material chemistry. The degree of cure is important to assess the material's brittleness, impact resistance, long term stability, creep, solvent resistance and integrity. [52]

4 Experimental Results

4.1 Density Tests

Density measurements were carried out testing three prism-shaped samples of each manufactured panel. Table 4.1.1 presents each density measure, as well as the average value for each specimen.

		ρ_c (g/cm³)	Mean ρ_c (g/cm³)
Reference composite 1	**Sample 1**	1,896	1,940
	Sample 2	1,967	
	Sample 3	1,958	
Reference composite 2	**Sample 1**	2,087	2,094
	Sample 2	2,106	
	Sample 3	2,087	
Dynamic composite	**Sample 1**	1,952	2,017
	Sample 2	2,047	
	Sample 3	2,052	

Table 4.1.1. Density measurements

After the visualization of the sample voids using SEM, density tests are also used for the characterization of voids. This technique relies on the accurate knowledge of the component's density and weight fraction and cannot provide information about the individual void size, shape or distribution, that meaning that two different composite samples with the same void volume fraction can have different mechanical behaviour. The need to know the constituent's physical properties prior to the material's characterization limits the use of this technique to already studied materials.

Nominal densities are obtained from the manufacturer's technical data sheets in the case of the reference matrix, but no density information is provided within the

dynamic epoxy data, so a common density value of 1,16 g/cm^3 is chosen. Choosing a random density matrix value contradicts the previously stated premise that the density values must be accurately known, but the results are reported even if more precise techniques which are out of the scope of this thesis could be implemented to improve the results reliability. Fibre's density is constant, while the exact matrix density is unknown as it depends on the cross-linking between hardener and epoxy resin. The chosen matrix's density is dependent on the quantity of hardener and resin mixed in the manufacturing of each sample. As part of the resin is bled during curing, the exact mixing ratio may have changed, so another source of uncertainty is introduced.

Void volume fraction can be calculated as the relative error found between the measured and the theoretical rule of mixture density or using the following formula:

$$V_v = 100 - \rho_c \left(\frac{\%_{m-matrix}}{\rho_{matrix}} + \frac{\%_{m-fibre}}{\rho_{fibre}} \right)$$

where V_v is the volume void fraction, $\%_{m-}$ and ρ are the mass fraction and density of the pristine required constituents. [70]

Table 4.1.2 includes the nominal and mean measured composite's density along with the calculated void fraction.

	$\boldsymbol{\rho_c}$ **(g/cm³)**	**Measured** $\boldsymbol{\rho_c}$ **(g/cm³)**	$\boldsymbol{V_v}$ **(%)**
Reference composite 1	2,092	1,940	7,27
Reference composite 2	2,214	2,094	5,42
Dynamic composite	2,056	2,017	1,90

Table 4.1.2. Density error measurements

Table 4.1.3 includes the void fraction obtained with the two implemented characterization techniques. The reliability of each technique cannot be assessed, as the real void fraction cannot be accurately known, but the comparative variation.

	V_v – Archimedes (%)	V_v – SEM (%)
Reference composite 1	7,27	3,76
Reference composite 2	5,42	2,18
Dynamic composite	1,90	1,79

Table 4.1.3. Void fraction obtained with density tests and SEM

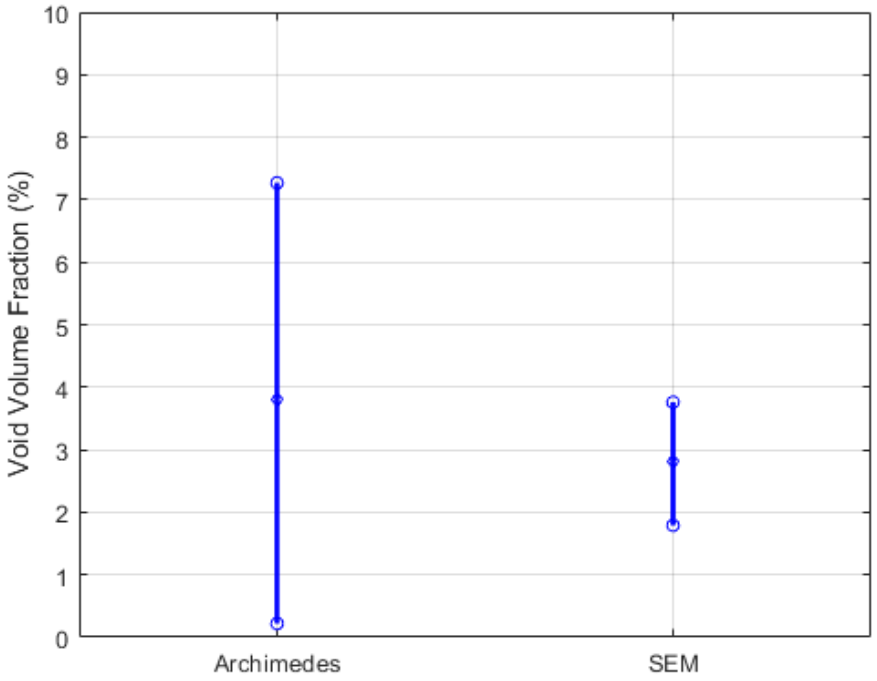

Figure 4.1.1. Comparison of the void volume fraction calculated using the Archimedes principle (Mohr – Westphal balance) and SEM

Both techniques show the same tendency when considering the manufacturing technique, which implies that using the hot press procedure is more convenient for our purpose. The vacuum bag's method is generally used to manufacture composites, but whenever the used resin has a low viscosity, it tends to be sucked because of the vacuum pressure, generating porosities within the material.

The average void volume fraction is significantly higher for both the reference samples using the Archimedes' principle because no massive defects were present in the surface of the analysed samples, whereas the dynamic composite void fraction

values are more homogeneous since it shows a remarkable superficial void. Using the Mohr Westphal's balance not only the surface can be reached, but the volume, so generally the void fraction values tend to be higher.

4.2 Dynamic Mechanical Analysis (DMA)

According to ASTM D7028 [62], the standard definition for DMA T_g is based on intersecting two tangent lines from a semi-logarithmic plot of the storage modulus versus temperature. The first tangent line is selected at a temperature before the transition, while the second line is defined at the inflection point to approximately the midpoint of the storage modulus drop.

T_g value depends on the determination test method, so it may not coincide with the values reported by other measurement techniques. This stresses the fact that the glass transition occurs over a temperature range. DMA T_g and DSC T_g will be compared in section 4.3.

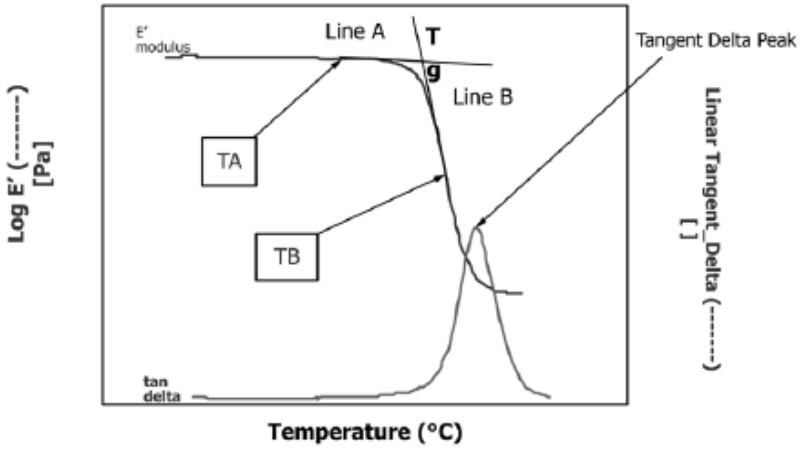

Figure 4.2.1. Definition of DMA T_g in ASTM D7028 [62]

DMA T_g can be also be defined as the peak temperature of the tan δ curve, so it will be included in this study for comparison reasons. The standard DMA T_g is a more conservative value, but generally the peak tan δ curve temperature is chosen as T_g as the accurate placement of the tangents is subject to more uncertainty than the definition of the peak. [63]

Figure 4.2.2 is an example of a performed test in which the trends of storage and loss moduli, as well as tan δ with respect to time are reflected.

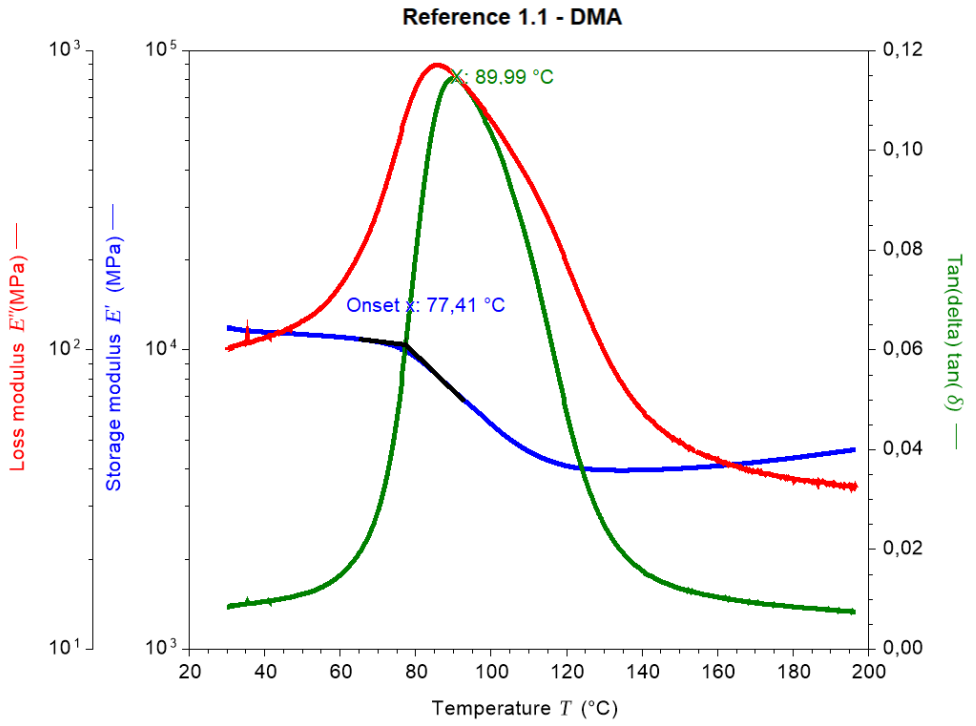

Figure 4.2.2. Example of DMA measure

Table 4.2.1 summarizes the results using both T_g definitions for the reference and dynamic composite. The indexes 1 and 2 correspond to the different tried manufacturing techniques. Tests were repeated twice for each manufacturing process. Even if the first and second trial samples have not the same mean composition, they are formed by the same materials, so the average value is reported for further comparison purposes with the DSC T_g values.

	T_g (°C)					
	Standard		**Peak tan δ**		**Average**	
	1	2	1	2	Standard	Peak tan δ
Reference	77,41	77,88	89,99	97,06	77,86	93,00
	78,20	77,96	92,87	92,08		
Dynamic	-	163,96	-	173,70	163,58	175,52
	-	163,20	-	177,33		

Table 4.2.1. DMA Tg measurements

Dynamic and reference samples show a great difference in the T_g value, which is mainly induced by the fact that the dynamic sample underwent a post-curing process, while the reference was just cured, and the manufacturer technical sheet data curing times were adapted to reduce the manufacturing time.

DMA single frequency assessment is completed by studying the composite's complex modulus (see Section 3.2). It will be compared to the calculated value using the rule of mixture considering the void fraction (see Section 2.2.1.1). Mohr – Westphal's void fraction values will be used for the calculation to obtain more conservative results.

$$E_c = E_f \cdot f + E_m \cdot (1 - f - V_v) + E_v \cdot V_v$$

Reference values are used for the different component's moduli ($E_f = 72\ GPa$, $E_m = 2\ GPa$ and $E_v = 0\ Pa$, as void corresponds to trapped air). Rule of mixtures is generally used for unidirectional composites, while the used glass fibre fabric is bidirectional, so the fibre modulus contribution is mitigated.

Table 4.2.2 resumes the obtained results and the obtained error using E_c as reference modulus.

	E* (MPa)	**E_c (MPa)**	**Error (%)**
Reference 1	14719,27	17083,02	-13,84
Reference 2	22151,87	20120,88	10,09
Dynamic	15284,68	18743,47	-18,45

Table 4.2.2. Measured complex modulus and rule-of-mixture modulus

Greater difference is found between the measured complex modulus and the rule-of-mixtures Young's modulus (error ranges from 10 to almost 20% in absolute value) than between the Mohr-Westphal's and rule-of-mixtures density even if the reference values are calculated using an equivalent formulation. Among the suspected causes are the use of a bidirectional fibre fabric and the difficulty of

assessing a coefficient to introduce the contribution of the fibre to the Young's modulus; manual lay-up which can cause misalignment among the fibre layers; the slightly differences in the definition of the complex modulus and the Young's modulus (ideally complex modulus and Young's modulus should be equivalent, but generally Young's modulus is referred to tensile tests, while the carried out DMA tests are performed under a flexural load and in the case of composites, value can significantly change) or the need of a more precise assessment of the void fraction. Error range between the complex and computed modulus is greater than the one that it could be acceptable in industrial productions, but it is still valid for the thesis' purpose.

In order to assess the effect of the volume fibre fraction and the void fraction on the composite's modulus value, one parameter is fixed and made equal to a reference value while the other is changed (shown in Figure 4.2.3).

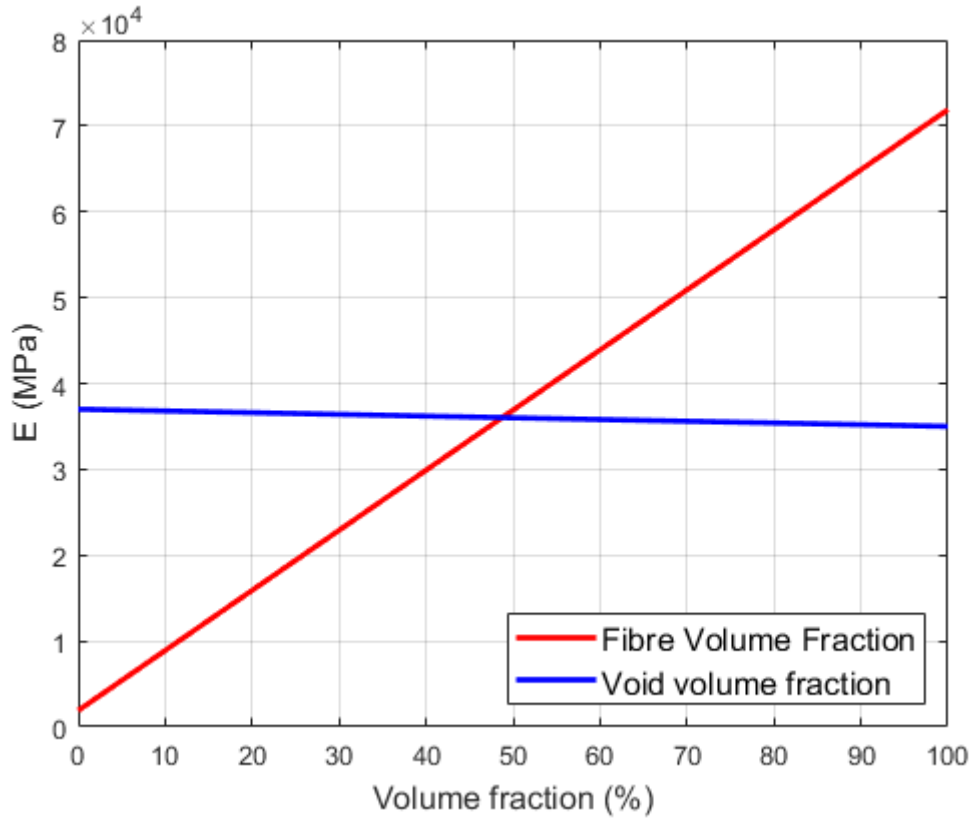

Figure 4.2.3. Change in E when varying the fibre or void volume fraction

As it was a priori supposed, fibre content is way more significant than the void one, but still the effect of the void is not negligible and most importantly, it may lead to the generation of larger defects which lead to a remarkable decrement of mechanical properties.

The results of the stress relaxation tests are presented below. To assess the relaxation modulus' evolution in time, the normalized relaxation modulus E/E_0 is plotted for each tested temperature. E_0 corresponds to the stress relaxation modulus value after the test temperature has been reached and stabilized.

Figure 4.2.4 and Figure 4.2.5 correspond to the reference composite's stress relaxation tests. The first test duration was 30 minutes, as the objective was to follow the procedure which was chosen in previous studies at Politecnico di Milano [48], while the second test was extended until 50 minutes in order to see if a noticeable behaviour raised.

Both tests indicate that a certain relaxation level is achieved in the T_g range (60 to 80°C), especially in the first test. No great differences should be found in both experiments results, as the samples are manufactured using the same materials, but comparing the plots, the first test shows a larger relaxation than the second one. The reason could be the errors induced by the manufacturing process. Fibre's modulus is one order of magnitude higher than the epoxy's modulus, so even if the resin can reach almost complete relaxation at temperatures around T_g, the fibre has greater influence on the stress relaxation modulus value. First sample's manufacturing leads to higher errors in the composite structure, including the misalignment of the reinforcement fibres with respect to the load direction, which results in a less effective fibre behaviour, giving more prominence to the matrix behaviour and its relaxation.

The dynamic composite's relaxation tests show a significant relaxation also when the T_g temperature range is reached (160, 180 and 200°C). It could be expected that increasing the temperature, relaxation should increase, but the tests show that the

relaxation is higher in the T_g range trial (160°C) than in the 180°C, but then increases again for 200°C.

If compared with the pure dynamic resin, reached relaxation levels are not even comparable due to the presence of the fibre fabric. In addition to the reinforcement modulus value, the second fibre effect is the homogenization of the stress relaxation behaviour, as the same tendency is observed in every test, regardless the temperature and the microstructure changes.

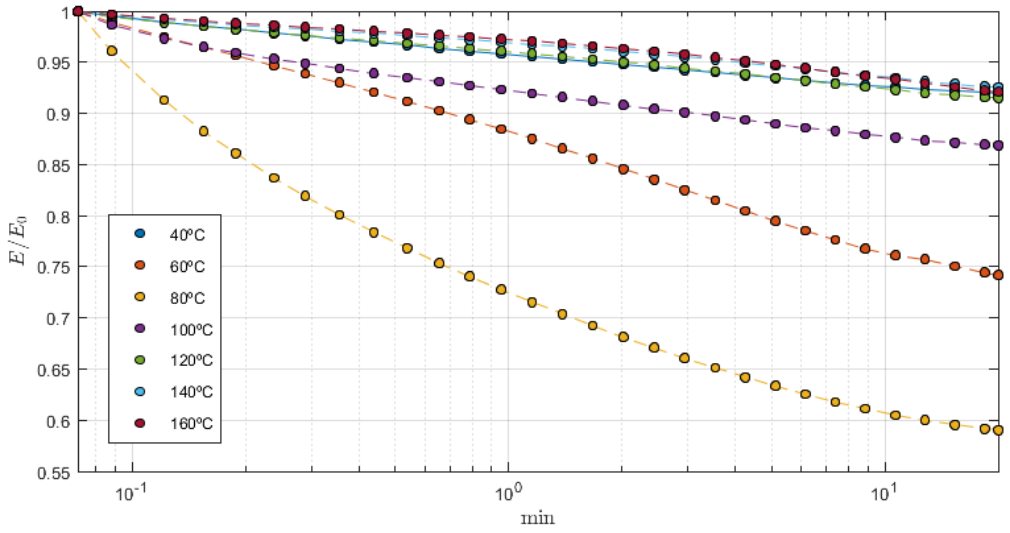

Figure 4.2.4. Reference composite 1: stress relaxation test

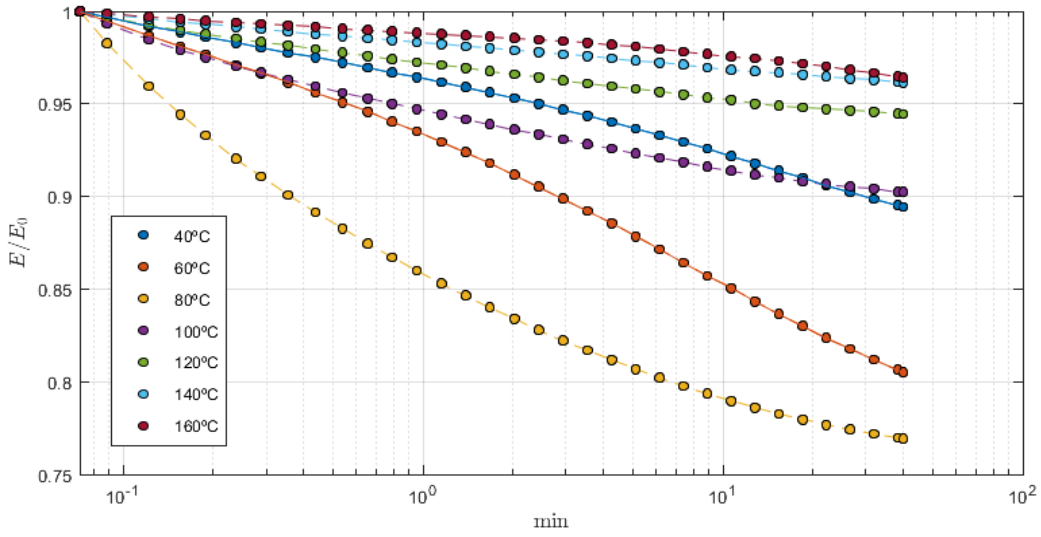

Figure 4.2.5. Reference composite 2: stress relaxation test

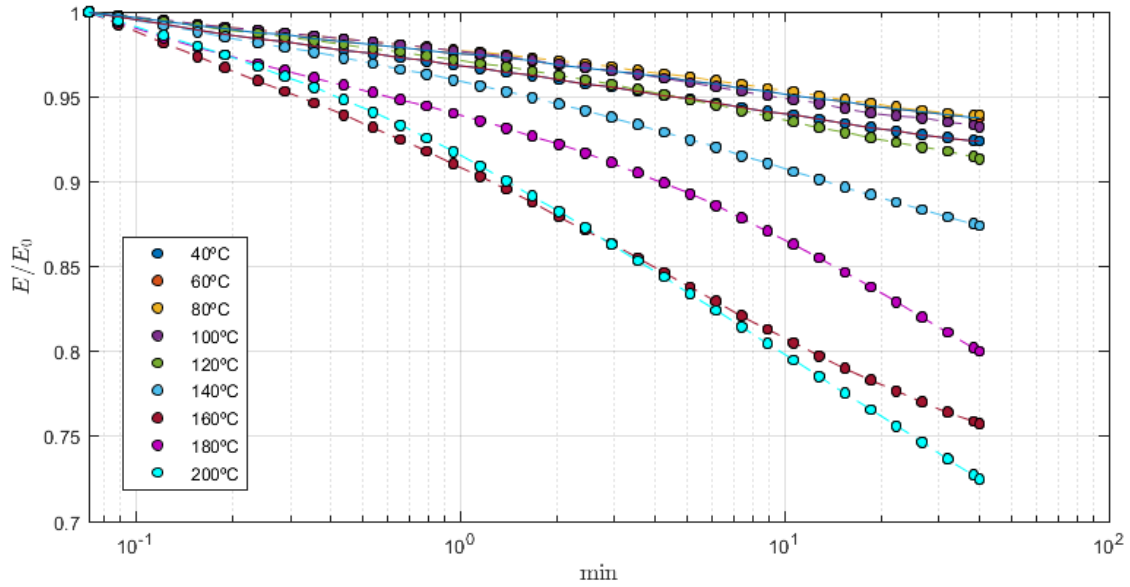

Figure 4.2.6. Dynamic composite: stress relaxation test

Table 4.2.3 lists the initial relaxation moduli at each test temperature for both reference and dynamic composites.

	Initial relaxation modulus (MPa)		
Testing temperature (°C)	**Reference 1**	**Reference 2**	**Dynamic**
40	10315	23154	12245
60	9608	23185	12652
80	5981	19328	12805
100	3624	16380	12968
120	3544	16638	13070
140	3724	16734	12965
160	3924	17084	12083
180	-	-	10941
200	-	-	10066

Table 4.2.3. Initial relaxation modulus in DMA stress relaxation mode

For every sample, the initial relaxation modulus tends to reduce when temperature is increased, but the rate of decline is more significant for the first reference sample than in the case of the hot press manufactured specimens. Moreover, the more remarkable decrease in the initial relaxation modulus is placed in the T_g range (approximately 80°C for the reference samples and 160°C for the dynamic one). Even if the tendency should be the decrement of the modulus with temperature, reference samples relaxation modulus slightly increases after the T_g range and dynamic sample right before the T_g range, which could be due to inaccuracy of the applied method or the changes in the resin nature after being subjected to relatively long high temperature tests.

Relaxation moduli values are of the same order of magnitude as the complex modulus and the rule-of-mixtures modulus, so it could also be used as measured moduli in exchange of the complex modulus. It is subjected to the same prior stated uncertainties.

4.3 Differential Scanning Calorimetry (DSC)

DSC results are obtained from the analysis of the normalized heat flow – temperature curve, in which the two implemented cycles can be observed (Figure 4.3.1). The start and final implemented temperatures are not reached due to the heating and cooling process happening within the DSC, but where assigned that values to cover an appropriate temperature range in which the value of T_g is expected. T_g does not correspond to a unique temperature value, but to a temperature range, but still a fixed value corresponding to the midpoint of this temperature range is chosen as the nominal value of T_g. The glass transition zone is characterized by a sudden decrease in heat flow. This process is made manually choosing approximately the initial and final value of the temperature range using the TRIOS software, so some dispersion in the results is found.

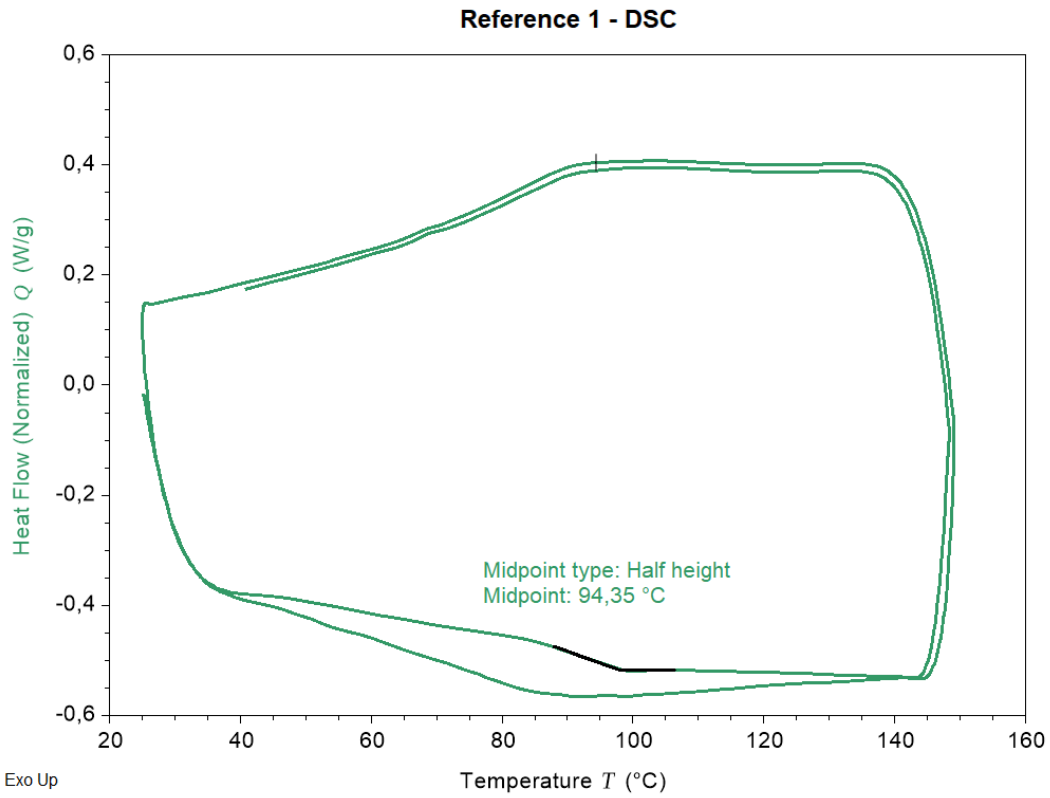

Figure 4.3.1. Example of DSC measure

No residual exothermic peak was found, which leads to the conclusion that complete curing is achieved for both reference and dynamic networks.

Table 4.3.1 includes the obtained T_g values. Indexes 1 and 2 again correspond to the manufacturing techniques.

	T_g (°C)		
	1	**2**	**Average**
Reference composite	94,35	84,36	89,36
Dynamic composite	-	167,04	167,04

Table 4.3.1. DSC T_g measurements

As before stated, definition of a single T_g value is obtained using standard conventions which are affected by the fact that the temperature range limits are selected manually. The user should be as accurate as possible selecting the temperature points in which the effects of the transition are markedly perceptible, but still dispersion is unavoidable.

Moreover, DSC and DMA samples are not comparable in size and shape, so the prescribed temperature ramps and gradients affect them differently. DSC samples weight ranges from 10 to 19 mg, so its heating rate can be considered homogeneous, while DMA samples are subjected to thermal gradients due to the epoxy's thermal properties.

DMA T_g values are lower than the ones of DSC for both samples, but they are approximately in the same temperature range. Reference composite's first DSC measurement was conducted one week after the manufacturing procedure which recommended curing at room temperature, while the second sample was measured straightaway, so its value shows an appreciable different T_g value with respect to DMA.

	DSC T_g (°C)	DMA T_g (°C)
Reference composite	89,36	77,86
Dynamic composite	167,04	163,58

Table 4.3.2. DSC and DMA T_g comparison

To complete the T_g assessment, the comparison between Paolillo's dynamic epoxy work [48] and our composite is included in Table 4.3.3, so to see if the values where analogous, as the presence of the fibre should not markedly affect the resin crosslinking process, and therefore its T_g.

	DSC T_g (°C)	DMA T_g (°C)
Dynamic epoxy	168,81	169,88
Dynamic composite	167,04	163,58

Table 4.3.3. DSC and DMA T_g comparison among the dynamic epoxy and the dynamic composite

5 Additional Functionalities

5.1 Mechanochromism

Mechanochromism is a colour change of a material induced by an external stimulus. It offers new potential functional properties in biomimetic camouflage devices, strain sensors, improvement of the understanding of stress transfer and identification of processes which can lead to mechanical failure. Mechanochromic behaviour can originate from changes in the molecular structure, disruption of intermolecular interactions or conformational arrangements. [72][73]

Regarding composites, the most relevant potential application is damage detection due to low- and medium-energy impacts, which until now can be only detected during aircraft's scheduled maintenance inspections, as it is located inside the laminate and can endanger the aircraft's structural integrity. Most common impact sources include hail, runway debris, ground collisions, engine rotor burst tools impact or bird strike.

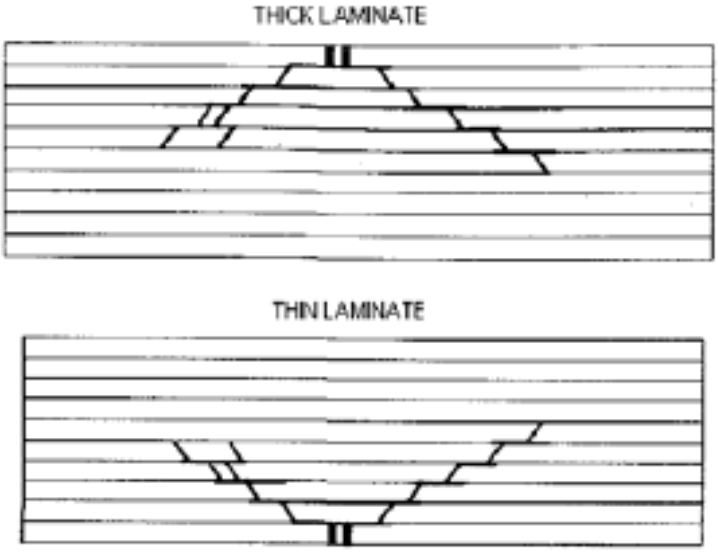

Figure 5.1.1. Delamination scheme after impact in thick and thin laminates

Current visual inspections in the field cannot reliably detect minor defects which may compromise the structure and non-destructive inspections (NDI) are difficult to implement, so the development of materials which are able to self-detect defects could greatly facilitate composites' maintenance and enhance composites' operation, as a faster detection and thus reparation could expand the boundaries of their use. [74]

The test specimen consists in a 100x100 mm three-fabric-layer dynamic composite's plate, which has been post-cured (see 2.2.1.2). The plate is subjected to an impact test which is carried out by letting fall vertically a spherical-end steel rod onto the sample. The rod is placed within a graduated plexiglass tube to assure a vertical fall, as impact energy depends on the fall characteristics, as it is assumed equal to the potential energy ($E_p = mgh$). To assess different impact energies, impact at various heights ranging from 10 to 180 cm are performed.

Figure 5.1.2. Steel rod and transparent plexiglass tube

Figure 5.1.3. Impact experiment setting

In case green coloration appears, the recovery of the original colour is first assessed at room temperature. The aim is studying the extension and intensity of the green coloration with different impact energies, the eventual breakage of the sample and the generated delamination. The latter is visualized using SEM.

Figure 5.1.4 and Table 5.1.1 resume the behaviour of the sample when impacted at different heights.

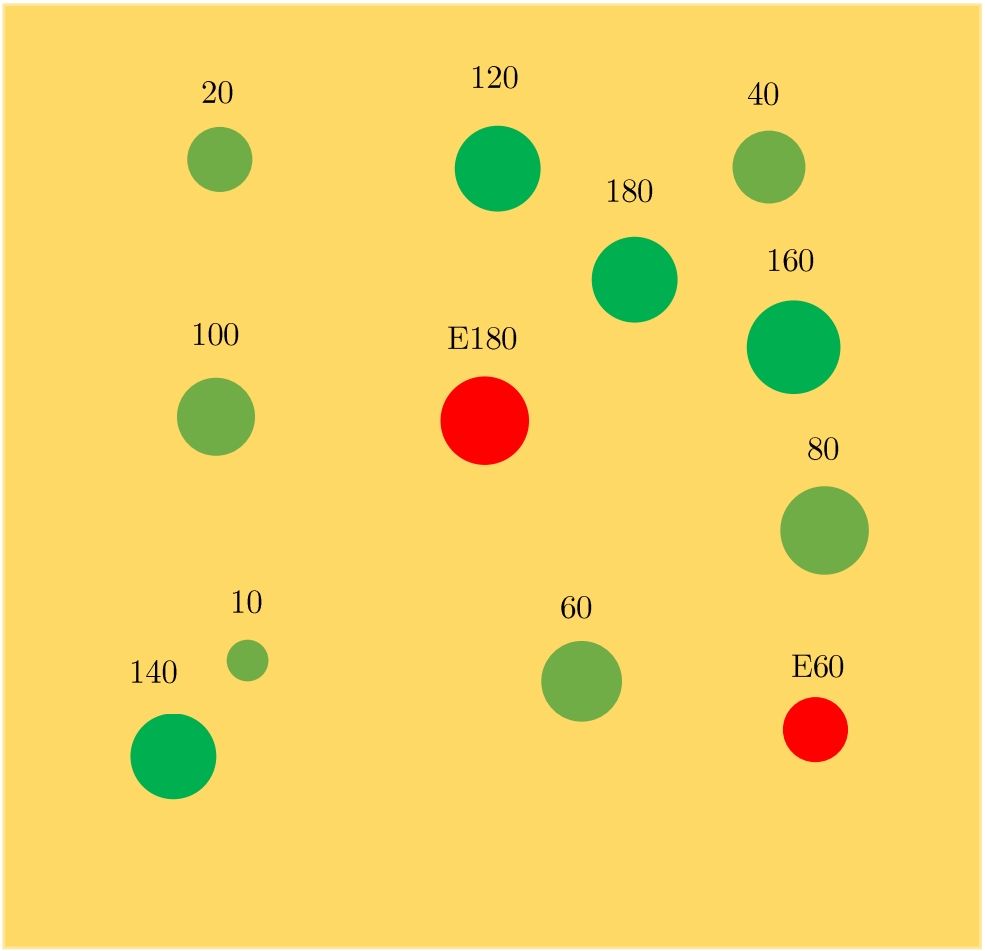

Figure 5.1.4. Impact tests scheme

Height (cm)	Impact energy (J)	Sample's behaviour
10	0,96	Light green coloration
20	1,92	Light green coloration

40	3,84	Light green coloration
60	5,76	Light green coloration Repeated (uncontrolled first impact)
80	7,68	Light green coloration
100	9,60	Light green coloration
120	11,52	Intense green coloration
140	13,44	Intense green coloration
160	15,36	Intense green coloration
180	17,28	Intense green coloration Repeated (uncontrolled first impact)

Table 5.1.1. Sample's impact behaviour

Compared to the pure epoxy resin, dynamic composite shows a remarkable and more straightforward mechanochromic response, as it is already visible even when subjected to low impact energies and can undergo medium-energy impacts without breaking. Due to the process' instrumentation, higher impact energies cannot be tested accurately, but observing the sample, breakage is likely to occur slightly increasing the received energy, as looking at the back part of the sample, it is observed that intrinsic damage has almost tear down the plate. Even for the tested heights, the experiment had to be carried out twice for the 60 and 180 cm trials due to an unstable fall of the rod. [48]

Green zone features are analysed using Image Pro Plus ©, ImageJ/Fiji and Matlab. Images were taken after each impact in order to have several images to measure the green zone area. Measurements are influenced by the user, as it is not an automated process, so the larger the quantity of images, the better accuracy of the measurement.

Figure 5.1.5 reports the green zone's characteristic area trend with the increment of impact height. As it can be observed, the zone tends to grow with impact energy following approximately a parabolic trend characterized by a significant rise for the

first impact tests (10 to 80 cm) and an almost asymptotic trend for higher impact energy tests. This behaviour agrees approximately with the change in the green coloration intensity, as the lower energy impacts are not as bright as the medium energy ones. The change in the intensity and the reduction in the coloured area may be due the generated delamination, as less energy is available for material deformation.

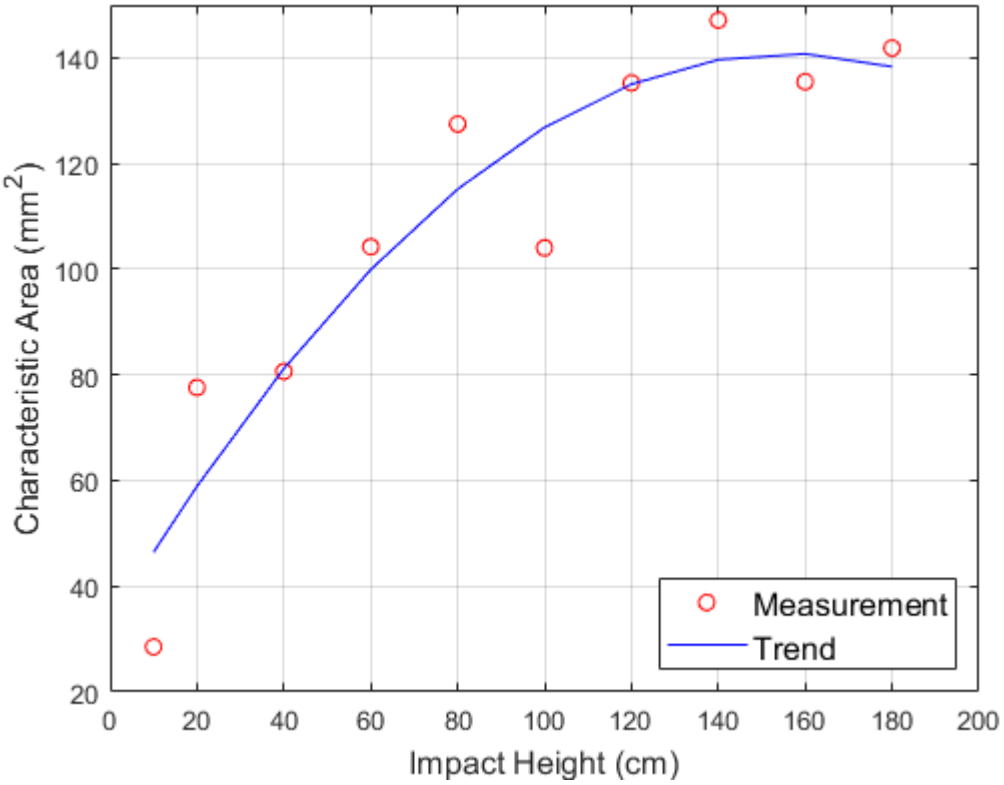

Figure 5.1.5. Green zone characteristic area vs Impact height

Intensity is measured using the RGB additive colour model. Considering each impact's intensity as the vector sum of each colour channel, the graph in Figure 5.1.6 is obtained. Measurements are obtained using the Matlab's Image Processing Toolbox. Figure 5.1.7. is provided as an example of how the intensity calculation is obtained.

Measurements follow a slightly decreasing linear trend which goes in line with the previously mentioned change in green coloration. Considering 100% intensity as

yellow colouring (no impact zone) and 0% intensity as the 180 cm impact, whenever impact energy increases, green colouring brightness is more remarkable and therefore further from yellow colouring.

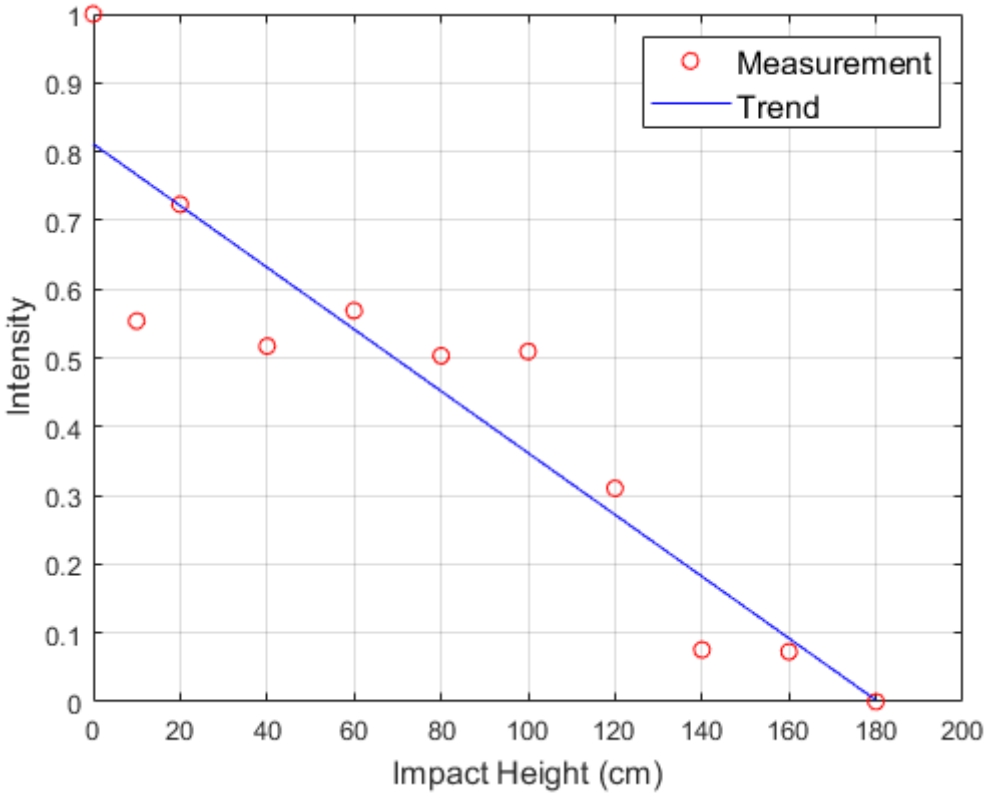

Figure 5.1.6. Color intensity vs Impact height

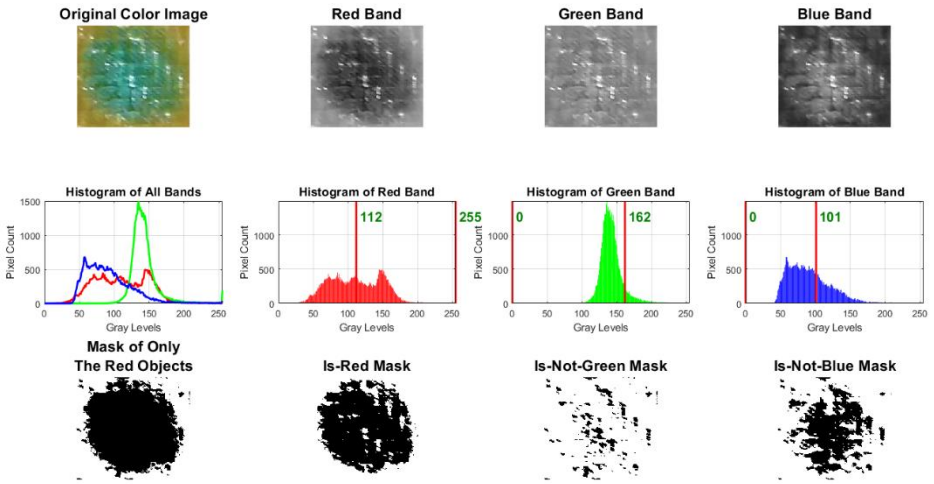

Figure 5.1.7. Example of intensity colouring calculation

Finally, the duration of the effect is assessed. As in Rekondo *et al.* [50], green coloration diminishes with time until it finally disappears.

First, green coloration behaviour is assessed at room temperature. Following images show the advance of green coloration with time at room temperature (right after impact, after 2 hours and 24 hours).

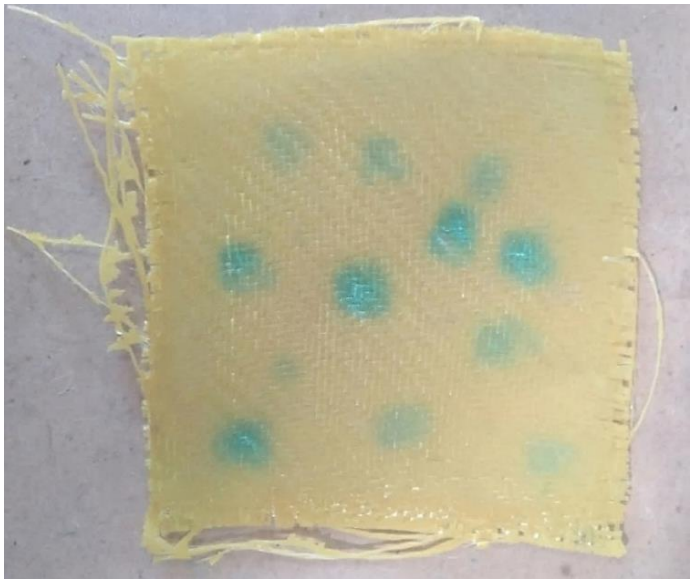

Figure 5.1.8. Sample after impact (room temperature): 0 hours

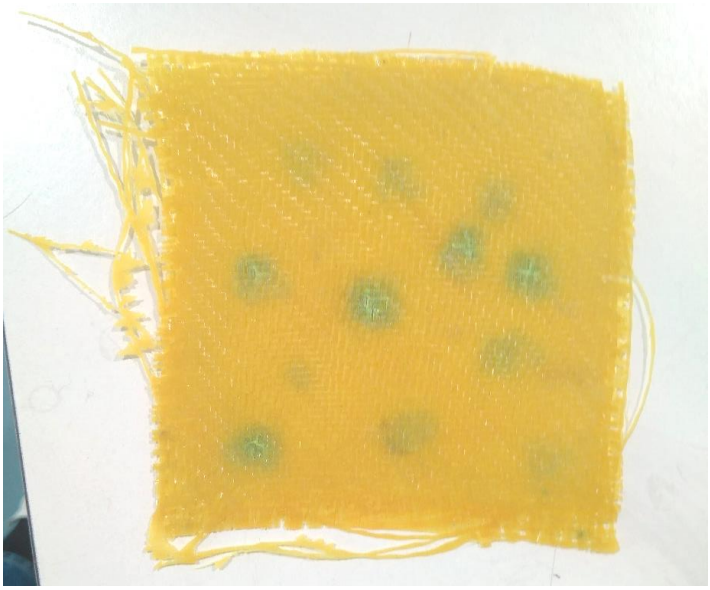

Figure 5.1.9. Samples after impact (room temperature): 2 hours

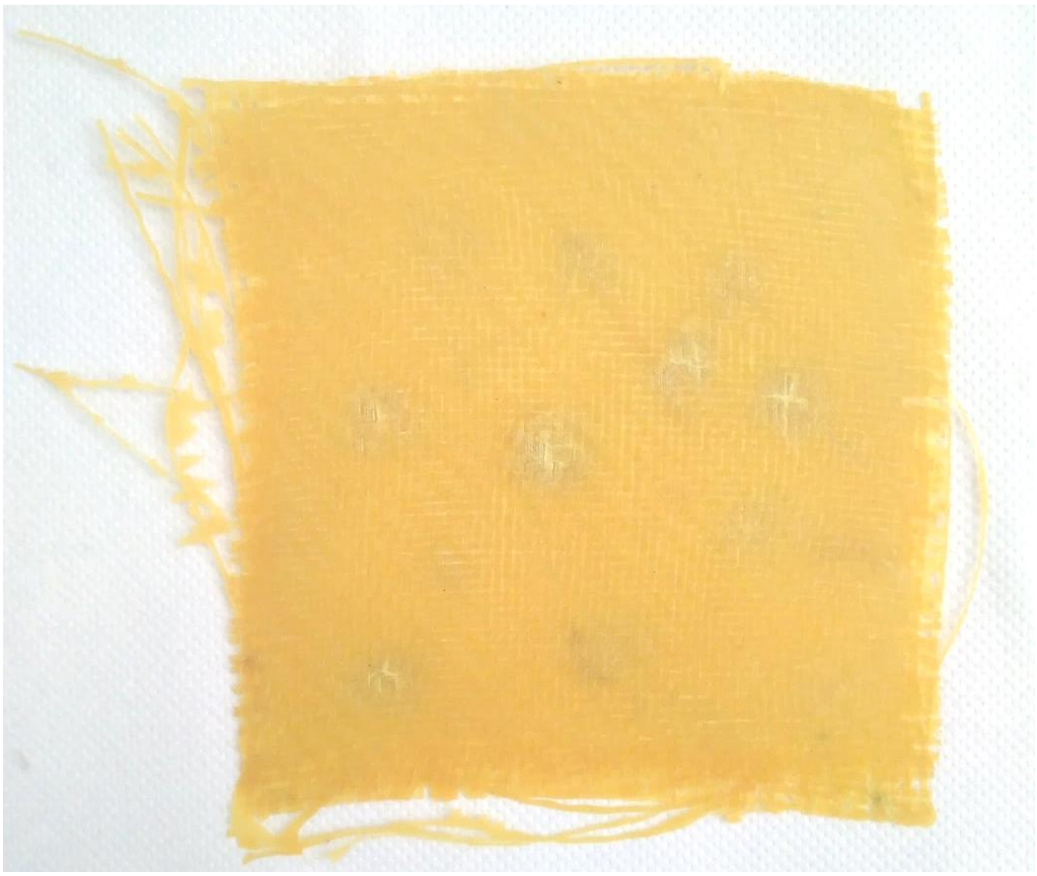

Figure 5.1.10. Sample after impact (room temperature): 24 hours

Further impact tests were performed in order to assess the influence of temperature on the mechanochromic behaviour and the structural recovery. Samples are subjected to 100 cm height impacts and then heated in the Memmert oven at 140 and 190°C, which means values under and upper the T_g, or frozen at -20°C. Height was chosen as a mean value of the performed impact tests.

	Temperature (°C)	**Time until disappearance**
Freezer	-20	< 4 days
Room temperature	25	~ 24 hours
Under T_g	140	30 – 40 seconds
Upper T_g	190	20 – 25 seconds

Table 5.1.2. Influence of temperature on green coloration duration

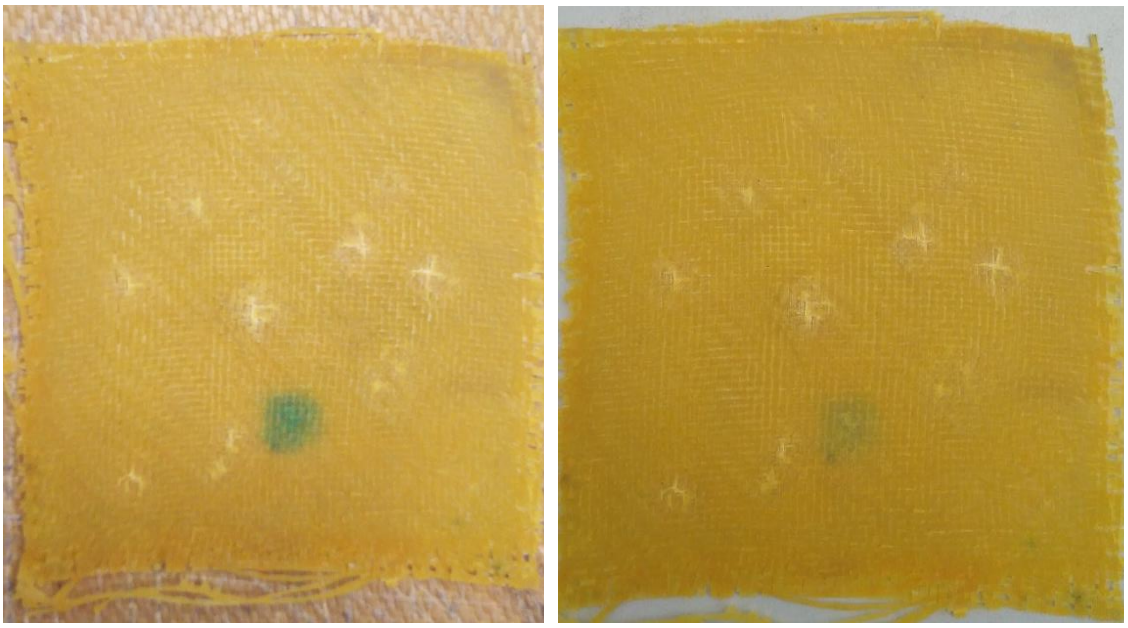

Figure 5.1.11. Change in green coloration (impact time, left and after 4 days, right) on a frozen sample

The difference in disappearance time shows that the mechanochromic feature is both time and temperature dependent. Increasing the temperature, polymer chains gain mobility, even when the used temperature is lower but close to T_g, so the mechanochromic behaviour duration is reduced. On the contrary, when temperature decreases, green coloration is maintained for several days and does not disappear during the experimental procedure duration (see in Figure 5.1.11).

Supposedly self-healing behaviour should also follow this trend. In order to assess the self-healing composite capability, the plate is cut to obtain both DMA and SEM samples to analyse the composite's modulus and delamination structure.

DMA trials follow the single frequency mode approach (see Section 4.2). Both samples include impact tests with the highest tested energy, equivalent to 180 cm height impact.

As explained in Section 4.2, error has multiple sources of uncertainty, so its value is not highly reliable. Still it is remarkable that even with a damaged inner structure,

the complex modulus value is in the range of the non-damaged samples, which means that the sample can undergo medium energy impacts without losing completely its integrity.

	E* (MPa)	**E_c (MPa)**	**Error (%)**
Sample 1	18313,37	18743,47	-2,29
Sample 2	13943,04		-25,61

Table 5.1.3. Effect of impact test on the complex modulus

Finally, 160 cm impact height sample is observed using SEM to assess the delamination structure using a visualization technique. A complete scan of the surface was made with 150x magnification.

Analysing the images, several delamination patterns can be observed along the scanned sample (Figure 5.1.12 along with 5.1.13, Figure 5.1.14 along with 5.1.15, Figure 5.1.16 along with 5.1.17 and Figure 5.1.18). Their extension varies with the distance to the impacted zone, being the largest one in Figure 5.1.16 and 5.1.17, and the presence of prior manufacturing defects.

Delamination spreads more easily, that meaning, with less energy transformation, when a void is already present within the structure. Nonetheless, delamination does not seem to affect the complete sample thickness, which means that the specimen could still sustain loads effectively before breakage. This feature is especially remarkable since this sample was only formed by three reinforcement layers and therefore its thickness is 30% lower than the one of the samples used for mechanical characterization.

Not complete extension of the delamination through-the-thickness goes in line with the relative preservation of mechanical properties observed in the DMA results. Further tests should be carried out to assess the energy needed for material complete breakage.

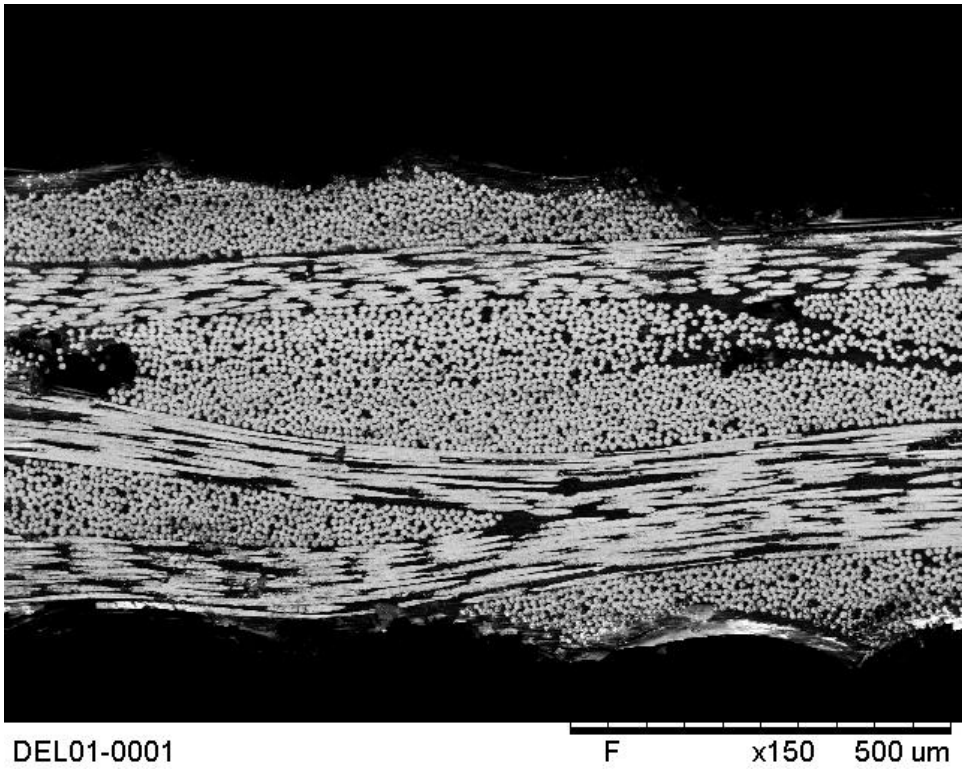

Figure 5.1.12. SEM: delamination structure (1)

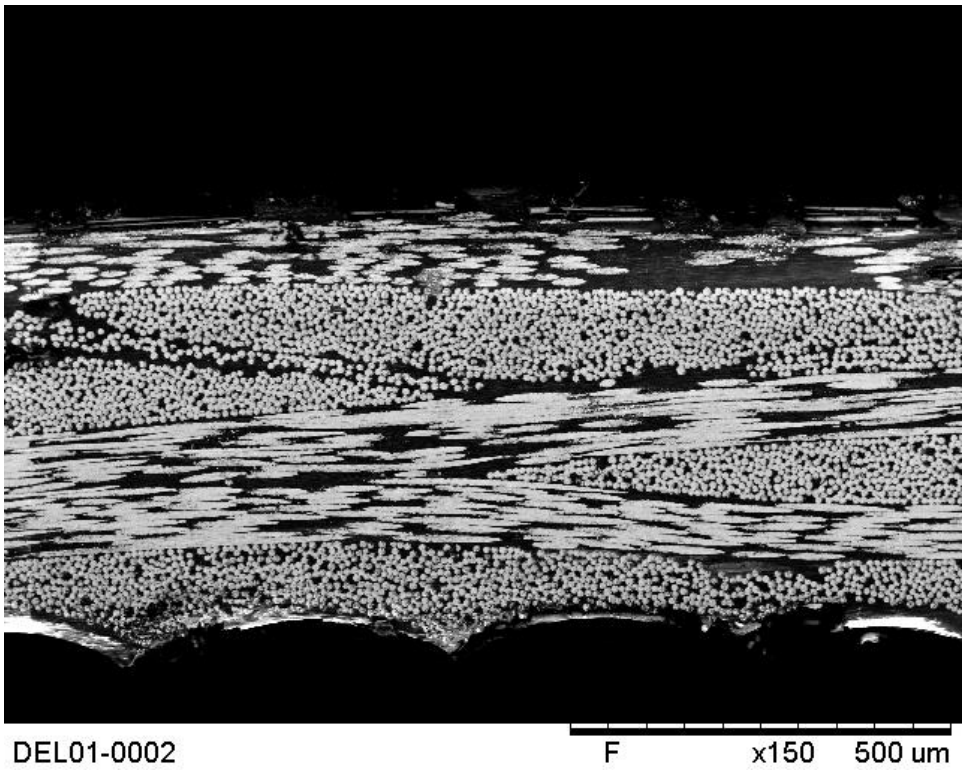

Figure 5.1.13. SEM: delamination structure (2)

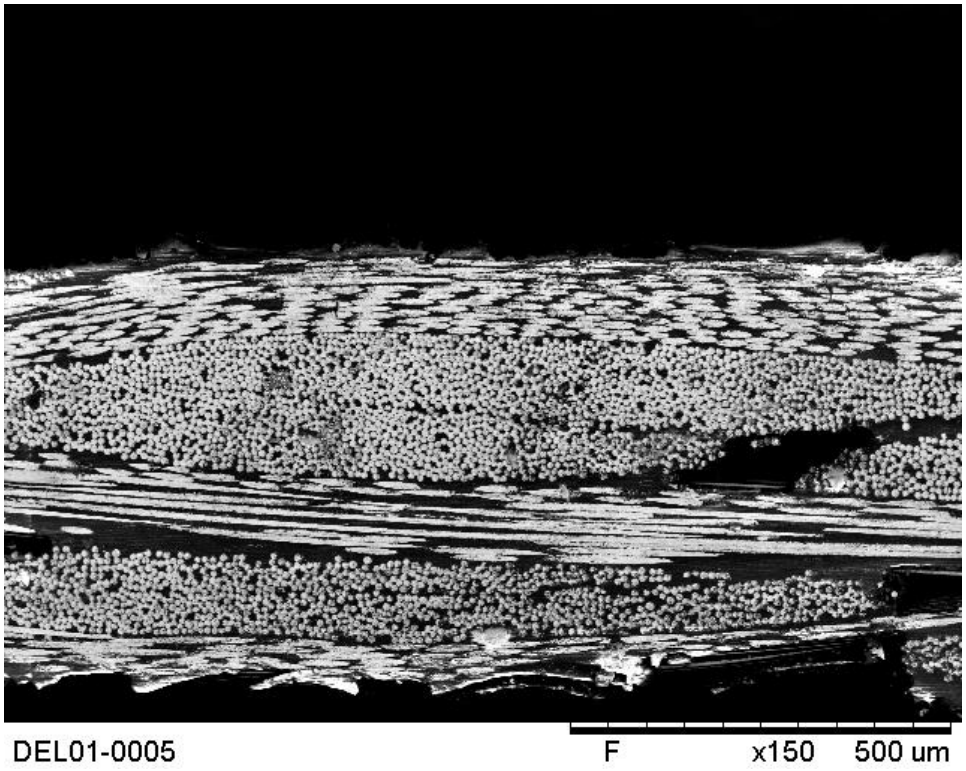

Figure 5.1.14. SEM: delamination structure (3)

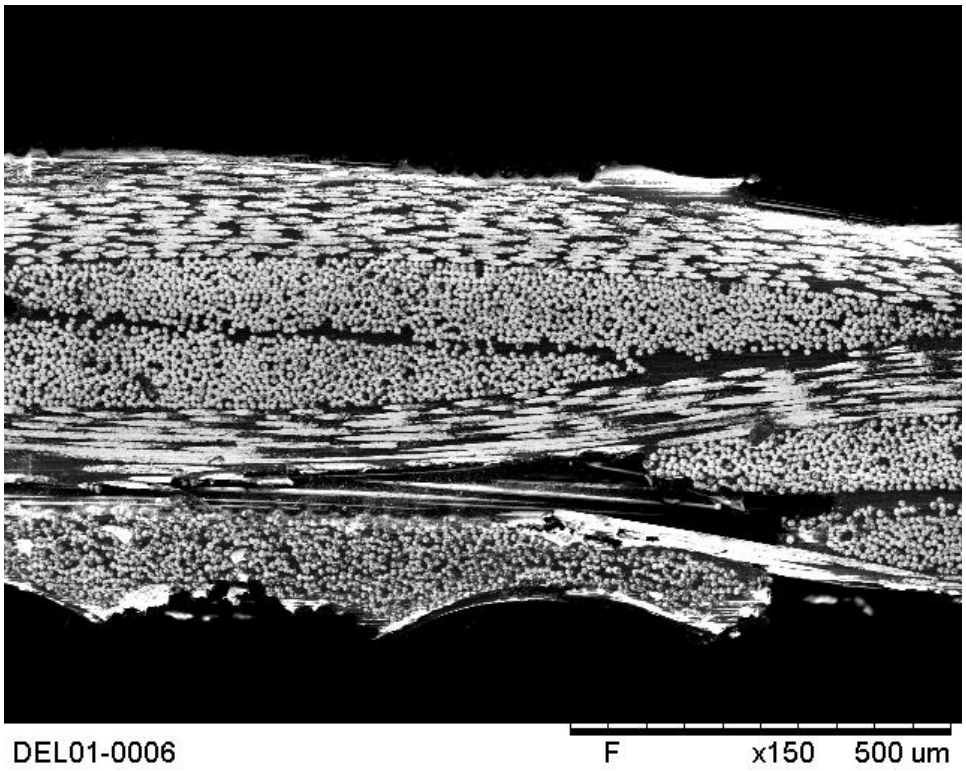

Figure 5.1.15. SEM: delamination structure (4)

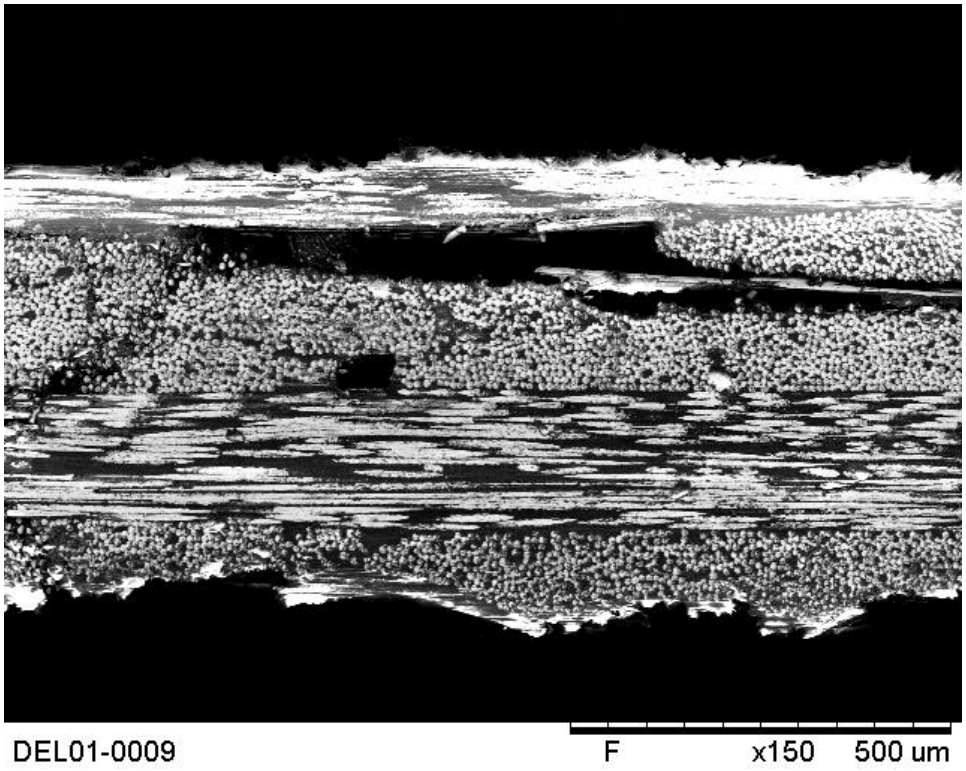

Figure 5.1.16. SEM: delamination structure (5)

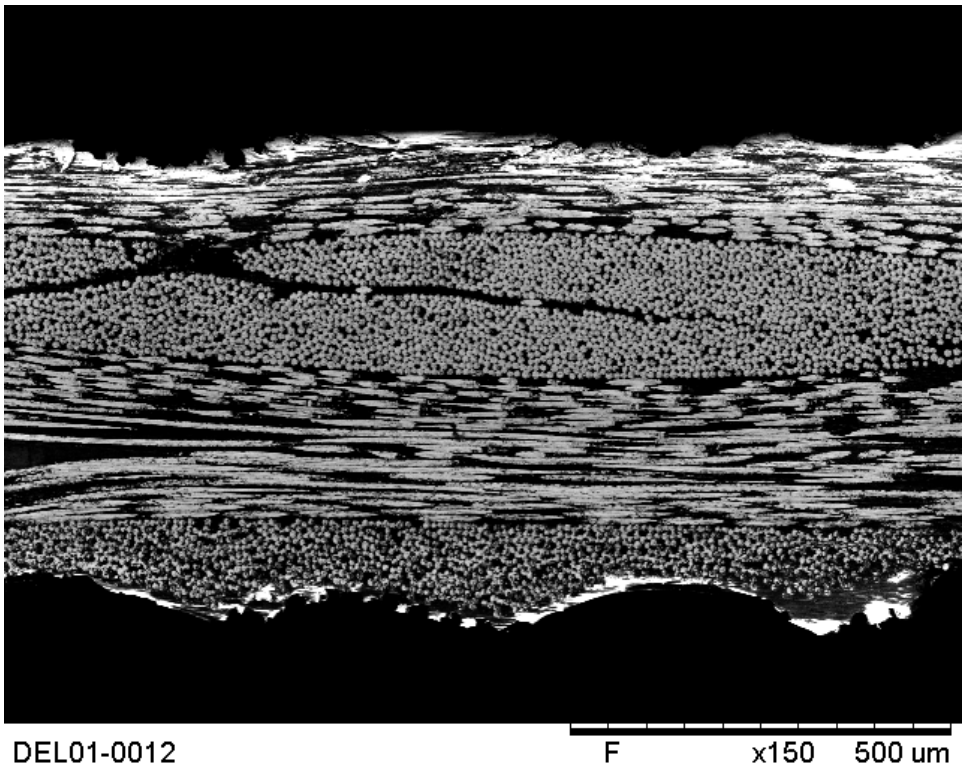

Figure 5.1.17. SEM: delamination structure (6)

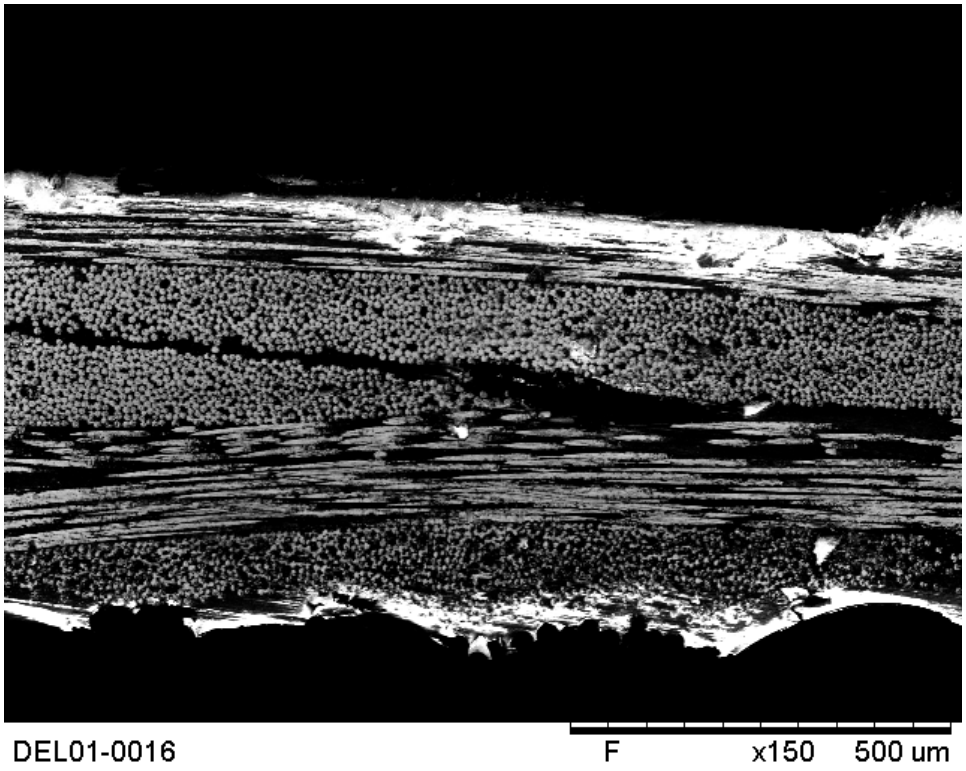

Figure 5.1.18. SEM: delamination structure (7)

5.2 Reprocessability

Thermoforming is one of the oldest, fastest and with higher efficiency plastics' forming processes characterized by low cycle time, low cost of tooling and relative cleanliness. Thermoforming process steps are explained in Figure 5.2.1. [77][78]

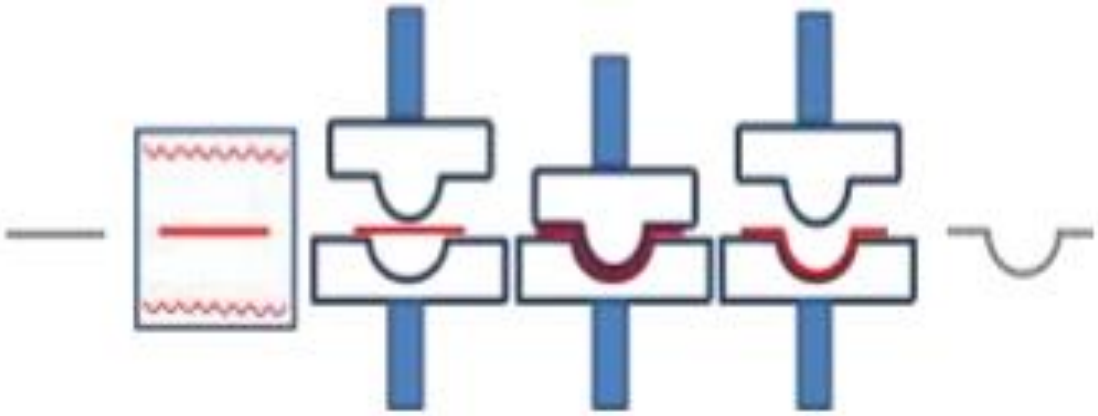

Figure 5.2.1. Thermoforming process: lay-up, preheating, positioning, pressure application, demoulding and component attainment (from left to right) [78]

So far thermoforming could be just applied to thermoplastics, but tests are carried out using dynamic covalent thermoset polymers to evaluate their eventual reprocessability. The introduction of thermoforming might mean the automatization of thermosets manufacturing techniques and therefore allowing mass production of high-performance composites. [78]

Within aerospace industry, one of the main applications of reprocessable composite structures could be corrugated structures production, which are a part of morphing wings. Along with self-healing materials, morphing structures are one of the most promising biomimetic approaches under development. Being able to modify the aircraft's structure during flight makes it possible to optimize the aircraft's configuration for each flight mission stage.

Corrugated structures main feature is their extremely anisotropic behaviour: high stiffness transverse to the corrugation direction and compliance along the

corrugation direction. This drives to high stiffness to weight ratio and high capacity of energy absorption, which are issues of critical importance for the aircraft's total weight and performance. Corrugated structures are chosen for morphing wings' manufacturing because they are stiff enough to withstand bending caused by aerodynamic forces, and flexible to deform according to the morphing actuation. [79]

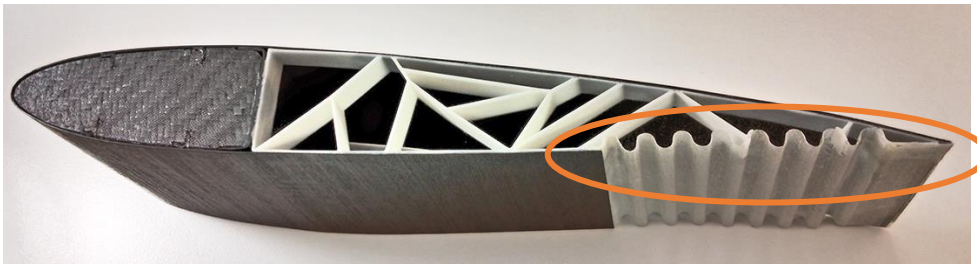

Figure 5.2.2. Morphing wing with corrugated structure [80]

Rekondo et al. [50] tested the dynamic composite thermoforming capability using a zig-zag shaped mould, so in order to increase the thermoforming complexity, the projected geometry prism-shaped mould with rounded edges. Cast is manufactured in aluminium.

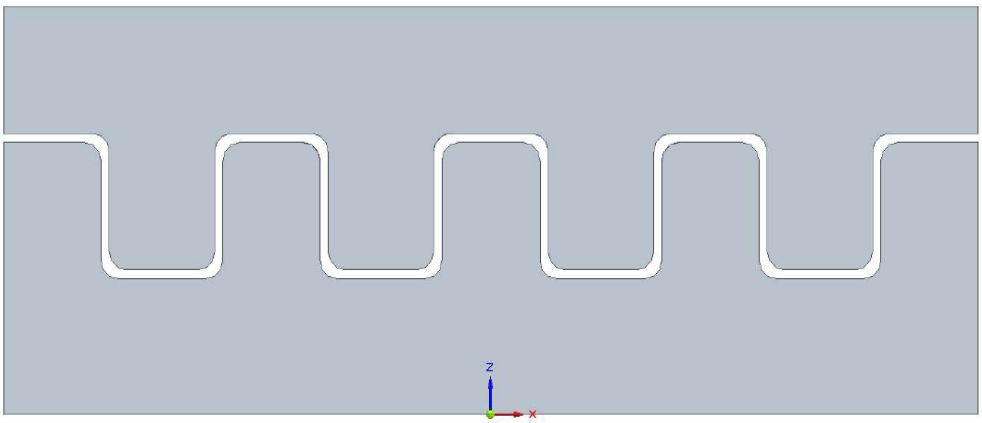

Figure 5.2.3. Mould 2D projection: geometry

To obtain the reprocessed sample, the mould is preheated with the sample placed within it till 200 °C and then 10 bar pressure is applied for 5 min maintaining temperature. Sample needs to be heated to enable material's relaxation.

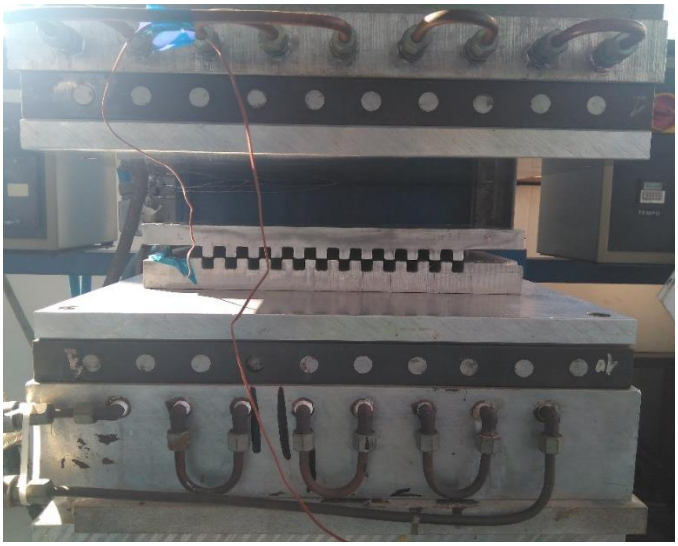

Figure 5.2.4. Sample and mould placed within the hot press before pressure application

Results of this test were partially satisfactory in terms of reprocessability, as the sample was in part reshaped. Due to the presence of vertical walls in the geometry and the small dimensional tolerance between the male and female offset, fibre reinforcement elongates until it breaks, as it is not able to adapt its shape to the mould shape, so further geometries should be tried in order to assess the material's reshaping capability.

Figure 5.2.5. Sample after reshaping 1

Figure 5.2.6. Sample after reshaping 2

Besides the sample breakage, maintaining the sample at high temperature while preheating and reprocessing causes the material's degradation. To avoid material degradation and favour reprocessability, several parameters of the experimental procedure can be improved: using a smaller mould to facilitate its handling and the specimen placing, so that it is subjected to 200°C less time and therefore the composite degradation is lowered and using a geometry with smoother radii of curvature and higher dimensional tolerance.

5.3 Repairability

Damage in composites is characterized by the presence of various damage mechanisms like progressive intra-laminar matrix damage, fibre-matrix interface debonding, abrasion, cracks, tensile and compressive fibres failure or inter-laminar delaminations, which occur in different load conditions such as shear, bending, transversely applied loads or impact under both monotonic or cyclic regimes. Current repair techniques are expensive and slow, since trained workers and special techniques are required, so to become more competitive against light alloys, faster and more straightforward methods need to be developed. The aim is allowing rapid reversible reactions under a convenient stimulus to restore the network's service conditions. [50]

Among the composite's failure mechanisms, it is worth briefly explaining how delamination works, at it is the most critical and a unique feature of composite materials in comparison to metallic materials. It is generated by inter-laminar stresses combined with low through-thickness strength. Due to the composite's configuration, fibres do not provide reinforcement through the thickness, so the matrix, which strength is neglectable in comparison to the one of the fibres, is in charge of sustaining loads in that direction. [81]

Several experimental procedures could be used as an approach to assess the composite's repair capability, as composites are subjected to several failure modes, as stated above. In this thesis, self-adhesion is evaluated by means of two rectangular 60x10x1 mm samples cut from the pristine dynamic plate which are subjected to pressure and high temperature (around 200°C). First, the sample is placed in the press under atmospheric pressure and high temperature for around 10 minutes to let the specimen relax and then pressure is applied for other 10 minutes. Figure 5.3.1 shows the used hot press. Accurate control of both pressure and temperature is difficult due to the press' configuration, but a thermocouple is

placed to control that the temperature does not vary greatly from the 200°C proposed range.

Figure 5.3.1. Hot press

Self-adhesion could be used as an alternative technique of mechanically fastened joints, as adhesively bonded joints have the advantage of involving few parts, full load transfer capability, sealing, weight reduction and no stress concentration. [82]

Figure 5.3.2 presents the sample before and after the self-adhesion test. As it can be seen, satisfactory results are obtained in terms of adhesion, since both samples remain bonded, but looking at the samples colour change, material's degradation is observed, which leads to lower mechanical properties. The main cause of material's degradation is that it must be subjected to high temperatures and that the degradation temperature may have been reached.

Used samples were first used in the impact tests (see Section 5.1), so delamination was present. After the adhesion test, delamination is still observable, so the use of a higher pressure may be advisable, as suggested by Ruiz de Luzuriaga *et al.* [40]

Pure dynamic epoxy resin samples show an analogous behaviour both in terms of adhesion and material's degradation, but longer relaxation time is needed, and lower pressure can be applied due to the material's mechanical properties, as higher-pressure values lead to breakage prior to the desired adhesion.

Figure 5.3.2. Samples before (left) and after (right) the adhesion test

In order to assess the adhesive strength of self-adhered samples, two samples with a smaller overlap area (left part in Figure 5.3.4) are generated. They are subjected to a tensile test, from which the stress-strain curve is obtained. Tests are performed using the Instron 4302 tensile testing machine and data are collected by Instron Series IX. Samples are tested with a constant speed of 1mm/min, which means that the sample is subjected to 1 mm deformation per minute.

Stress-strain curve is obtained from the load and displacement recorded data in order to calculate Young's modulus, which can be computed as the slope of the curve's elastic region and compared to the values obtained during the mechanical characterization (see section 4.2).

Figure 5.3.3. Instron 4302 tensile testing machine

First the samples are assessed visually after the performed tests. Tensile test samples usually contain a contraction area, which is the weakest part of the sample in which breakage occurs during tensile test. In our case, the adhesive area is equivalent to the contraction area, so as supposed, it is the zone in which samples break. Light green coloration can be observed, which means that defects are prone to have formed.

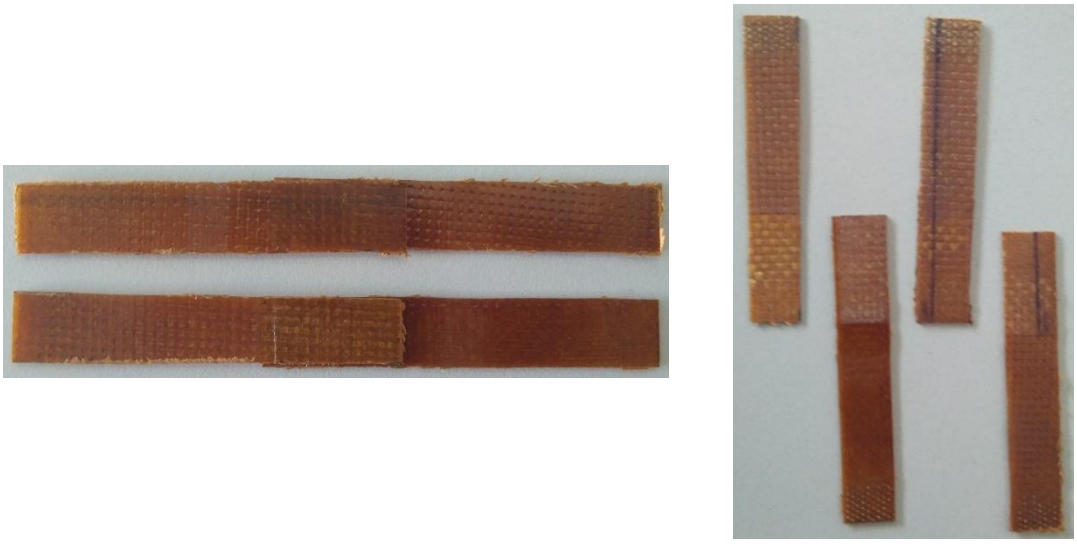

Figure 5.3.4. Tensile test samples before (left) and after (right) the tests

Stress-strain curves suggest a consistent mechanical behaviour of the adhered samples, as Young's modulus are comparable. Difference in breakage stress is just due to the different cross section area of the tested samples, as the first sample is thinner than the second one. Force-displacement and stress-strain curves are analogous, but with the purpose of computing the adhesive stress, force-displacement curve is plotted in Figure 5.3.5.

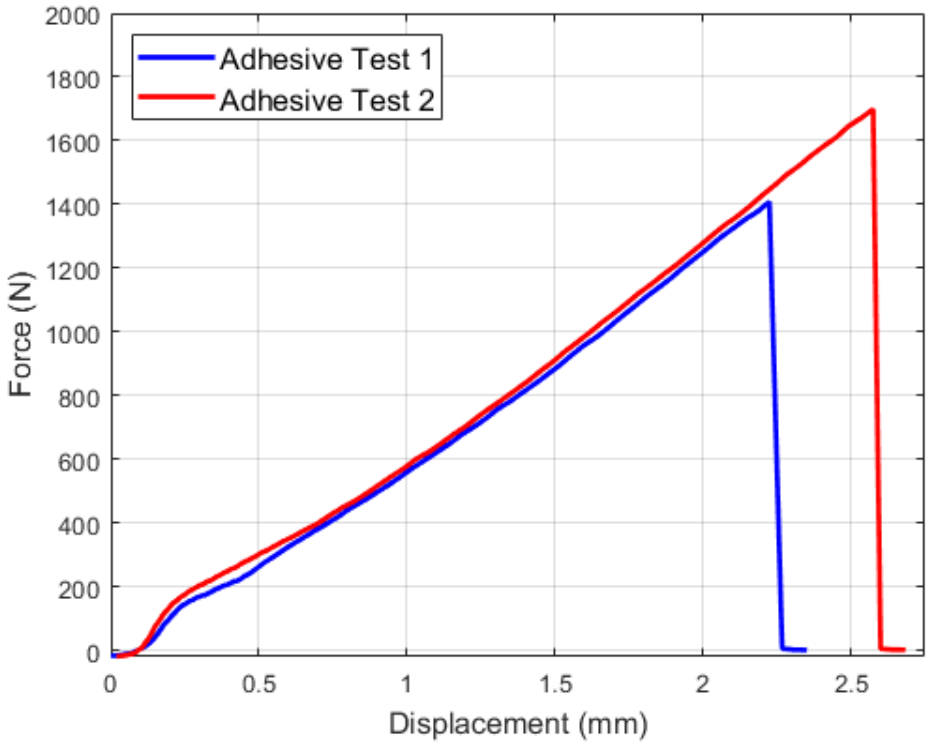

Figure 5.3.5. Stress-strain curve

Force and displacement at break, average elastic modulus and adhesive stress are resumed in Table 5.3.1. Adhesive stress is equivalent to the shear stress to which the overlap area is subjected, so it is calculated as the ratio of the maximum supported load and the adhered area. Difference in adhesive s

	Adhesive Sample 1	**Adhesive Sample 2**
Force at break (N)	1408	1699
Displacement at break (mm)	2.23	2.68
Elastic modulus (MPa)	20747	22371
Adhesive stress (MPa)	6.71	8.09

Table 5.3.1. Mechanical properties of adhesive samples

Comparing the elastic modulus value with the one obtained in DMA tests, adhesive samples show a higher stiffness than not adhesive ones, but it may be due to the fact that a tensile test instead of a flexural test has been carried out, so further tensile tests should be performed to record the pristine samples tensile elastic modulus.

6 Conclusions

This thesis has dealt with the manufacturing, mechanical characterization and functional assessment of an intrinsic self-healing glass fibre reinforced composite. The intention was to make a comparative study between a reference industrial epoxy network and a dynamic matrix maintaining the same fibre reinforcement. Therefore, the first step towards achieving this purpose was the choice of the sample's composition and the implemented manufacturing technique.

Reference epoxy network's parameters were chosen according to the technical data sheet, ensuring more reliable results. An exception was the implemented curing time at room temperature, which was reduced in order to harmonize the curing procedure with the one used for the dynamic matrix. Dynamic matrix is instead not completely characterized, so the hypothesis of stoichiometric mix ratio for the reaction of resin and hardener was made. Maintaining 4 – AFD as dynamic hardener, further research could be carried out tuning stoichiometry. This would lead to the obtention of materials with different mechanical properties and glass transition temperatures, which means more suitable materials for each desired application.

With respect to the manufacturing techniques, two different processes were tested: vacuum bagging and hot press. Both methods are standard procedures within the composite's manufacturing industry, but the fact that manual materials mixing and lay-up were chosen introduced uncertainty in the composite's structure and composition. Autoclave could have also been used for the composite's curing, but it would have been an energy waste considering the sample's simple shape and size.

The choice of the hot press as reference manufacturing procedure was based on the higher compliance of the 50% fibre volume fraction requirement and the lower void volume fraction values, assessed experimentally using SEM and the Archimedes' principle.

Voids and porosity are critical imperfections within the structure of fibre reinforced composites, so its characterization is crucial.

Archimedes' principle accuracy depends mainly on the precise knowledge of the reinforcement and matrix's density, as well as its weight fraction values. Dynamic matrix's density is unknown and weight fractions are calculated by weighting the introduced fibre reinforcement and matrix and the final obtained sample, but during the laminate's lay-up some fibres peel away, so required data for the density's calculation are slightly compromised and reference data are used reducing the method's accuracy.

SEM is a visual, destructive analysis technique which allows the characterization of the void's size, shape and distribution, but only in a 2D cross-section, which introduces again an error in the void characterization.

Little *et al.* [70] and Di Landro *et al.* [76] suggests further void characterization techniques, such as matrix burn-off, matrix digestion or micro-computed tomography which are out of the scope of this thesis. Still, it is worth mentioning that the obtained void fraction values are in line with their results despite the aforementioned error sources.

Mechanical characterization was completed carrying out DSC and DMA tests. Comparable thermal and mechanical properties are obtained when testing the dynamic composite with respect to the reference composite, which provides a positive picture for the future, since a more straightforward introduction of this kind of materials in industrial applications will be possible if they can provide the same level of performance.

The main challenge of the composite's characterization was the Young's modulus assessment, as DMA single frequency tests had to be repeated due to a first extremely large deviation from the theoretical rule-of-mixtures computed value. Still 10 to 20% error range are found due to the use of a bidirectional fibre

reinforcement, manual lay-up and the use of reference Young's modulus to calculate the theoretical rule-of-mixtures modulus value.

A distinguishing feature which is also assessed during the mechanical tests is the material's stress relaxation, which aim is characterizing the heat-induced malleability of materials. Tests showed a significant relaxation test around the T_g temperature range and higher temperatures. Results demonstrate that relaxation is higher when no fibre reinforcement is present, but still opens an opportunity to test if the proposed material has the capacity of changing its shape when subjected to high temperatures.

Reprocessability tests did not provide the complete reshaping of the tested sample, so further tuning of the test parameters should be carried out. Our trial aimed achieved a very complex shape, but still research is in early stages, so a more progressive approach could provide more satisfactory results.

Besides reprocessability, eventual repairability was also assessed by testing self-adhesion. Adhesion was achieved and material mechanical properties are consistent with the mechanical characterization results, so even if the material seem to be degradated, test results are promising and open the door for the development of further repairing techniques.

Finally, a significant and innovative feature found when testing the dynamic composite is mechanochromism. Mechanochromic behaviour is attributed to the creation of radicals when subjecting the dynamic composite to a test which induces energy into the composite's matrix structure. Depending on the temperature at which the sample is preserved, green coloration eventually disappears when radicals bond to generate again disulphide bridges. High temperatures facilitate chemical crosslinking by inducing mobility to the polymer chains. Moreover, extension and intensity of the coloured zone depends on the received energy, since the area tends to increase with energy till delamination starts, as less energy is available for material deformation.

Industrial-scale production of the proposed composite could be carried out since the used materials are readily available and as stated before, no innovative manufacturing techniques have been used. Thermomechanical performance values are in the same range as the ones presented by current fibre reinforced composites and furthermore, they have promising functional features which in the long run could reduce manufacturing costs, which is crucial to introduce this kind of materials in mass production sectors such as automotive industry, construction, renewable energy industry and obviously, aerospace industry.

Further research should be conducted to gain a broader insight into dynamic covalent chemistry and its benefits, so that this kind of smart materials' production becomes cheaper and therefore its clearly innovative properties can be widely exploited to create more sustainable engineering products.

Acknowledgements

In order to finish this thesis, I would like to thank all the people and institutions that made it possible.

First, I appreciate Politecnico di Milano for giving me the opportunity to come to Milan as a guest student as part of the Double Degree program, as I do really think it is a unique way to broaden horizons and acquire different perspectives towards engineering.

Focusing on the people, I would especially like to thank Dr. Ing. Antonio Mattia Grande for being so supportive, always willing to help and really committed to student's work.

Furthermore, I also need to thank Ing. Stefano Paolillo and Mrs. Maria Rosaria Pagano for constantly support me by sharing their experience and knowledge, and Dr. Ing. Matteo Boiocchi and Mr. Alessandro Maggiolini for helping me carry out my experimentation.

On the second place, I would also like to thank my home university, Escuela Técnica Superior de Ingeniería Aeronáutica y del Espacio. Being closed to the end of my studies, I can only realize that I made the right choice when I decided to study Aerospace Engineering at this university.

And last, but certainly not least, I would like to express my gratitude to my family and friends. Even most of you are back home, I have always felt you close. Particularly I would like to thank my parents for having always supported my decisions, and Ángel, for listening to all my ups and downs and staying always by my side. Somehow this work is yours.

Bibliography

[1] Chrzanowski, W., Khademhosseini, A. (2013). *"Biologically inspired 'smart' materials"*, Advanced Drug Delivery Reviews.

[2] Kamila, S. (2013). *"Introduction, classification and applications of smart materials: an overview"*. American Journal of Applied Sciences 10 (8), pp. 876-880.

[3] Garcia, S.J., Fischer, H.R. (2014). *"9-Self-healing polymer systems: properties, synthesis and applications"*. In: Aguilar, M.R., Román, J.S. (Eds.), *"Smart Polymers and Their Applications"*, Woodhead Publishing, pp. 271-298.

[4] NL Innovation (2013). *"Self healing materials: concept and applications"*, NL Agency.

[5] Van der Zwaag, S., Grande, A.M., Post, W., Garcia, S. J., Bor, T.C. (2014). *"Review of current strategies to induce self-healing behaviour in fibre reinforced polymer-based composites"*. Materials Science and Technology, 30:13, pp. 1633-1641.

[6] Hager, M.D.; Greil, P.; Leyens, C.; Van Der Zwaag, S.; Schubert, U.S. (2010). *"Self-healing materials".* Advanced Materials, Vol.22(47), pp. 5424-5430.

[7] Das, R., Melchior, C., Karumbaiah, K.M. (2016). *"11-Self-healing composites for aerospace applications"*. In: Rana, S., Fangueiro, R., *"Advanced Composite Materials for Aerospace Engineering: Processing, Properties and Applications"*, Woodhead Publishing, pp. 333-359.

[8] Bekas, D.G., Tsirka, K., Baltzis, D., Paipetis, A.S. (2015). *"Self-healing materials: A review of advances in materials, evaluation, characterization and monitoring techniques"*. Composites Part B: Engineering Volume 87, pp. 92-119.

[9] Wang, Y., Pham, D.T., Ji, C. (2015). *"Self-healing composites: A review"*. Cogent Engineering, 2(1), 1075686.

[10] Yuan, Y. C., Yin, T., Rong, M. Z., Zhang, M.Q. (2008). *"Self-healing in polymers and polymer composites. Concepts, realization and outlook: A review"*. eXPRESS Polymer Letters Vol.2, No.4, pp. 238-250.

[11] White, S. R., Sottos, N. R., Geubelle, P. H., Moore, J. S., Kessler, M. R., Sriram, S. R., Viswanathan, S. (2001). *"Autonomic healing of polymer composites"*. Nature, 409, pp. 794–797.

[12] Bond, I.P., Trask, R.S., Williams, H.R. (2008). *"Self-healing fiber-reinforced polymer composites"*. MRS Bulletin 33 (08), pp. 770-774.

[13] Hamilton, A.R., Sottos, N.R., White, S.R. (2010). *"Self-healing of internal damage in synthetic vascular materials"*. Advanced Materials 22 (45), 5159.

[14] Mphalele, K., Ray S. S., Kolesnikov, A. (2017). *"Self-healing Polymeric Composite Material Design, Failure Analysis and Future Outlook: A Review"*. Polymers 9, 535.

[15] Kalista Jr, S. J., Ward, T. C. (2007). *"Thermal characteristics of the self-healing response in poly(ethylene-co-methacrylic acid) copolymers"*. Journal of the Royal Society Interface 4, pp. 405-411.

[16] Varley, R. J., Shen, S., van der Zwaag, S. (2010). *"The effect of cluster plasticisation on the self healing behaviour of ionomers"* Polymer 51, pp. 679-686.

[17] Ghosh, S. K. (2009). *"Self-healing Materials: Fundamentals, Design Strategies and Applications"*. Wiley-VCH Verlag GmbH & Co. KGaA, Weinheim.

[18] Chen, J., Huang, Y., Ma, X., Lei, Y. (2018*). "Functional self-healing materials and their potential applications in biomedical engineering"*. Advanced Composite Hybrid Materials 1, pp 94-113.

[19] Scheiner, M., Dickens, T. J., Okoli, O. (2016). *"Progress towards self-healing polymers for composite structural applications"*. Polymer 83, pp 260-282.

[20] Min, Y., Huang, S., Wang, Y., Zhang, Z., Du, B., Zhang, X., Fan, Z. (2015). "Sonochemical Transformation of Epoxy-Amine Thermoset into Soluble and Reusable Polymers". Macromolecules 18, pp. 316-322.

[21] Jin, F., Li, X., Park, S. (2015). *"Synthesis and application of epoxy resins: A review"*. Journal of Industrial and Engineering Chemistry 29, pp. 1-11.

[22] Oliveux, G., Dandy, L. O., Leeke, G. A. (2015). *"Current status of recycling of fibre reinforced polymers: Review of technologies, reuse and resulting properties"*. Progress in Material Science 72, pp. 61-99.

[23] Matxain, J. M., Asua, J. M., Ruipérez, F. (2016). *"Design of new disulphide-based organic compounds for the improvement of self-healing materials"*. Phys. Chem Chem. Phys. 18, 1758.

[24] Grande, A. M., Martin, R., Odriozola, I., van der Zwaag, S., Garcia, S. J. (2017). *"Effect of the polymer structure on the viscoelastic and interfacial healing behaviour of poly(urea-urethane) networks containing aromatic disulphides"*. European Polymer Journal 97, pp. 120-128.

[25] Ruiz de Luzuriaga, A., Matxain, J. M., Ruipérez, F., Martín, R., Asua, J. M., Cabañero, G., Odriozola, I. (2016) *"Transient mechanochromism in epoxy vitrimer composites containing aromatic disulphide crosslinks"*. Journal of Materials Chemistry C 4, 6220.

[26] Azcune, I., Odriozola I. (2016). *"Aromatic disulphide crosslinks in polymer systems: Self-healing, reprocessability, recyclability and more"*. European Polymer Journal 84, pp. 147-160.

[27] Martín, R., Rekondo, A., Ruiz de Luzuriaga, A., Casuso, P., Dupin, D., Cabañero, G., Grande, H. J., Odriozola, I. (2016). *"Dynamic sulfur chemistry as a key tool in the design of self-healing polymers"*. Smart Materials and Structures 25, 084017.

[28] Saba, N., Jawaid, M., Alothman, O. Y., Paridah, M. T., Hassan, A. (2015). *"Recent advanced in epoxy resin, natural fiber-reinforced epoxy composites and their applications"*. Journal of Reinforced Plastics and Composites 0(0), pp. 1-24.

[29] Lehn, J. M. (2013). *"Dynamers: from supramolecular polymers to adaptive dynamic polymers"*. Advanced Polymer Science 261, pp. 155-172.

[30] Kloxin, C. J., Scott, T. F., Adzima B. J., Bowman, C. N. (2010). *"Covalent Adaptable Networks (CANs): A Unique Paradigm in Crosslinked Polymers"*. Macromolecules 43(6), pp. 2643-2653.

[31] Baker, A., Dutton, S., Kelly, D. (2004). *"Composite Materials for Aircraft Structures"*, 2nd ed., AIAA Education Series, Reston, VA.

[32] Niu, M. C. (1992). *"Composite Airframe Structures"*, 1st ed., Hong Kong Conmilit Press Limited, Hong Kong.

[33] González, F., Guenther, B. (2003). *"Determination of the epoxide equivalent weight of epoxy resins based on diglycidyl ether of bisphenol A (DGEBA) by proton nuclear magnetic resonance"*, Polymer Testing 22, pp. 51-56.

[34] Denissen, W., Winne, J. M., Du Prez, F. E. (2016). *"Vitrimers: permanent organic networks with glass-like fluidity"*. Chemical Science 7, 30.

[35] Denissen, W., De Baere, I., Van Paepegem, W., Leibler, L., Winne, J., Du Prez, F. E. (2018). *"Vinylogous Urea Vitrimers and Their Application in Fiber Reinforced Composites"*. Macromolecules 51, pp. 2054-2064.

[36] Chen, X. X., Wudl, F., Mal, A. K., Shen, H. B., Nutt, S. R. (2003). *"New thermally remendable highly cross-linked polymeric materials"*. Macromolecules 36 (6), pp. 1802-1807.

[37] Park, J. S., Kim, H. S., Hahn, H. T. (2009). *"Healing behaviour of a matrix crack on a carbon fiber/mendomer composite"*. Composites Science and Technology 69, pp. 1082-1087.

[38] Roy, N., Bruchmann, B., Lehn, J. M. (2015). *"DYNAMERS: dynamic polymers as self-healing materials".* Chem Soc Rev 44, 3786.

[39] Montarnal, D., Capelot, M., Tournilhac, F., Leibler, L. (2011). *"Silica-Like Malleable Materials from Permanent Organic Networks".* Science Vol. 334, Issue 6058, pp. 965-968.

[40] Ruiz de Luzuriaga, A., Martin, R., Markaide, N., Rekondo, A., Cabañero, G., Rodríguez, J., Odriozola, I. (2016). *"Epoxy resin with exchangeable disulphide crosslinks to obtain reprocessable, repairable and recyclable fiber-reinforced thermoset composites"*. Materials Horizons 3, 241.

[41] Takahashi, A., Ohishi, T., Goseki, R., Otsuka, H. (2016). *"Degradable epoxy resins prepared from diepoxide monomer with dynamic covalent disulphide linkage"*. Polymer 82, pp. 319-326.

[42] Wei, C., Chen, M., Liu, D., Zhou, W., Khan, M., Wu, X., Huang, N., Li, L. (2015). *"A recyclable disulphide bond chemically cross-linking, high toughness, high conductivity ion gel bases on re-shaping and restructuring in the gel state"*. Polymer Chemistry 6, 4067.

[43] Johnson, L. M., Ledet, E., Huffman, N. D., Swarner, S. L., Shepherd, S. D., Durham, P. G., Rothrock, G. D. (2015). *"Controlled degradation of disulphide-based epoxy thermosets for extreme environments"*. Polymer 64, pp. 84-92.

[44] Abdolah Zadeh, M., Grande, A. M., van der Zwaag, S., García, S. J. (2016). *"Effect of curing on the mechanical and healing behaviour of a hybrid dual network: a time resolved evaluation"*. RSC Advances 6, 91806.

[45] Nevejans, S., Ballard, N., Miranda, J. I., Reck, B., Asua, J. M. (2016). *"The underlying mechanisms for self-healing of poly(disulphide)s"*. Phys. Chem. Chem. Phys.

[46] Zhou, F., Guo, Z., Wang, W., Lei, X., Zhang, B., Zhang, H., Zhang, Q. (2018). *"Preparation of self-healing, recyclable epoxy resins and low-electrical resistance composites based on double-disulfide bond exchange"*. Composites Science and Technology 167, pp. 79-85.

[47] Abdolah Zadeh, M., Esteves, A. C. C., van der Zwaag, S., García, S. J. (2014). *"Healable Dual Organic-Inorganic Crosslinked Sol-Gel Based Polymers: Crosslinking Density and Tetrasulfide Content Effect"*. Journal of Polymer Science, Part A: Polymer Chemistry 52, pp. 1953-1961.

[48] Paolillo, S. (2018). *"Characterization of a Dynamic Epoxy Network: Curing and Functional Properties"*. Master Thesis, Politecnico di Milano.

[49] Rekondo, A., Martín, R., Ruiz de Luzuriaga, A., Cabañero, G., Grande, H. J., Odriozola, I. (2014). *"Catalyst-free room-temperature self-healing elastomers based on aromatic disulphide metathesis".* Materials Horizons 1, 237.

[50] Martín, R., Rekondo, A., Ruiz de Luzuriaga, A., Cabañero, G., Grande, H. J., Odriozola, I. (2014). *"The processability of a poly(urea-urethane) elastomer reversibly crosslinked with aromatic disulphide bridges"*. Journal of Materials Chemistry A 2, 5710.

[51] Mutlur, S. (2004). *"Thermal Analysis of Composites Using DSC"*. In: Kessler, M. R., *"Advanced Topics in Characterization of Composites"*, Trafford Publishing, pp. 11-34.

[52] Sichina, W. J. (2000). *"Characterization of Epoxy Resins Using DSC"*. PerkinElmer, Inc.

[53] Mike Compositi, TM. *"Scheda Tecnica Prodotto Linea Resine Epossidiche SX8 EVO"*.

[54] Callister Jr., W. D., Rethwisch, D. G. (2007). *"Materials Science and Engineering: An Introduction"*, 7th Ed. John Wiley & Sons, Inc.

[55] John Wiley & Sons, Inc. (2015). *"Encyclopedia of Polymer Science and Technology"*.

[56] PerkinElmer, Inc. (2013). *"Dynamic Mechanical Analysis"*.

[57] Nixon, W.C. (1971*). "A Discussion on New Developments in Electron Microscopy with Special Emphasis on their Application in Biology"*. Philosophical Transactions of the Royal Society of London, Series B, Biological Sciences, Vol. 261, No. 837, pp. 45-50.

[58] Hardis, R. (2012). *"Cure kinetics characterization and monitoring of an epoxy resin for thick composite structures"*. Master Thesis, Iowa State University.

[59] Wellen, R. M. R., Canedo, E. L. (2014). *"On the Kissinger equation and the estimate of activation energies for non-isothermal cold crystallization of PET"*. Polymer Testing 40, pp. 33-38.

[60] Sis, H. (2009). *"Application of Model-free Methods for Analysis of Combustion Kinetic of Coals with Different Ranks"*. Energy Sources, Part A, 31:12, pp. 1016-1027.

[61] TA Instruments (2002). *"DMA 2980 Dynamic Mechanical Analyzer Operator's Manual"*.

[62] ASTM D7028-07 (2015). *"Standard Test Method for Glass Transition Temperature (DMA Tg) of Polymer Matrix Composites by Dynamic Mechanical Analysis (DMA)"*. ASTM International, West Coshohocken, PA.

[63] Artiaga, R., García, A. (2005). *"Fundamentals of DMA"*. Departamento de Ingeniería Inustrial II, Escola Politécnica Superior, Universidade da Coruña.

[64] Obaid, N., Kortschot, M. T., Sain, M. (2017). *"Understanding the Stress Relaxation Behavior of Polymer Reinforced with Short Elastic Fibers"*. Materials 10, 472.

[65] Prime, R. B. (2005). *"Dynamic Mechanical Analysis of Thermosetting Materials"*. IBM.

[66] Grzys, M. *"Thermal Applications Note, Guidelines for Performing DMA Creep Experiments"*. TA Instruments.

[67] ®™ Trademark of The Dow Chemical Company ("Dow") or an affiliated company of Dow. *"Epoxy Resins Product Overview Guide"*.

[68] HEXCEL ® (2015). *"HexFORCE ® 01102 1000 TF970 E Glass Fabric"*.

[69] PPG Industries © (2014). *"G75 Single End Yarn Product Bulletin"*.

[70] Little, J. E., Yuan, X., Jones, M. I. (2012). *"Characterisation of voids in fibre reinforced composite materials"*. NDT&E International 46, pp. 122-127.

[71] Graham-Jones, J., Summerscales, J. (2015). *"Marine Applications of Advanced Fibre-reinforced Composites"*. Woodhead Publishing Series in Composites Science and Engineering.

[72] Wang, Z., Fan, W., He, Q., Wang, Y, Liang, X., Cai, S. (2017). *"A simple and robust way towards reversible mechanochromism: Using liquid crystal elastomer as a mask"*. Extreme Mechanics Letters 11, pp. 42-48.

[73] Calvino, C., Neumann, L., Weder, C., Schrettl, S. (2016). *"Approached to Polymeric Mechanochromic Materials"*. Journal of Polymer Science Part A Polymer Chemistry 55(4).

[74] Chisholm, S. A., Rufin, A. C., Chapman, B. D., Benson, Q. J. (2016). *"Forty Years of Structural Durability and Damage Tolerance at Boeing Commercial Airplanes"*. Boeing Technical Journal.

[75] Jiang, Y. (2014). *"An outlook review: Mechanochromic materials and their potential for biological and healthcare applications"*. Materials Science and Engineering C 45, pp. 682-689.

[76] Di Landro, L., Montalto, A., Bettini, P., Guerra, S., Montagnoli, F., Rigamonti, M. (2017). "Detection of Voids in carbon/Epoxy Laminates and Their Influence on Mechanical Properties". Polymers & Polymer Composites, Vol. 25, No. 5.

[77] Stack, R. M., Lai, F. (2013). *"Development in Thermoforming Thermoplastic Composites"*. University of Massachusetts Lowell.

[78] Markaide, N., Ruiz de Luzuriaga, A., Hoyos, G., Rekondo, A., Grande, H. J. (2017). *"Composites termoestables reprocesables, reparables y reciclables"*. Materiales Compuestos, Vol 2, Nº1

[79] Dayyani, I., Shaw, A.D., Flores, S., Friswell, M.I. (2015). *"The mechanics of composite corrugated structures: A review with applications in morphing aircraft"*. Composite Structures, Vol. 133, pp. 358-380.

[80] Ermanni, P., Jenny, P., Mazza, E., Morari, M. (2009) *"Smart Airfoil"*. ETH Zürich.

[81] Wisnom, M. R. (2012). *"The role of delamination in failure of fibre-reinforced composites"*. Philosophical Transactions of the Royal Society A 370, pp. 1850-1870.

[82] Dorworth, L. C., Dillingham, G. (2017). *"Fundamentals of Adhesive Bonding of Composite Materials"*. AeroDef Manufacturing.